STUDIES ON THE MOLECULAR PATHOGENESIS OF NEURONAL CEROID LIPOFUSCINOSES IN THE ANIMAL MODELS OF CLN8 AND CLN10

Mervi Kuronen

Folkhälsan Institute of Genetics,

Neuroscience Center and Department of Medical Genetics, University of Helsinki

and Helsinki Graduate Program in Biotechnology and Molecular Biology

Academic Dissertation

To be publicly discussed,
with the permission of the Faculty of Medicine of the University of Helsinki,
in the Folkhälsan lecture hall Arenan, Topeliuksenkatu 20, Helsinki,
on Friday September 28th 2012 at 12 noon

Helsinki 2012

Supervised by

Docent Outi Kopra, PhD

Folkhälsan Institute of Genetics, Neuroscience Center and Department of Medical Genetics, University of Helsinki

Helsinki, Finland

Professor Anna-Elina Lehesjoki, MD, PhD

Folkhälsan Institute of Genetics, Neuroscience Center and Department of Medical Genetics, University of Helsinki

Helsinki, Finland

Reviewed by

Senior Lecturer Hannah Mitchison, PhD

Institute of Child Health, University College London

London, United Kingdom

Docent Tapio Heino, PhD

Department of Biosciences, University of Helsinki

Helsinki, Finland

Opponent

Professor Frances M. Platt, PhD

Department of Pharmacology, University of Oxford

Oxford, United Kingdom

Cover image: immunohistochemically stained myelin sheaths in the mouse cerebral cortex.
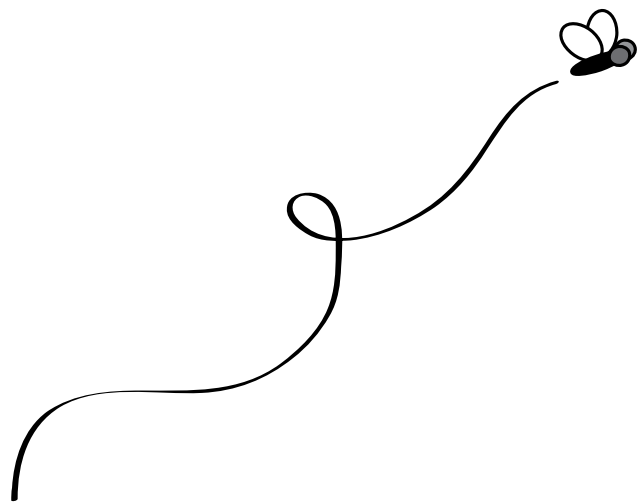
To all of you who have made my brain cells sparkle

TABLE OF CONTENTS

LIST OF ORIGINAL PUBLICATIONS

I   Kuronen M, Talvitie M, Lehesjoki AE, Myllykangas L. Genetic modifiers of degeneration in the *cathepsin D* deficient *Drosophila* model for neuronal ceroid lipofuscinosis. *Neurobiol Dis.* 36: 488–493. 2009.

II   Kuronen M, Lehesjoki AE, Jalanko A, Cooper JD, Kopra O. Selective spatiotemporal patterns of glial activation and neuron loss in the sensory thalamocortical pathways of neuronal ceroid lipofuscinosis 8 mice. *Neurobiol Dis.* 47: 444–457. 2012.

III   Kuronen M, Hermansson M, Manninen O, Zech I, Talvitie M, Laitinen T, Gröhn O, Somerharju P, Eckhardt M, Cooper JD, Lehesjoki AE, Lahtinen U, Kopra O. Galactolipid deficiency in the early pathogenesis of neuronal ceroid lipofuscinosis model *Cln8mnd*: implications to delayed myelination and oligodendrocyte maturation. *Neuropathol Appl Neurobiol.* 38: 471–486. 2012.

The publications are referred to in the text by their Roman numerals. Unpublished data are also presented.

The original articles are reproduced with the permission of the respective copyright holders (Elsevier, Wiley-Blackwell Ltd.).

ABBREVIATIONS

Abbreviations that appear more than once and in more than one section are presented here.

A2B5	antigen for gangliosides
ALS	amyotrophic lateral sclerosis
AMP	adenosine monophosphate
ATP	adenosine triphosphate
ATP13A2	P5-type ATPase
Ca^{2+}	calcium ion
cathB	*cathepsin B*
cathD	*cathepsin D*
CD68	cluster of differentiation 68
CDase	*Ceramidase*
cDNA	complementary DNA
CerS	ceramide synthase
CGT	UDP-galactose:ceramide galactosyltransferase
CLN1-10	ceroid lipofuscinosis, neuronal, 1-10
CNS	central nervous system
CSPα	cysteine string protein alpha
CTSD	cathepsin D
DNAJC5	DNAJ/HSP40 homolog, subfamily C, member 5
EEG	electroencephalogram
EPMR	progressive epilepsy with mental retardation
ER	endoplasmic reticulum
ERG	electroretinogram
ERGIC	endoplasmic reticulum Golgi intermediate department
GABA	gamma-aminobutyric acid
GAL4	yeast transcription activator protein
GalC	galactoceramide
GFAP	glial fibrillary acidic protein
HDL	high density lipoprotein
HMGCR	3-hydroxy-3-methyl-glutaryl coenzyme A reductase

Hsc70	*heat shock 70 kDa protein cognate*
HSP70	heat shock 70kDa protein
lag1	*longenvity assurance gene*
LFB	Luxol fast blue
LGNd	dorsal lateral geniculate nucleus
loe	*löchrig/AMP-activated protein kinase gamma subunit*
MBP	myelin basic protein
MFSD8	Major facilitator superfamily domain-containing 8
mnd	*motor neuron degeneration* mouse mutation
MOG	myelin and oligodendrocyte glycoprotein
MRI	magnetic resonance imaging
mRNA	messenger RNA
NCL	neuronal ceroid lipofuscinosis
nclf	*neuronal ceroid lipofuscinosis* mouse mutation
NeuN	antigen for neuronal nuclei
NG2	Chondroitin sulphate proteoglycan 4
Olig2	Oligodendrocyte lineage transcription factor
PAS	Periodic acid-Schiff
PCR	polymerase chain reaction
PDGF	platelet-derived growth factor
PLP	proteolipid-protein
Po	posterior nucleus of thalamus
PPT1	palmitoyl-protein thioesterase 1
S1	primary somatosensory cortex
S1BF	primary somatosensory cortex, barrel field
S2	secondary somatosensory cortex
Sap-r	*Saposin-related*
SEP	somatosensory evoked potential
sGalC	sulfatide
shi	*shibire*
Sod	*Superoxide dismutase*
TLC	TRAM-Lag1p-CLN8 protein domain
TNFα	tumor necrosis factor alpha
Tor	*Target of rapamycin*
TPP1	tripeptidyl-peptidase 1

TRAM	translocating chain-associated membrane protein
Trxr-1	*Thioredoxin reductase 1*
UAS	upstream activating sequence
UDP	uridine diphosphate
V1	primary visual cortex
VEP	visual evoked potentials
VPL	ventral posterior lateral nucleus of thalamus
VPM	ventral posterior medial nucleus of thalamus
wt	wildtype

ABSTRACT

The neuronal ceroid lipofuscinoses (NCLs) are a group of pediatric neurodegenerative syndromes. They are characterized by epilepsy, mental and motor regression, loss of vision and early death. Pathological findings include accumulation of lysosomal storage material together with neuron loss and glial activation in affected brains. Mutations in at least ten genes are reported to cause NCL disease. Apart from human disease, NCL phenotypes are widely present in the animal kingdom. However, the events leading to NCL disease onset and progression remain elusive and without a possibility to intervene.

In this study these events were assessed in two forms of NCLs, the CLN8 and CLN10 diseases. Late-infantile onset CLN8 disease and the more protracted progressive epilepsy with mental retardation are caused by mutations in the *CLN8* gene. CLN8 is a resident of the endoplasmic reticulum membrane and linked to a lipid metabolism-related protein family. Mutations in the *cathepsin D* (*CTSD*) gene cause the most severe form of NCL, CLN10, which typically leads to death shortly after birth. The lysosomal aspartic protease CTSD is involved in cellular protein degradation and apoptosis. Two animal models were used in this study, the *Cln8mnd* mouse carrying a spontaneous mutation in the mouse *Cln8* gene, and the previously generated *cathepsin D* deficient *Drosophila*, *cathD¹*. Both model the respective human NCL diseases with intracellular storage and neuronal death.

The *Drosophila cathD¹* was characterized with degenerative changes in the retina. This phenotype could be utilized to study the genetic pathways of *cathD* in a hypothesis-based modifier screen using *Drosophila* genetics and histological techniques. Seven candidate modifiers involved in lipid metabolism regulation, endocytosis and oxidative stress were identified as enhancers of the retinal degeneration of *cathD¹*. Similar processes have been described affected in other *Drosophila* models for NCLs, suggesting that *Drosophila* NCL proteins may act in overlapping genetic pathways. While the importance of these pathways needs to be assessed in the human disease, their overlap suggests a possibility for a common mechanism of neurodegeneration.

Similarly to previously characterized NCL models, the CLN8 disease model *Cln8mnd* showed neuron loss and glial activation in sensory thalamocortical pathways. By using stereological methods and histology, neuron loss in the visual thalamocortical pathway was shown to appear relatively late compared to the previously described retinal degeneration in *Cln8mnd*. This suggests that the visual areas of the brain are spared even with diminished or absent input from the retina. The somatosensory thalamocortical pathway was affected first. While the cerebral cortical sensory areas were relatively spared, neuron loss progressed rapidly in the thalamic component of these pathways. Thalamic sensory nuclei have shown particular vulnerability in the majority of NCL models, indicating a common pathological pathway

proceeding from thalamus to the cortex. In the future, knowledge of the differentially affected components of distinct pathways may be utilized in therapies, which should be targeted to the primary sites of pathology. In CLN8 disease these appear to be the retina and somatotosensory thalamus.

Glial cells were observed to contribute to the *Cln8^mnd* neuropathology. Especially microglial activation preceded neuron loss in *Cln8^mnd* brain. Decreased axonal myelination, studied by stereology, light and electron microscopy, was observed even before microglial activation, yet myelination reached normal levels by the time of major brain pathology. By protein and gene expression profiling we were able to show a delayed maturation of oligodendrocytes in the *Cln8^mnd* mouse brain and *in vitro*. These results suggest that perturbations in the glia-neuron-glia signaling occur well in advance of the neurodegeneration in *Cln8^mnd*. With increasing information on the mechanisms of these interactions it may be possible to find a specific target for therapies for CLN8 or NCLs in general.

The myelination defect in *Cln8^mnd* was observed through large-scale brain lipid analysis, where decreased amounts of myelin-specific galactolipids were found in *Cln8^mnd* cortex, especially in the early stages of *Cln8^mnd* disease. Subsequent analyses showed a persistent defect in the galactolipid synthesis by the UDP-galactose:ceramide galactosyltransferase enzyme. The connection of CLN8 to lipid synthesis regulation is in agreement with the sequence-based hypothesis of a role for CLN8 in lipid metabolism regulation, while further studies are required to indicate a specific function.

In conclusion, this study resulted in increased knowledge on the CLN8 and CLN10 disease pathogenesis and on the cellular functions of the affected proteins. Results from both *cathD^1 Drosophila* and *Cln8^mnd* mouse suggest both similarities and differences to other NCL models. In the future, increased knowledge on the molecular changes may take us towards targeting these diseases with therapies.

TIIVISTELMÄ

Neuronaaliset seroidilipofuskinoosit (NCL-taudit) muodostavat yleisimmän syyn lapsuusiän hermorappeumaan. Vaikka tautien taustalla olevat geenivirheet pääosin tunnetaankin, molekyylitason tapahtumat, jotka johtavat taudin syntyyn, ovat edelleen pitkälti selvittämättä. Taudin etenemistä ei myöskään kyetä pysäyttämään tai tautia parantamaan.

Tässä väitöskirjassa tutkittiin NCL-tauteihin lukeutuvien CLN8- ja CLN10-tautien taustalla olevien proteiinien toimintaa. Synnynnäisen NCL-taudin, CLN10:n taustalla ovat katepsiini D (*CTSD*) –geenin virheet. Solun sisällä lysosomeihin paikantuva CTSD on proteiineja pilkkova entsyymi. Työssä käytimme apuna CTSD-poistogeenistä banaanikärpästä (*cathD¹*), jolla on NCL-taudeille tyypillistä solunsisäistä kertymämateriaalia ja hermosolujen rappeumaa. Teimme seulonnan, jossa tarkastelimme 17 geenin mutaatioiden vaikutusta *cathD¹*-kärpäsen ilmiasuun. Histologiseen analyysiin perustunut seulonta vahvisti, että *cathD¹*:n solukuolema voimistuu, kun kärpäsellä on häiriöitä rasva-aineenvaihdunnassa, endosytoosissa ja solujen suojautumisessa happiradikaaleilta. Samankaltaisten reittien on havaittu vaikuttavan myös muiden NCL-banaanikärpäsmallien ilmiasuihin. Näitä reittejä voidaan tarkemmin tutkia banaanikärpäsessä ja muissa NCL-tautien solu- ja eläinmalleissa.

CLN8-geenin mutaatiot voivat aiheuttaa paitsi lapsuusiän NCL-taudin, myös nuoruusiällä puhkeavan, suomalaisen tautiperimän tauteihin kuuluvan Pohjoisen epilepsian. CLN8-toiminta on tuntematon, mutta proteiinin tiedetään paikantuvan solujen endoplasmakalvostoon ja sekvenssiyhtäläisyyksien perusteella sen on arveltu liittyvän rasva-aineenvaihdunnan säätelyyn. Tautimallina CLN8-tutkimuksissa käytettiin *Cln8^mnd*-hiirikantaa, jossa on luonnollisesti syntynyt *Cln8*-geenin mutaatio. CLN8-taudin etenemistä tutkittiin eri-ikäisistä hiiristä kerätyissä aivoleikkeissä ja käytettiin kvantitatiivisia menetelmiä, joiden avulla saatiin luotettava kuva hermosolukuoleman laajuudesta. Näyttääkin siltä, että aiemmin kuvattujen NCL-tautimallien lisäksi myös *Cln8^mnd*-hiiren aivopatologia keskittyy isoaivokuoren ja talamuksen välisiin yhteyksiin ja alkaa tunto- ja kipuaistimuksia välittävältä somatosensoriselta aivoradalta. Toisin kuin useissa aiemmin kuvatuissa NCL-malleissa, aivojen näköaivorata säilyi vahingoittumattomana hyvin pitkään, vaikka *Cln8^mnd*-hiiren tiedetään sokeutuvan varhain. Tietoa tautimuutosten etenemisestä voidaan toivottavasti käyttää hyväksi, kun pyritään kehittämään hoitomuotoja CLN8-tautia vastaan.

Muutokset glia- eli hermotukisoluissa edelsivät hermosolukatoa tutkituilla aivoalueilla. Jo varhain ennen hermosolukuolemaa havaittiin aivojen immuunipuolustuksen aktivaatioon viittaavia muutoksia mikrogliassa. Vielä aiemmin muutoksia nähtiin oligodendrosyyteissä, jotka muodostavat hermosolujen viejähaarakkeita ympäröivän myeliinitupen. Myeliiniä, joka on välttämätöntä nopealle signaalinvälitykselle, muodostui *Cln8^mnd*-hiirellä normaalia hitaammin. Tämän havaittiin liittyvän myeliiniin rikastuneiden rasva-aineiden, galaktolipidien

vähentyneeseen valmistukseen. Tulokset viittaavat siihen, että CLN8:n toiminta liittyisi rasva-aineiden valmistukseen, mutta lisätutkimuksia tarvitaan, jotta pystyttäisiin selvittämään tarkka biologinen mekanismi.

Väitöskirjatyön tuloksena saatiin lisää tietoa NCL-tautien aiheuttamasta aivopatologiasta ja siihen vaikuttavista tekijöistä. NCL-taudit ovat keskenään hyvin samankaltaisia. Tämä tutkimus tukee oletusta, että tautimekanismeissa on samankaltaisuuksia. Esimerkiksi rasva-aineenvaihdunnan häiriöiden havaittiin vaikuttavan sekä CLN8- että CLN10-tautimalleissa. Tautimekanismit ovat kuitenkin myös hyvin erilaiset, mikä nähtiin vertailtaessa eri NCL-malleissa tehtyjä tutkimuksia isoaivokuoren ja talamuksen välisistä radoista: NCL-taudit eivät noudata samaa kaavaa siinä, miltä alueilta tautimuutokset alkavat. Näiden vertailujen kautta saatu tieto on hyödyllistä, kun NCL-tauteja vastaan kehitetään hoitomuotoja.

1 INTRODUCTION

I said in Dorian Gray that the great sins of the world take place in the brain: but it is in the brain that everything takes place.... It is in the brain that the poppy is red, that the apple is odorous, that the skylark sings.

-Oscar Wilde

Why do we have a brain? As Oscar Wilde says, to see, to smell, to hear. With a nervous system we are able to observe the environment with senses such as sight, smell, hearing, taste, touch, pain, and balance. Sensations arouse a diversity of behaviours: in Wilde's case, he got an idea, took a pen and wrote, performing the acts of the human brain. Performed acts – that is the other half of the answer. We have a brain to act according to our perceptions of the environment. Sometimes the act is deliberate, directed movement such as the movement of fingers and hands. Sometimes the result is a chain of reasoning, consideration of previous experiences, leading to the conscious decision not to act.

Why study the nervous system of another animal species in order to understand the human brain? We may do so out of pure curiosity, since in evolution many variations have been generated to adjust to environmental challenges. Yet with shared environment and ancestors many of the adjustments are similar between us animals. That is what we make use of when tackling a certain problem in an experimental model organism. Brains of different species do have much in common: they are comprised of nerve cells, neurons, which signal electrically and are interconnected via synapses, structures that join the cells together and enable signal transduction in a network of cells.
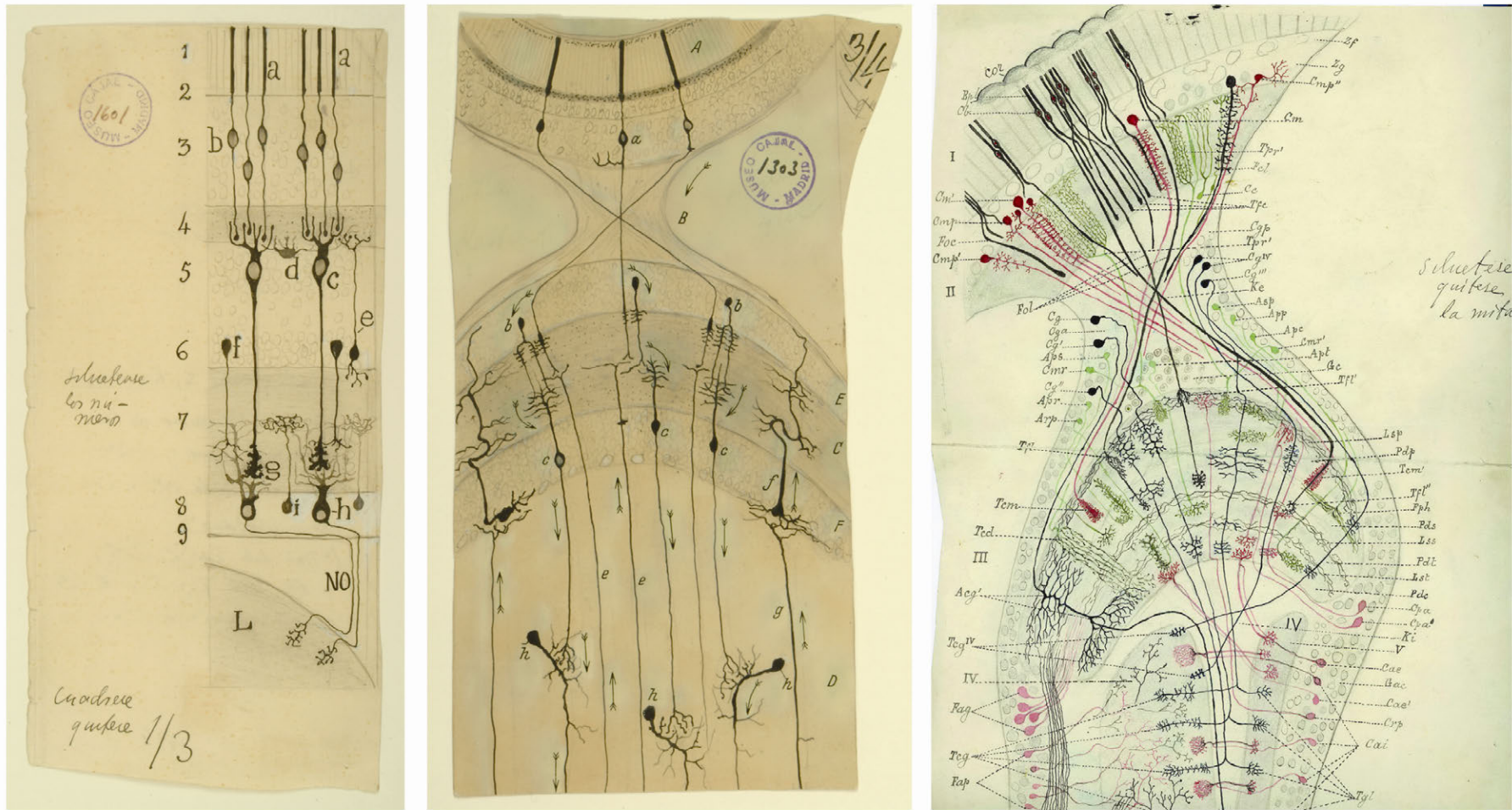
Figure 1. Drawings of Santiago Ramón y Cajal depicting the organization of the visual system (from left to right) of a vertebrate, a cephalopod (*Sepia*) and an insect (housefly, *Musca*). This illustration shows the physical dimensions of the neuronal circuits: vertebrate neurons are larger than those of a cephalopod which again are larger than those of an insect (Llinas 2003). Reprinted with permission from Instituto Cajal (CSIC), Madrid, Spain.

2 REVIEW OF THE LITERATURE

2.1 CELL TYPES OF THE CENTRAL NERVOUS SYSTEM

> *… l'écorce cérébrale est pareille à un jardin peuplé d'arbres innombrables, les cellules pyramidales, qui, grâce à une culture intelligente, peuvent multiplier leurs branches, enfoncer plus loin leurs racines, et produire des fleurs et des fruits chaque fois plus variés et exquis.*
>
> *… the cerebral cortex is similar to a garden filled with trees, the pyramidal cells, which, thanks to intelligent culture, can multiply their branches, sending their roots deeper and producing more and more varied and exquisite flowers and fruits.*
>
> *-Santiago Ramón y Cajal*

The fact that the brain is formed by a network of connected but separate individual cells that communicate specifically with each other was demonstrated by Santiago Ramón y Cajal, Nobel Prize laureate in Physiology or Medicine, 1906. Ramón y Cajal described and illustrated a plethora of nervous system cell types, subtypes and the pathways they formed. He utilized a variety of organisms in his work, including material from humans and other mammals, birds, frogs, cephalopoda and insects, and had a substantial contribution to the field of comparative neuroanatomy (Fig. 1).

Ramón y Cajal's work was the basis of the Neuron Doctrine, the principle of the neuron as the single anatomical and functional unit in the nervous system. Ramón y Cajal also acknowledged the other major cells types in the nervous system, collectively called the glia, by speculating on their functions in attention, sleep and wakefulness (Garcia-Marin *et al.* 2007). However, until recent decades, glial cells have mostly been regarded as connective tissue and named as the 'nerve glue' (Virchow 1846; according to (Baumann & Pham-Dinh 2001). While the active roles of glial cells are still being discovered, neurons are no longer considered as the single functional units of information flow in the brain - they are aided to a great extent by glial cells in forming and maintaining neural circuits. Established functions of glia include supporting neurotransmission, maintaining ionic balance in the extracellular space, and insulating axons to speed up electrical communication (Allen & Barres 2009). The main cell types of the vertebrate central nervous system (CNS), the astrocytes, oligodendrocytes, microglia and neurons (Fig. 2) are introduced in the following sections 2.1.1-2.1.4. Notes on invertebrate (*Drosophila*) neurons and glia are given in section 2.1.5.
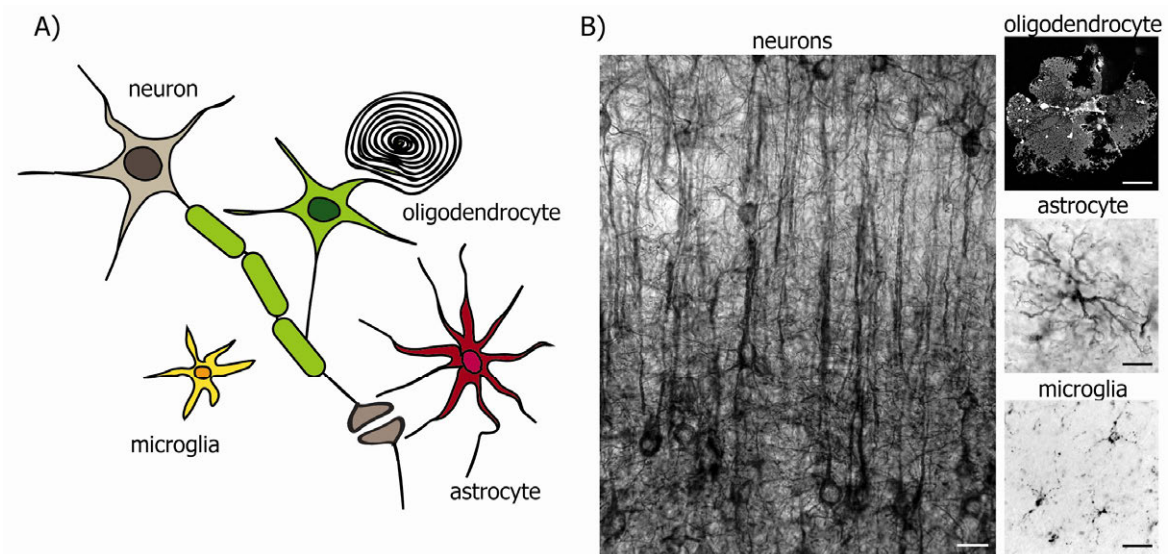
Figure 2. The four main cell types of the vertebrate central nervous system. A) Schematic illustration of a neuron, myelin forming oligodendrocyte, an astrocyte and a microglial cell. B) Neurons and glial cells observed through antibody-based staining methods. Scale bars 20 μm.

2.1.1 NEURONS

Morphologically, a neuron consists of a cell soma (or cell body), one axon and usually several dendrites. There are a multitude of neuron types in the vertebrate nervous system. Classification relies on the cellular morphology, electrophysiology, use of neurotransmitters and other chemical properties, and on the synapses and connections they make. However, the simplest classification of neurons in the vertebrate nervous system is according to the distance of the axon projection. Neurons connecting to more distant parts of the nervous system are called projection or relay neurons, and neurons with short-distance axons that connect to local circuits are called interneurons (Kandel *et al.* 2000). In this section, properties of mammalian cerebral cortical and thalamic neurons are introduced.

2.1.1.1 Neurons of the cerebral cortex

Pyramidal cells (Fig. 3A) are the major projection neurons and the most abundant neuron type of the neocortex (70-80% of neurons). In addition, they are the main excitatory neurons of the cerebral cortex releasing glutamate or aspartate as neurotransmitters. Pyramidal neurons are identified by their large size, triangular-shaped soma, large number of dendrites and dendritic spines and highly polarized shape. However, their structure exhibits high regional variation. Spiny stellate cells are another excitatory cell type of the cortex, but as opposed to pyramidal neurons, they are local interneurons. (Elston 2003; Markram *et al.* 2004; Squire *et al.* 2003)
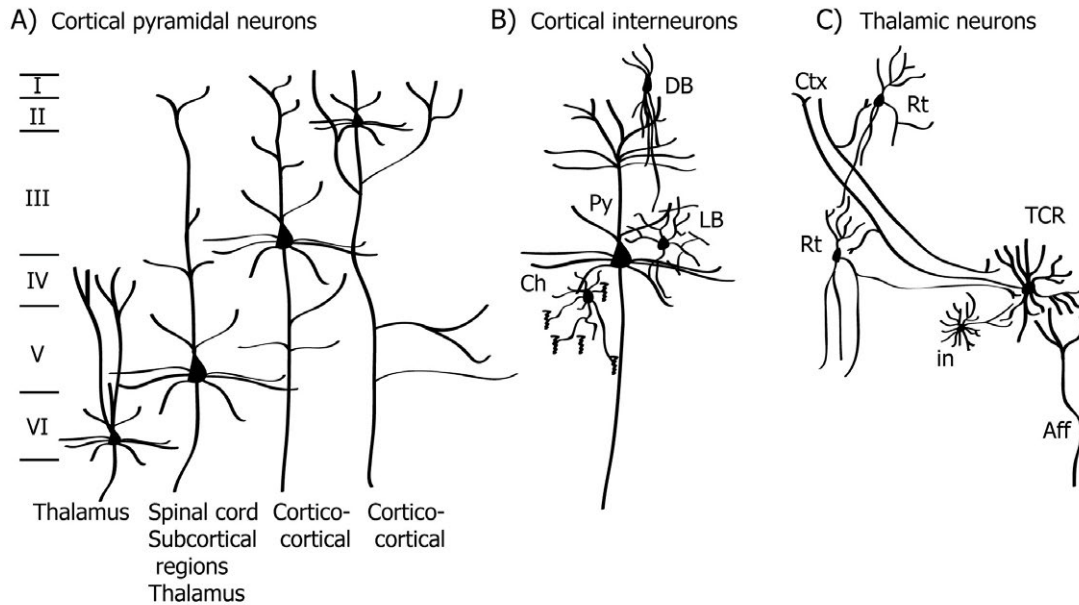
Figure 3. Neuron subtypes in the cerebral cortex and thalamus. A) Excitatory pyramidal cells project to the spinal cord, subcortical and to other cortical regions. B) Large basket cells (LB), double bouquet cells (DB) and chandelier cells (Ch) are illustrated surrounding a layer III pyramidal neuron. C) Thalamocortical relay neurons (TCR) receive information through afferent neurons (Aff) and project to cortical regions (Ctx), sending collateral projections to thalamic reticular nucleus (Rt). The reticular nucleus also receives collaterals from the cortical axons projecting to thalamus. Local interneuron (in) is also depicted. Illustrations modified from (DeFelipe 2011; Jones 2009; Squire *et al.* 2003).

The major inhibitory neurons of the cerebral cortex include the basket cells, chandelier cells and double bouquet cells (Fig. 3B). They predominantly synapse with pyramidal cells and use gamma-aminobutyric acid (GABA) as the neurotransmitter. These GABAergic interneurons can be distinguished by their morphological, electrophysiological and molecular properties. Especially the calcium-binding proteins parvalbumin, calbindin and calretinin serve as valid molecular markers. Approximately 50% of all inhibitory interneurons are basket cells, which are further divided into large, small and nest basket cells. They target the somata and proximal dendrites of pyramidal cells and are thus considered to control the integrated synaptic response. Meanwhile the chandelier cells target the axons where they give a strong inhibitory input. Double bouquet cells target the pyramidal cell dendrites. (Markram *et al.* 2004; Squire *et al.* 2003)

The cerebral cortical layers differ according to which neuron types they contain (Fig. 3A and section 2.3.1.1). Pyramidal cells are mainly located in layers III, V and VI. Spiny stellate cells are most highly concentrated in layer IV of primary sensory areas. The basket cells, chandelier cells and double bouquet cells predominately localize in layers III and V where they inhibit the distant-projecting pyramidal cells. (Markram *et al.* 2004; Squire *et al.* 2003)

2.1.1.2 Neurons of the thalamus

The thalamus is an important relay system between the cerebral cortex and other regions of the CNS. Mammalian thalamic nuclei contain excitatory relay neurons and local interneurons (Fig. 3C). The thalamic reticular nucleus consists of GABAergic interneurons and acts to integrate and modulate information received and sent by the thalamus. While many thalamic nuclei of mice and rats appear to lack local interneurons, the major inhibitory action is executed by the reticular nucleus (Arcelli *et al.* 1997). The thalamic relay neurons largely share a common morphology, including a symmetrical, bushy dendritic field. Interneuronal dendrites show rich terminal branching and swellings, while the discoid dendritic arbors of a reticular interneuron are situated in the plane of the cell nucleus. (Jones 2009; Sherman & Guillery 2006)

The importance of the thalamic communication with cortex is illustrated by the synaptic input it receives: the majority of inputs to a typical sensory relay neuron are from cerebral cortex (almost 50% of the synapses) while the inputs from the sensory receptors account only for 5-15% of the synapses. A large number of inhibitory inputs is mostly derived from the reticular nucleus (approximately 30% of the synapses). Similarly, cortical inputs predominate in the reticular nucleus cells, where 70% of synapses are from the cortex. (Jones 2009; Van Horn *et al.* 2000)

2.1.2 ASTROCYTES

Astrocytes populate all CNS regions and constitute the most abundant cell type in the brain. Astrocytes form networks through gap junction channels that allow intercellular information flow, such as the calcium (Ca^{2+}) transients that may serve as a means of communication within and between astrocytes, other glial cells and neurons. Astrocyte morphology, functions and molecular expression pattern changes during CNS injury or disease in a process of reactive astrocytosis. (Allen & Barres 2009; Giaume *et al.* 2010; Sofroniew & Vinters 2010)

2.1.2.1 Astrocyte morphology and functions

In normal brain, astrocytes can be divided into at least two phenotypes: protoplasmic astrocytes are found in grey matter and fibrous astrocytes in white matter. The less studied fibrous astrocytes contact neuronal axons at the nodes of Ranvier. Protoplasmic astrocytes form a few main branches that give rise to several processes which contact neuronal dendrites, synapses and other astrocytes. (Sofroniew & Vinters 2010)

With their close contacts to synapses, it is not surprising that astrocytes have various roles in the synapse. They recycle neurotransmitter molecules released to the synaptic cleft through the glutamate-glutamine cycle. Thus, potentially excitotoxic amounts of glutamate are

efficiently removed and inactivated. In addition, astrocytes release molecules such as thrombospondins, to induce synaptogenesis and increase synaptic activity. Astrocytes are proposed to modulate neuronal excitability through releasing 'gliotransmitters' glutamate, adenosine triphosphate (ATP) and D-serine. There are neuronally evoked fluctuations in the astrocytic Ca^{2+} concentration that have been proposed to trigger gliotransmitter exocytosis to the synaptic cleft. However, the debate continues on the significance of this phenomenon. (Barres 2008; Hamilton & Attwell 2010)

Besides the synapses, astrocytes contact the blood vessels and form an imperative part of the neurovascular unit comprising neurons, glia and vascular cells (endothelia, pericytes and vascular smooth muscle cells). Astrocytes regulate the cerebral microcirculation through inducing vasodilation/vasoconstriction, possibly depending on the neuronal activity and involving Ca^{2+} waves in astrocytes. While astrocytes act as the main glycogen storage in the CNS, they are likely to participate in the increased metabolic requirements evoked by synaptic activity. (Iadecola & Nedergaard 2007; Sofroniew & Vinters 2010)

2.1.2.2 Reactive astrocytosis

Reactive astrocytosis is defined as the astrocytic response to all CNS perturbations, manifesting as changes of astrocyte molecular expression, morphology and function that depend on the severity of the insult (Fig. 4). Astrocytosis is a regulated phenomenon including inter- and intracellular signalling. All CNS cell types can release signalling molecules to trigger reactive astrocytosis, including growth factors, cytokines and neurotransmitters. (Sofroniew & Vinters 2010)

Morphologically, reactive astrocytes exhibit cellular hypertrophy with thickened processes. Reactive astrocytes are characterized by the upregulation of cytoskeletal intermediate filament proteins, especially of the glial fibrillary acidic protein (GFAP). In severe astrocytosis, proliferative astrocytes may originate from local or migrated glial cell progenitors or as a result of the cell cycle re-entry of mature astrocytes. Glial scar formation is a response to severe insult requiring a complex interplay of astrocytes with fibromeningeal and other glial cells. A glial scar establishes a physical barrier to the site of the injury, restricting the entry of inflammatory cells but also preventing axonal regeneration. (Pekny & Pekna 2004; Sofroniew 2009; Sofroniew & Vinters 2010)

Reactive astrocytosis can have both beneficial and detrimental effects on neurons and other cell types. The beneficial functions have been observed by experiments where reactive astrocytosis has been attenuated. Loss of reactive astrocytosis can lead to excitotoxic neurodegeneration due to failure in the synaptic glutamate uptake. It also results in enhanced synaptic degeneration in response to cortical lesions. Loss of astrocyte barrier functions may increase the effects of inflammation or infection. The detrimental effects may be caused by

the production of cytotoxic molecules such as pro-inflammatory cytokines through which astrocytosis may lead to chronic inflammation or neuropathic pain. Reactive astrocytosis may exhibit two stages, showing beneficial effects in the acute stage after CNS injury, but later inhibiting the CNS regeneration and leading to increased inflammation. (Milligan & Watkins 2009; Pekny & Nilsson 2005; Sofroniew 2009)
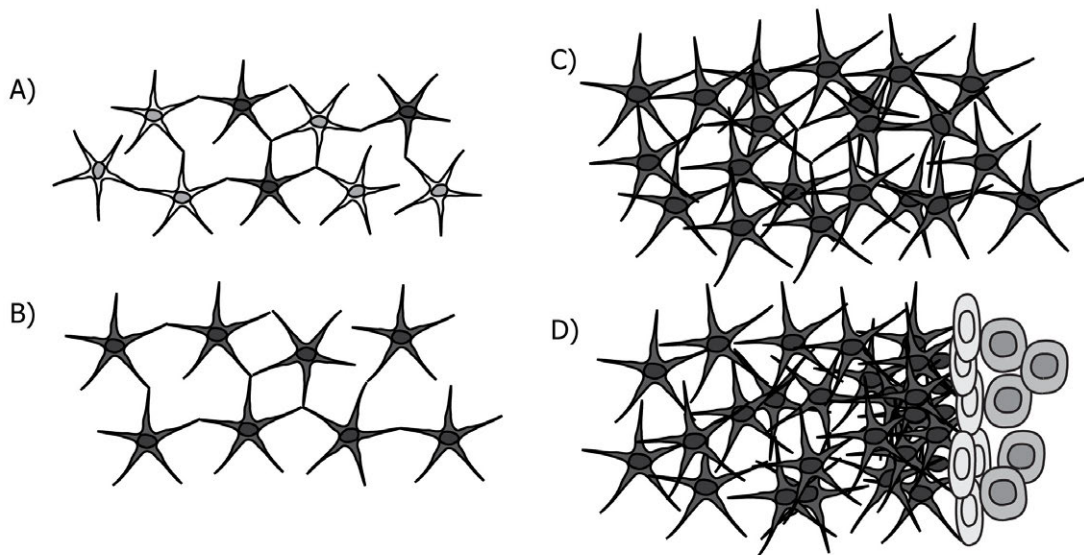
Figure 4. Different grades and progression of reactive astrocytosis. A) In normal brain, astrocytes inhabit separate domains and only some express GFAP (dark grey cells). B) Hypertrophy and molecular changes (GFAP expression) are seen in cases such as moderate metabolic or molecular insults or milder inflammatory activation. This phenotype can reverse if the triggering insult is removed. C) Molecular expression changes, overt cellular hypertrophy and proliferation are typical in areas surrounding severe lesions, infection or in regions of chronic neurodegeneration. D) Glial scars envelop areas of overt tissue damage and inflammation. It includes proliferation of astrocytes and other cell types. Glial scars restrict entry of inflammatory cells (round light grey cells) to the site of injury. Illustration based on (Sofroniew & Vinters 2010).

2.1.3 OLIGODENDROCYTES

In vertebrates, oligodendrocytes are essential for rapid electrical communication between neurons and their targets. Oligodendrocytes generate myelin sheets that enclose axons enabling the saltatory conduction of action potentials. In addition, myelination induces clustering of ion channels thereby further enhancing conduction velocity (Allen & Barres 2009). Other roles of oligodendrocytes include providing trophic and metabolic support to the neuronal axons (Nave 2010). Schwann cells, the peripheral counterparts of oligodendrocytes, which will not be introduced here in detail, ensheathe and support

peripheral nerves and display similarities but also differences to the CNS oligodendrocytes (Baumann & Pham-Dinh 2001).

2.1.3.1 Myelin

In brain, myelin is formed by the expanded and specialized plasma membrane of a mature, myelinating oligodendrocyte. The compactly multilayered and segmented structure of myelin, low water content and high lipid content account for its insulation properties. Structurally, myelin sheath segments or internodes are separated by the nodes of Ranvier, where myelin is lacking and the axon is exposed to the extracellular milieu. Rapid saltatory nerve conduction is established through the axonal impulse jumping from node to node over the well-insulated internodes. (Baumann & Pham-Dinh 2001)

Myelin membrane has a protein to lipid ratio of 1:3 while other biological membranes have a ratio of 1:1-4:1. The lipid composition is unique (Fig. 5) with exceptionally high proportions of glycosphingolipids galactoceramide (cerebroside, GalC) and its sufated form, sulfogalactoceramide (sulfatide, sGalC). These lipids differ from other glycosphingolipids since they consist of a galactose (instead of glucose) headgroup, they incorporate very-long-chain fatty acids and they are solid at body temperature. Other major myelin lipids include cholesterol, which decreases the fluidity of the membrane, and phospholipids, of which ethanolamine-containing plasmalogen is highly myelin-enriched. A large proportion of fatty acids in galactolipids and phospholipids are saturated. These lipid characteristics contribute to the decreased membrane fluidity and permeability that enhance the insulation capacity of the myelin membrane. (Aggarwal *et al.* 2011; Chrast *et al.* 2011; Siegel *et al.* 1999)

The multilayered myelin membrane is compacted by specific oligodendrocyte expressed proteins (Fig. 5). The myelin basic protein, MBP, and the proteolipid-protein, PLP, account for 60-80% of total myelin proteins and are the major structural proteins in CNS myelin (Fig. 5). MBP joins the cytoplasmic membrane leaflets in close apposition. Membrane spanning PLP is suggested to function in the adhesion of the extracellular leaflets. (Aggarwal *et al.* 2011; Siegel *et al.* 1999)

Synthesis of the myelin components is under strict developmental regulation and needs to progress rapidly before and during the active period of myelination (section 2.1.3.2). The activity of UDP-galactose:ceramide galactosyltransferase (CGT), catalyzing the last step of galactolipid synthesis, increases notably in rodent brain just before the maximal rate of myelin formation and then gradually declines. MBP synthesis and integration to myelin is very rapid and occurs in free ribosomes associated with the myelin membrane. PLP is synthesized in the bound ribosomes in the perikaryon and transported to the oligodendrocyte processes possibly together with cholesterol and galactolipids. A pool of PLP accumulates in the late endosomes

of premyelinating oligodendrocyte processes that are released and integrated once the myelination is initiated. (Siegel *et al.* 1999; Simons & Trotter 2007)
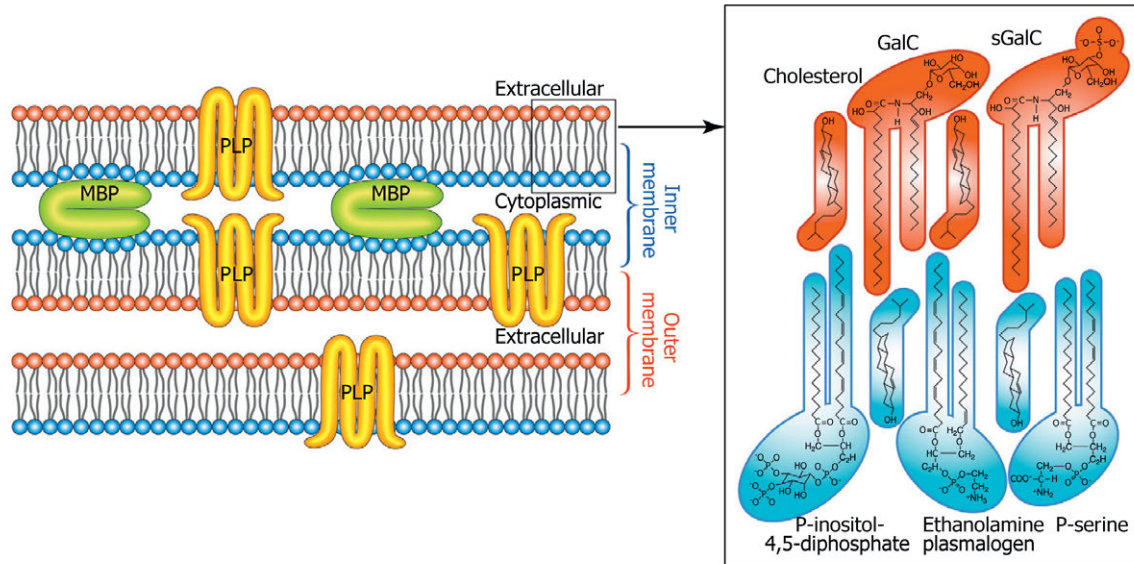
Figure 5. Major components of the myelin membrane. Cholesterol and galactolipids are enriched on the extracellular side of the myelin membrane, while ethanolamine plasmalogen is localized to the cytoplasmic side of the bilayer. The cohesive effect of MBP is mainly established through its interactions with phosphatidylserine and phosphatidylinositol-(4,5)-bisphosphate. Reprinted from Aggarwal *et al.* 2011, with permission from Elsevier.

2.1.3.2 Oligodendrocyte development and myelination

Myelination is a spatiotemporally regulated process that requires the oligodendrocytes to proliferate, migrate and synthesize myelin membrane. In the mouse CNS, myelin formation starts at birth in the spinal cord and optic tract, and by 45–60 days postnatally the brain is completely myelinated. In humans the myelination peak occurs during the first year after birth, yet the process already starts during the second half of fetal life from the spinal cord. Myelination occurs until 20 years of age, especially in the associative areas of the cerebral cortex. Myelination progresses caudorostrally in the brain, opposite to the spinal cord where the progression is rostrocaudal. (Baumann & Pham-Dinh 2001)

In the mammalian cortex, oligodendrocytes as well as neurons and astrocytes are generated from the proliferating neuroepithelial cells of the telencephalic ventricular and subventricular zone (SVZ). Oligodendrocyte progenitors migrate from these zones, continuously extending and retracting their processes. This may serve to sense other nearby oligodendrocyte progenitors and establish correct spacing. The process of sensing the surrounding

oligodendrocytic cells continues throughout postmigratory oligodendrocytic development. Different stages of oligodendrocyte development are characterized by changes in cell morphology and molecular expression pattern (Fig. 6). (Baumann & Pham-Dinh 2001; Simons & Trotter 2007).
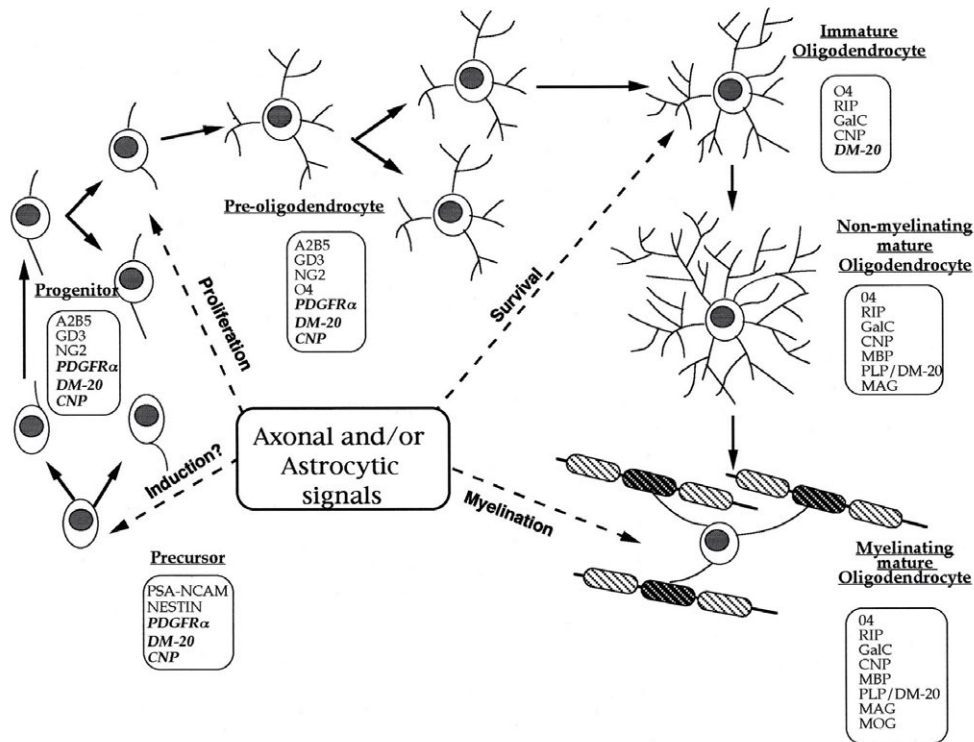
Figure 6. Morphological and molecular changes during oligodendrocyte development. Oligodendrocyte progenitors have bipolar morphology or extend only a few processes and can be detected with markers such as gangliosides (A2B5) and chondroitin sulfate proteoglycan (NG2). These cells are migratory and proliferate, also *in vitro,* in response to specific growth factors and signals. Preoligodendrocytes are multiprocessed cells that have mostly lost their mitogenic response to PDGF and are post-migratory. An immature oligodendrocyte obtains the marker GalC and loses A2B5 antigens. A mature oligodendrocyte expresses markers such as MBP, PLP and myelin and oligodendrocyte glycoprotein (MOG). Adapted from Baumann & Pham-Dinh, 2001, use permitted by the American Physiological Society.

In oligodendrocyte development signals from axons control the timing of progenitor differentiation to ensure correct timing of myelination. In addition, they are important in matching the number of oligodendrocytes to the axons requiring myelination. Trophic factors and growth factors, such as platelet-derived growth factor (PDGF) and fibroblast-derived growth factor (FGF), secreted by neurons and astrocytes regulate oligodendrocyte proliferation and survival. Myelination is influenced by the electrical activity of neurons, possibly through secretion of adenosine from neurons and by indirect signals from astrocytes. At the same time, oligodendrocytic support to neurons is required for axonal protein

clustering at the nodes of Ranvier. Oligodendrocytes also modify the axonal cytoskeleton and transport. (Simons & Trajkovic 2006)

2.1.4 MICROGLIA

Microglia comprise 5-20% of the glial cells in CNS. They derive from the hematopoietic lineage, unlike neurons, astrocytes and oligodendrocytes, which all have a neuroectodermal origin. Microglia are the resident immune cells of the CNS that survey the brain for damage and infection and phagocytose dead cells and debris. Activated microglia are present in most if not all neuropathological conditions, but whether they are helpful or harmful in these conditions remains mostly an open question. (Allen & Barres 2009)

Developmentally, microglial cells enter the brain from the blood circulation early in development, in both embryonic and early postnatal stages. In the CNS microglial precursors proliferate and migrate to populate the CNS. While migrating, microglia differentiate and their early developmental amoeboid phenotype is replaced by the ramified state. Neurons induce and sustain the ramified state by direct signalling, but also astrocytes and epithelial cells affect the change. Even in the ramified state, often misleadingly called the resting state, microglia are highly motile cells constantly extending and withdrawing processes. (Hanisch & Kettenmann 2007; Tambuyzer *et al.* 2009).

The activation of microglia affects their morphology and molecular expression. The gradual changes from ramified, surveying microglia to the activated, alert microglia are characterized by cellular hypertrophy and thickened processes giving the cells a "bushy" appearance (Fig. 7). Under a persisting stimulus, microglia acquire the amoeboid morphology and become fully functional phagocytotic cells that express molecular markers of macrophages. At this stage, there often is another population of macrophage marker expressing cells, the acutely CNS-infiltrated macrophages. These two types of immune cells are both required for the maintenance of CNS integrity. Apart from phagocytosis microglia regulate the immune reaction by releasing immunoregulatory substances. Interleukin-1 (IL-1) and tumor necrosis factor α (TNFα) are major pro-inflammatory cytokines whereas anti-inflammatory cytokines include IL-10, transforming growth factor β (TGFβ) and IL-1 receptor antagonist. (Carson *et al.* 2007; Hanisch & Kettenmann 2007)

Phagocytotic microglia migrate towards the chemotactic stimulus and proliferate at the target. Microglia clear the target cells or debris, such as the remnants of neurons eliminated by developmental apoptosis. Microglia are implicated in synaptic remodelling during the development of the nervous system, since they have been proposed to remove inappropriate synaptic connections through phagocytosis. Microglia are also involved in synaptic remodelling during pathological conditions, by efficiently removing excitatory synapses and so limiting neuronal excitability and glutamate toxicity. This 'synaptic stripping' has been

described in spinal motor neurons but may occur in other regions of the CNS as well. (Eroglu & Barres 2010; Tambuyzer *et al.* 2009).
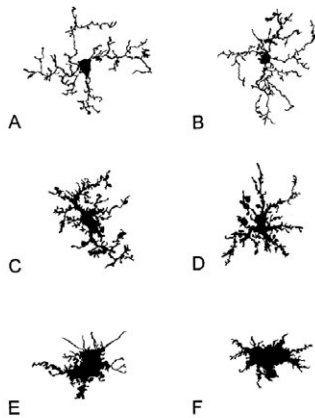
Figure 7. Morphology of the microglia in the rat brain, depicting ramified (A,B), hypertrophied (C,D) and bushy cells (E,F). Reprinted from Sołtys *et al.* 2001, with permission from John Wiley and Sons.

Healthy neurons and possibly other CNS cell types release signals to inhibit microglial activation. When these signals are disrupted, e.g. by blocking the neuronal activity, microglial activation is triggered. Neurotransmitters are proposed to act as such signals. In addition, microglial activation can be induced by factors that are not normally present (viral or bacterial structures) or that show abnormal states (released intracellular components, protein aggregates). (Hanisch & Kettenmann 2007; Tambuyzer *et al.* 2009)

2.1.5 *DROSOPHILA* NEURONS AND GLIA

Similarily to mammals, the fruit fly *Drosophila melanogaster* has sensory neurons, interneurons and motor neurons. The neuronal structure is widely homologous among invertebrates and vertebrates, but differences do exist. . Vertebrate somatosensory neurons are derived from the CNS migratory precursors, are unipolar, and their somata locate to dorsal root ganglia (see section 2.2.1.4) from where their processes grow bidirectionally both towards the CNS and to innervate the periphery. The corresponding *Drosophila* neurons are bi- or multipolar, are born and located in the periphery and grow axons unidirectionally towards the CNS. In addition, vertebrate projection axons are myelinated and located in defined white matter tracts. Comparable axons in *Drosophila* locate to synaptic regions (neuropil) and individual axons lack glial ensheathment (Sanchez-Soriano *et al.* 2007). The structural arrangements of the *Drosophila* CNS are described in section 2.2.2.

Drosophila neurons are usually smaller in size (see Fig. 1) and there are less of them: it has been estimated that the adult *Drosophila* brain consists of 100 000 - 200 000 neurons (Nichols 2006)

while the human brain consists of 10^{11} neurons and mouse brain (C57Bl/6J strain) of 75 000 000 neurons (Kandel *et al.* 2000; Williams 2000). Then number of glial cells is also lower: the *Drosophila* glia constitute 25% of the total brain cells while some estimates point that 65% of the mouse brain cells and 90% of the human brain cells are glial cells (Allen & Barres 2009).

The functional classes of *Drosophila* glia resemble the vertebrate glial classes. Cortex glia, forming close contacts with neuronal cell bodies, the blood-brain barrier and tracheal elements, are very similar to vertebrate astrocytes. The *Drosophila* blood-brain barrier is formed by surface glia that tightly separate neurons and other glia from surrounding hemolymph. Neuropil glia resemble oligodendrocytes since they extend sheathlike membranes around target axons to provide an isolated space for neuronal action potentials and trophic support. *Drosophila* peripheral glia perform these functions in the periphery, similarly to the Schwann cells of vertebrates. Microglia do not appear to have a specific counterpart, but all glial types may perform immune cell-like functions. (Freeman & Doherty 2006)

2.1.6 DIFFERENTIATING BETWEEN THE CELLS OF THE CENTRAL NERVOUS SYSTEM

Cell type and developmental stage-specific morphological and molecular characteristics can be utilized in identifying the cells of the nervous system. Having started this section with Santiago Ramón y Cajal, it is reasonable to end it by crediting Camillo Golgi, who shared the Nobel Prize in 1906 with Ramón y Cajal. Although wrong in his theory of a continuous, fluid exchanging neural network, his staining technique paved the way for Ramón y Cajal's neuroanatomical discoveries.

Histological staining is used for selectively highlighting cells and cellular components. In staining procedures, chemical reactions between chemicals and components within a tissue are utilized. Immunohistochemistry refers to a staining process where antibodies are used for specific recognition of molecules in the material of interest. Many of the molecular characteristics of certain cell types or the developmental status of the cell can be distinguished using the immunohistochemical procedures (see Table 6 in Methods, section 4.2.3).

Apart from differentiating between cell types and cellular components, histological staining is utilized in the study of basic anatomy of the tissue, as well as examining the pathology, that is, regions of damaged tissue. The topics of functional anatomy and pathologies of the CNS are covered in the following sections 2.2 and 2.3.

2.2 ANATOMICAL ORGANIZATION OF THE NERVOUS SYSTEM

Estimated amount of glucose used by an adult human brain each day, expressed in M&Ms: 250.

Harper's Index

Neural pathways including a sensory input, a motor output and the information-integrating interneuron is highly conserved in all animal nervous systems. Very early in evolution, nervous systems were organized to form distinct modules performing different tasks. Early forms of centralized nervous systems consist of a longitudinal nerve cord and an anterior collection of nerve cells, a ganglia or a brain, at the cephalic end of the organism. This structure is found in flatworms (phylum *Platyhelminthes*). A more complex CNS is found in insects (phylum *Arthropoda*), brains of which are divided into regions performing different functions. During vertebrate nervous system evolution, the importance of the cerebral hemispheres and especially the cerebral cortex as the association centre becomes increasingly evident. (Lentz and Erulkar in Encyclopædia Britannica, www.britannica.com)

The peripheral nervous system (PNS) lies outside of the CNS structures, and in vertebrates can be divided into somatic and autonomic peripheral nerves. Somatic division consists of the sensory neurons of dorsal root and cranial ganglia innervating the skin and musculature. Autonomic division controls the smooth muscles and the exocrine glands (Kandel *et al.* 2000).

2.2.1 VERTEBRATE CENTRAL NERVOUS SYSTEM ORGANIZATION

The main regions of the vertebrate CNS include the spinal cord, cerebellum, brain stem (comprised of medulla, pons and midbrain), diencephalon and cerebral hemispheres (Fig. 8). Spinal cord and brain stem function as relays between the CNS and PNS and contain pathways to and from the brain: sensory information is carried via ascending pathways, while the motor commands and regulation runs via descending pathways (see section 2.2.1.3). The thalamus (section 2.2.1.2) and hypothalamus are diencephalic structures. Hypothalamus regulates the autonomic nervous system and, through the pituitary, the hormonal balance of the body. The cerebral hemispheres consist of the cerebral cortex (section 2.2.1.1) and the underlying white matter, the basal ganglia, the hippocampus and the amygdala. The basal ganglia are formed by a group of interconnected nuclei, the striatum (composed of the caudate and putamen), the globus pallidus, the substantia nigra and the subthalamic nucleus and they contribute to movement regulation and cognition. The amygdala and hippocampus are part of the limbic system, which is suggested to process emotional reactions through regulating the autonomic nervous system and endocrine system. Hippocampus is also

involved in memory storage and spatial navigation. The cerebellum integrates motor, somatosensory and vestibular information in order to coordinate the movement. (Kandel *et al.* 2000)
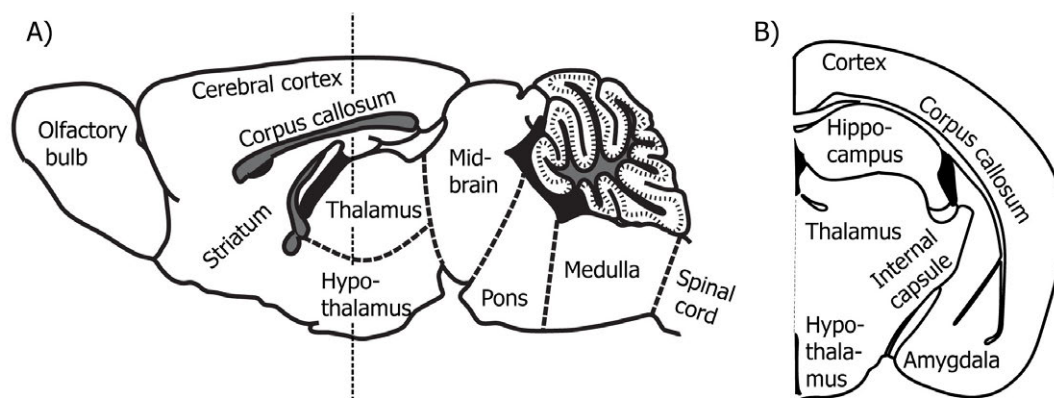
Figure 8. Mouse brain visualized in A) sagittal (cross-section from the midline) and B) coronal section (left hemisphere; the plane of cross-section is shown in A). Some major brain structures and white matter tracts are illustrated. Modified from Paxinos & Franklin 2001.

2.2.1.1 Cerebral cortex

Cerebral cortex is organized into distinct functional areas that have a characteristic pattern of connections. Most of the cortical surface in mouse is involved in sensory and motor information processing (Fig. 9A). Primary sensory cortical areas are the first areas in cortex to receive sensory information from the periphery while the primary motor cortex projects directly to the spinal cord. Higher order sensory cortex integrates information from the primary cortex, while higher order motor areas send processed information to primary motor cortex. (Kandel *et al.* 2000)

Apart from the regional division, the cerebral cortex is organized into six layers (I-VI). Layer I below the pial surface is mainly composed of axons that run laterally and make contacts with the apical dendrites of the lower layer neurons. Layers II and III are composed of pyramidal neurons connecting to other cortical regions making association connections (within the hemisphere) and callosal projections (between hemispheres through the corpus callosum, see section 2.2.1.7). Layer IV neurons receive inputs from the thalamus and send information to projection neurons in layers III, V and VI. Layers V and VI comprise the major sites of outputs from the cortex, layer VI pyramidal neurons connecting to the thalamus and the large layer V pyramidals descending to the basal ganglia, brain stem and spinal cord (Fig. 10B, see also Fig. 3A). Depending on the cortical area, the size of the individual layers varies. Layer IV is thicker in primary sensory areas that receive vast subcortical input while motor cortex layer V is expanded giving rise to descending motor pathways. (Kandel *et al.* 2000)
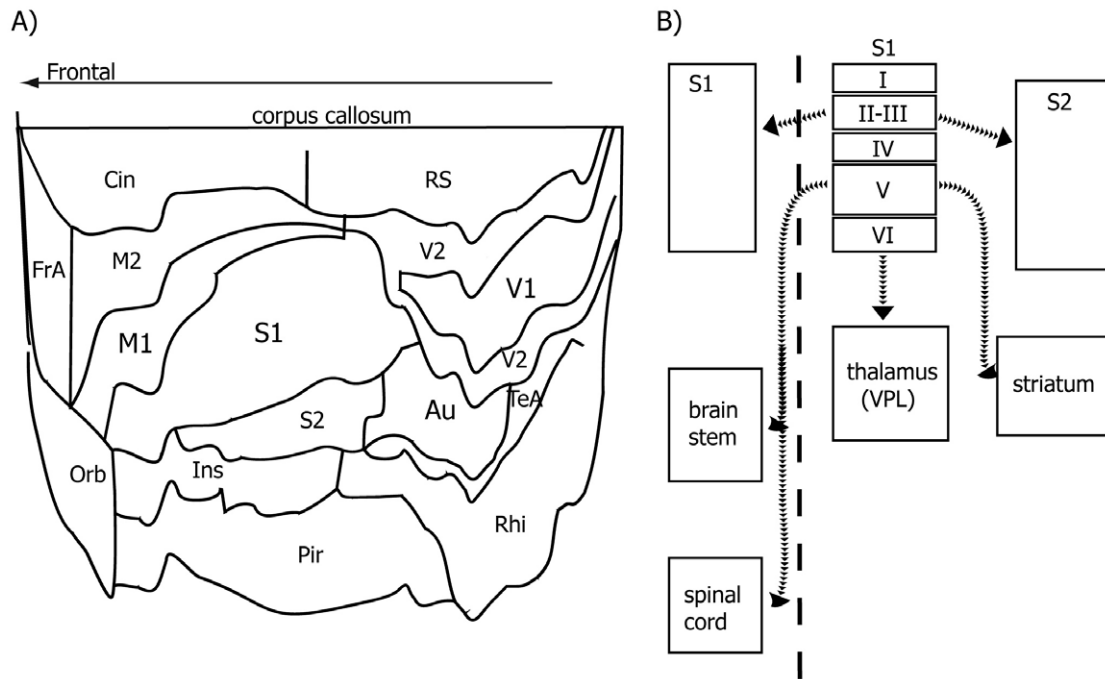
Figure 9. Regional and laminar organization of the cerebral cortex. A) The flattened mouse cerebral cortex shows the proportions of cortical regions, such as the primary sensory regions (somatosensory, S1, visual, V1 and auditory, Au) and primary motor cortex M1. The map is constructed from a full set of mouse coronal sections (see Fig. 8), the top representing the medioventral limit of the cortex (the corpus callossum) of each section. The vertical (y) axis represents distance from the medioventral margin measured around the surface of the cortex. Au, auditory (primary and secondary), Cg, cingulate, FrA, frontal association, Ins, insular, M1, primary motor, M2, secondary motor, Orb, orbital, Pir piriform (olfactory), Rhi, rhinal (entorhinal, ectorinal, perirhinal), S1, primary somatosensory, S2, secondary somatosensory, RS, retrosplenial, TeA, temporal association, V1, primary visual cortex, V2, secondary visual cortex. Modified from (Paxinos & Franklin 2001). B) Cerebral cortex is organized into layers, from which neurons project to distinct areas in the brain. Shown are the subcortical somatosensory projections from layers V and VI, and cortico-cortical connections from layers II and III, boh association connections within the same hemisphere or callosal projections to the other hemisphere. Dashed line presents the midline. VPL, ventral posterior lateral nucleus. Modified from Kandel *et al.* 2000.

2.2.1.2 Thalamus

The thalamus acts as the major relay system of the information passing to the cerebral cortex from other regions of the CNS or from the cerebral cortex itself. Distinct groups of neurons, nuclei, are separated based on the information that they transmit and the connections they make. All sensory information received by other areas of the CNS pass through the thalamus, with the exception of the olfactory afferents. The thalamus also relays motor information from the cerebellum and the basal ganglia to the motor cortex. Thalamic nuclei and their

major inputs and projections are listed in Table 1. (Kandel *et al.* 2000; Sherman & Guillery 2006)

Table 1. Major thalamic nuclei are divided to specific relay nuclei that have well-defined inputs and connections to functionally specific cortical areas. Association nuclei receive most of their inputs from cortex and project to cortical association areas. Modified from Kandel *et al.* 2000.

THALAMIC NUCLEUS	PRINCIPAL INPUT	MAJOR OUTPUTS	INFORMATION RELAYED
Specific relay nuclei			
Ventral posterior	Spinal cord / trigeminal nerve	Somatosensory cortex	Somatosensory
Lateral geniculate	Retina	Visual cortex	Visual
Medial geniculate	Cochlea	Auditory cortex	Auditory
Ventral anterior / ventral lateral	Spinal cord / Globus pallidus / cerebellum	Motor cortex	Motor
Association nuclei			
Anterior group	Hypothalamus	Cingulate gyrus	Limbic
Medial dorsal	Amygdala, hypothalamus	Prefrontal cortex	Limbic
Lateral dorsal	Hypothalamus, Cingulate gyrus	Cingulate gyrus	Emotional expression
Posterior group	Spinal cord, cortical regions	Somatosensory cortex (primary / secondary)	Integration of sensory information
Other			
Midline	Reticular formation, hypothalamus	Basal forebrain	Limbic
Intralaminar	Reticular formation, spinal cord, cerebral cortex	Basal ganglia and cortex	Attention/arousal
Reticular	Cerebral cortex, thalamic nuclei	Thalamic nuclei	Modulation of thalamic activity

2.2.1.3 General organization of the sensory and motor pathways

Separate pathways carry visual, auditory, somatosensory and motor information and can be further divided into specialized pathways, e.g. the somatosensory pathway has distinct subsystems for sensations of pain and light touch. The sensory and motor neural pathways are topographically organized, that is, the spatial relationship of the peripheral receptive/output surface is preserved along the CNS relay systems (Kandel *et al.* 2000). Below is an introduction to the main pathways of somatosensory, visual and motor information carried to/from the cerebral cortex (Fig. 10).

Somatosensory pathways

Ascending somatosensory pathways deliver information from the receptors in the skin, joints and muscles of the trunk and limbs. The main two subdivisions, the medial lemniscal pathway and the anterolateral pathway (Fig. 10), mediate sensations of light touch and of pain and temperature, respectively. In both pathways the first order neuron soma is located in the dorsal root ganglion (DRG), from where it connects to the peripheral sensory receptor. The thalamocortical connection is generated by the third order neuron, which lies in the thalamus and projects its axon to layer IV of the primary somatosensory cortex. The pathways differ mainly in the location and behaviour of the second order neuron. In the medial lemniscal pathway, the soma of the second order neuron is in the nuclei of the medulla, from where its axon crosses the midline and projects to the thalamus. The tract from medulla to thalamus is called the medial lemniscus, from where the name of the pathway derives. The second order neuron of the anterolateral pathway is located in the dorsal horn of the spinal cord, from where it crosses the midline and ascends to synapse in the reticular formation, midbrain or thalamus. The thalamic nuclei innervated by the medial lemniscal pathway are the ventral posterior lateral (VPL) and posterior (Po). Apart from these two nuclei, the anterolateral pathway has intralaminar nuclei connections. (Kandel *et al.* 2000)

Visual pathway

In the retina, the light-sensitive photoreceptor cells synapse with bipolar cells, which then synapse to retinal ganglion cells. The axons of retinal ganglion cells project to the dorsal lateral geniculate nucleus (LGNd) in thalamus, axons from the nasal half of the retina crossing the midline in the optic chiasm. The pathway from LGNd to the primary visual cortex mediates the visual perception. A minor proportion of retinal connections are made to the midbrain and the superior colliculus, which control the papillary reflexes and eye movements, respectively. (Kandel *et al.* 2000)

Corticospinal motor pathway

The corticospinal motor pathway (or pyramidal tract, Fig. 10) is responsible for the execution of voluntary movements. In human brain, half of the corticospinal tract axons originate from

layer V pyramidal neurons of the primary motor cortex. The rest of the axons originate from the supplementary and premotor areas. Regulatory inputs to the motor cortex arrive from the somatosensory and sensory association cortex, thalamus (ventral lateral nucleus), basal ganglia and the cerebellum. The motor cortical axons descend through the white matter structures of internal capsule and cerebral peduncle in the midbrain to pyramids of the medulla. Most of the axons cross the midline in the medulla and reach the lateral column of spinal cord and constitute the lateral corticospinal pathway. Some 10% cross only until they reach the anterior column of the spinal cord (anterior corticospinal pathway). In the ventral horn of the spinal cord, pyramidal axon synapses with the lower motor neuron. (Kandel *et al.* 2000)
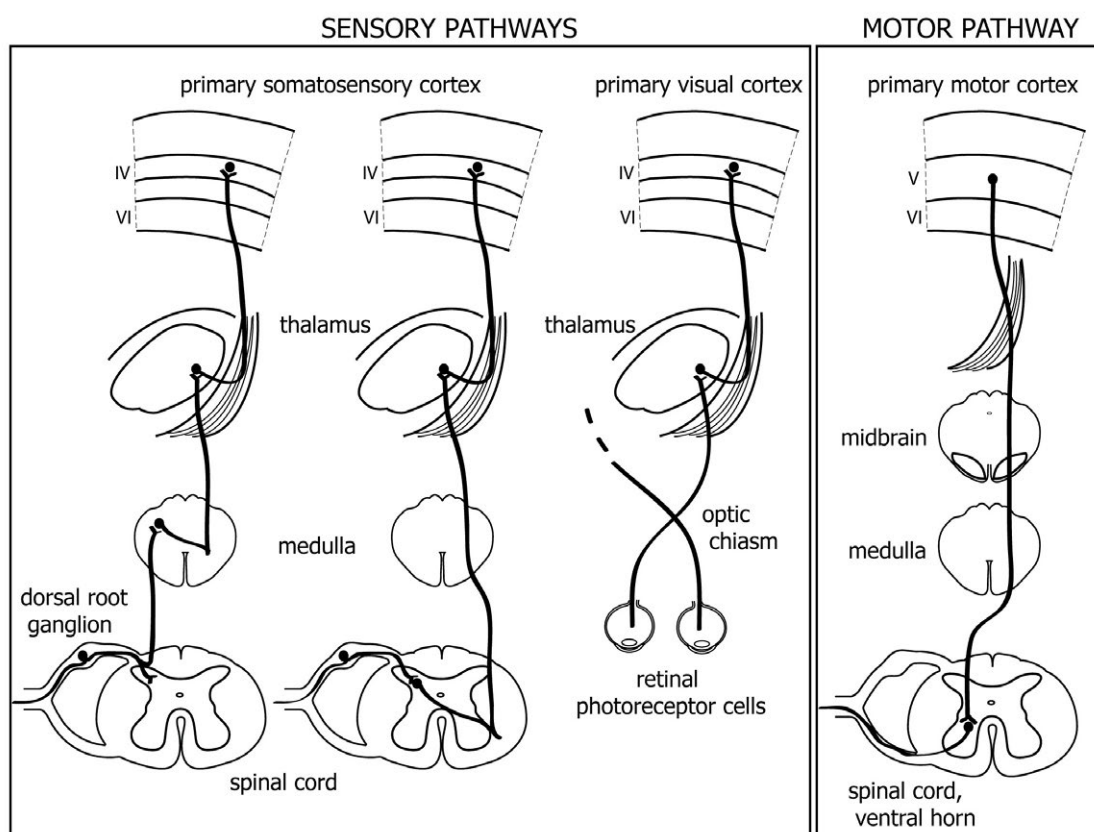
Figure 10. Somatosensory (medial lemniscal pathway on the left, anterolateral pathway on the right) and visual pathways carry information from the sensory receptors to the cortex. Motor pathway delivers motor commands from the cortex to the target muscles. Modified from Kandel *et al.* 2000; Squire *et al.* 2003.

White matter components

The axons in the described neural pathways project long distances and require efficient myelination for efficient conduction velocities. Bundles of these myelinated axons form the projection white matter tracts in CNS. The internal capsule is a white matter structure formed by the tracts to/from the thalamus, cortex and basal ganglia, as well as of the corticospinal

tract for motor information. In the brain stem, the medial lemniscal tract and cerebral peduncle/pyramidal tracts constitute the white matter tracts of somatosensory and motor information, respectively. Commissural tracts, such as the anterior and the posterior commissure and the largest fiber bundle in the brain, the corpus callosum, serve to connect the two cerebral hemispheres.

2.2.2 INVERTEBRATE NERVOUS SYSTEM ORGANIZATION

The *Drosophila* brain includes neural circuits for vision, olfaction, locomotion, and complex behaviors for mating, aggression, circadian rhythms as well as learning and memory. In comparison to vertebrate CNS, many aspects such as neurotransmitter systems are highly conserved. However, many adaptatations are notably different, such as the fly compound eye, introduced in the following section.

2.2.2.1 Basic structure of the adult *Drosophila* visual system

The entire adult *Drosophila* visual system consists of the retina, lamina, medulla, lobula, and lobula plate (Fig. 11 and Fig. 12). Genetic mutations or environmental conditions that alter the precise and repeating structure of the adult eye either in development or aging are relatively simply detected. This has been utilized in the study of human neurodegenerative disorders (see section 2.3.2.2).

The *Drosophila* eye consists of approximately 800 ommatidia (Fig. 11) each containing a cluster of eight photoreceptor cells. Of these, six extend through the retina (R1–6), and the remaining two (R7, R8) locate to the upper and lower halves of each ommatidium. Each photoreceptor contains one rhabdomere, consisting of microvilli that function in light reception. The ommatidia are surrounded by primary and secondary pigment cells, which prevent the off-angle light from entering the photoreceptor system. Overlying the photoreceptors are the cone cells that secrete lens material and the pseudocone and transparent cornea for light focusing (Montell 1999; Wang & Montell 2007), Interactive Fly, http://www.sdbonline.org/fly/aimain/1aahome.htm.)

From each ommatidium, eight photoreceptor axons project to distinct neuropils in the *Drosophila* brain. The R1–6 axons form synapses in the lamina, situated directly below the retina, whereas the R7–8 axons project through the lamina to the medulla. Lamina is linked to medulla and medulla to lobula by two successive chiasmata. Throughout the visual system, neurons are arranged as topographic arrays representing the arrangement of ommatidia. Lobula plate neurons connect the optic lobes of the two hemispheres and the lobula complex neurons project to the central brain. (Wang & Montell 2007), the FlyBrain project, http://flybrain.neurobio.arizona.edu/Flybrain/html/index.html)
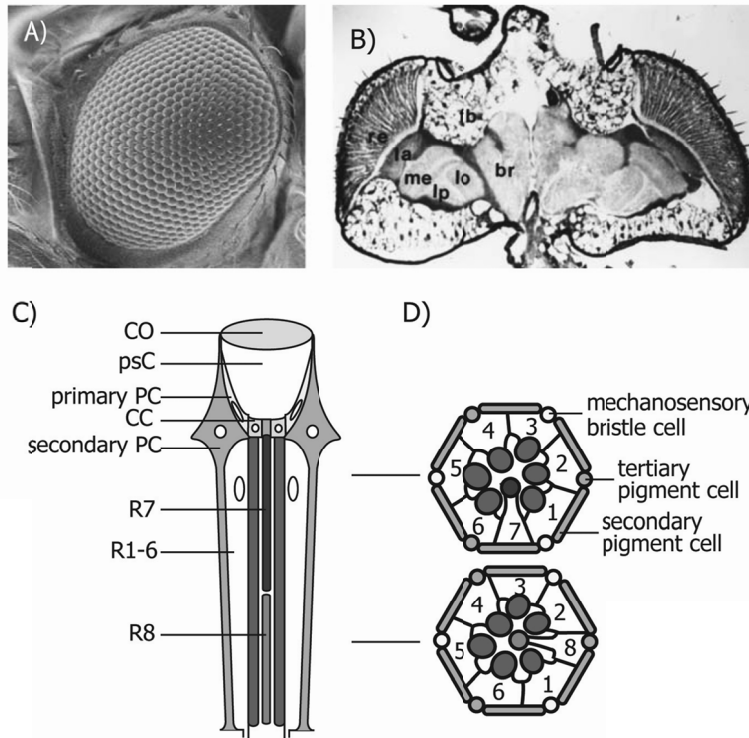
Figure 11. Structure of the adult *Drosophila* compound eye. A) Scanning electron microscopy picture of the *Drosophila* compound eye. B) Coronal section through an adult fly head: br, brain; fb, fat body; la, lamina; lo, lobula; lp, lobula plate; me, medulla; re, retina. C) Sructure of an ommatidium: CO, cornea; psC, pseudocone; PC, pigment cell; CC, cone cell; R1–6, R7, R8, photoreceptor cells 1–8. D) Cross-sections through the distal and proximal regions of the ommatidia. Rhabdomeres are represented with ovals and the photoreceptor (R) cell bodies are numbered 1-8. Reprinted from Wang & Montell 2007, with permission from Springer.

Despite very different architecture the vertebrate and fly eye development and function have molecular similarities. Functional comparisons can be made between ommatidial and vertebrate photoreceptors. The outer segments of vertebrate rods and cones resemble the rhabdomere structure. Both outer R1–6 cells and rods are very light-sensitive, express a single visual pigment, and constitute the majority of photoreceptor cells. The inner R7–8 cells and cones are less sensitive to light but show high-acuity, and express multiple visual pigments. (Montell 1999; Wawersik & Maas 2000)

2.2.2.2 Basic structure of the adult *Drosophila* central brain

The *Drosophila* brain, the neuronal cell bodies and the associated glial cells are arranged in the superficial layers of the brain (cortex), while the interior consists of neuron projections (axonal tracts and synaptic domains) and associated glial processes (neuropil). The major *Drosophila* brain structures are illustrated in Fig. 12.

The protocerebrum is a part of circuits controlling higher order behaviours such as the circuits mediating circadian behaviours. Mushroom bodies are structures within the protocerebrum and are involved in olfactory learning and memory. The central body complex comprises the ellipsoid body and the fan shaped body. These mediate aspects of learning, locomotion, and courtship and are associated with the protocerebrum. The antennal lobes are the first order neuropils in olfactory information processing. Antennal lobe neurons are innervated by the antennal sensory neurons and send projections to the mushroom bodies. Subesophageal ganglion neurons are involved in gustatory information processing. They receive input from taste neurons and mediate feeding behaviors. (Nichols 2006; Rein *et al.* 2002), the FlyBrain project, http://flybrain.neurobio.arizona.edu/Flybrain/html/index.html.)
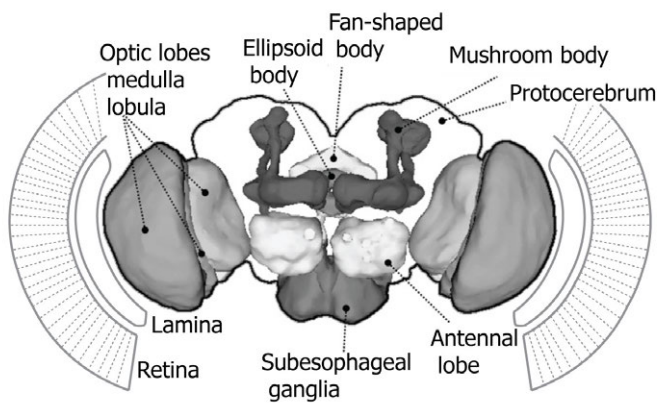

Figure 12. Major structures of the adult *Drosophila* brain. Reprinted and modified from Nichols 2006, with permission from Elsevier.

2.3 PATHOLOGICAL CONDITIONS OF THE NERVOUS SYSTEM

De todas las reacciones posibles ante una injuria, la más hábil y económica es el silencio.

Of all the possible reactions to an insult, the most effective and efficient one is silence.

-Santiago Ramón y Cajal

The American National Institute of Neurological Disorders and Stroke lists over 400 neurological conditions including chronic pain, epilepsy and Alzheimer's disease (http://www.ninds.nih.gov/disorders). Both common and rare forms of these pathological conditions cause disability and suffering for both affected individuals and those close to them.

In the study of human disease, the etiology (the cause of the disease), pathogenesis (mechanism through which the disease develops), nature of the changes and the clinical outcome need to be determined. Causes including insults such as head injury or stroke, infections or inheritance may underlie a human neurological disorder. Inheritance contributes to a variety of developmental, degenerative and cerebrovascular diseases such as hydrocephalus, Parkinson's disease or susceptibility to ischemic stroke.

2.3.1 INHERITED DISORDERS OF THE CNS

Inheritance of a disorder can manifest as a genetic predisposition (complex inheritance) or as monogenic (Mendelian) inheritance, where either one or two mutated copies of a gene can cause the disease. While monogenic diseases may be undervalued due to their rarity, they are valuable as models for complex, more common disease. For example, the rare inherited forms of Alzheimer's and Parkinson disease have been crucial for dissecting the molecular background of these diseases. An interesting entity for genetic research has been the Finnish population. Due to the characteristics of the population history, a group of rare hereditary diseases are overrepresented in Finland and constitute the so-called Finnish disease heritage (Norio 2003b). Importantly, the establishment of the genetic basis of these 36 monogenic disorders has resulted in efficient molecular diagnosis but also provided novel avenues for basic research.

2.3.2 ANIMAL MODELS OF HUMAN CNS DISORDERS

Nobel prize winning research has been performed in experimental animals including the fruit fly *Drosophila melanogaster*, sea snail *Aplysia californica*, roundworm *Caenorhabditis elegans,* chicken

Gallus gallus domesticus and mouse *Mus musculus*. Thus, these model systems have a long research tradition and are extremely well characterized. They can be studied along the whole spectrum of their development, even prior to the manifestation of disease symptoms, which is not normally possible in the humans. Experimental animals can be adjusted for specific needs of the study in question by selecting a suitable strain or characteristic, by manipulating the environmental factors and by genome manipulation techniques.

In human disease modelling, there are two basic approaches for genetic manipulation. The forward genetics or phenotype-driven approach relies on screens for disease phenotypes after induced mutagenesis. Random mutations are generated by radiation, chemicals or by insertional mutagenesis, and the location of the mutation is mapped to find the cause for the interesting phenotype. In the reverse genetics or genotype-driven approach the known gene of interest is manipulated in order to study the phenotypic effects of the mutations. In addition, spontaneously occurring disease in larger animals, especially in dogs and sheep, have proven very advantageous in human disease modelling (Cooper 2010; Gagliardi & Bunnell 2009; Tecott 2003).

2.3.2.1 Mouse

Perhaps the most widely used model system in human genetic disorder research is the mouse. Compared to humans, mice exhibit similar nervous system organization and similar behaviours. Even complex behaviours can be monitored in mice due to well-developed behavioural tests. Almost every human gene has a counterpart in the mouse genome, since 97% of our genes are similar. In addition, mice are particularly suitable for genetic studies because of the availability of genetic manipulation techniques. Well-established methods exist to destroy a functional gene through removing or altering the gene sequence (knock-out mice), to mimic the effect of human mutation by producing a similar mutation in the mouse gene (knock-in mice) and to insert an extra gene into the mouse genome (transgenic mice). Apart from these genetically manipulated mice, the relatively long tradition of induced mutagenesis has resulted in mutations in genes relevant for human disease. (Hafezparast *et al.* 2002; Harper 2010; Tecott 2003)

2.3.2.2 *Drosophila*

The fruit fly *Drosophila melanogaster* has been a powerful genetic tool for over one hundred years and during this time its genome, anatomy, physiology, behaviour and development have been characterized in detail. Its short reproduction cycle together with easy and low-cost maintenance make it an appealing laboratory organism. Through the analysis of naturally occurring and induced mutations a plethora of molecular pathways have been discovered and proven to be evolutionarily conserved. Especially the disease-causing genes appear to be widely conserved, since approximately 75% of human disease genes have homologues in the

Drosophila genome (Bier 2005). Established *Drosophila* models of neurodegenerative diseases suggest that mechanisms of neurodegeneration are well-conserved (Bilen & Bonini 2005; Muqit & Feany 2002).

The power of *Drosophila* genetics is illustrated by the vast number of mutant lines available for research. The largest *Drosophila* strain resource, the Bloomington *Drosophila* Stock Center, lists nearly 50 000 stocks (http://flystocks.bio.indiana.edu/). Targeted gene deletions can be generated through the use of transposable element-based excision strategies (Ryder & Russell 2003). Of particular importance is the ability to express/silence genes in a cell type-specific manner using the UAS-GAL4 system (Brand & Perrimon 1993). A *Drosophila* line carrying the yeast GAL4 transcription activator under the control of a cell or tissue-specific promoter is crossed with another line, where the gene of interest or an RNA interference (RNAi) construct is fused to the yeast upstream activator sequence (UAS). The controlled gene expression or gene silencing effect is observed in the resulting progeny.

The possibility to access molecular pathways relevant to disease pathogenesis has made *Drosophila* disease modelling especially attractive. In genetic modifier screens an established disease phenotype is utilized to search for modifying effects by crossing the mutant to *Drosophila* lines carrying mutations in other genes. In this approach, second-site mutations or genome-wide RNAi libraries can be used for screening the enhancement or suppression of the original phenotype in an unbiased manner. The prerequisite for large-scale screening is a robust phenotype such as the rough-eye phenotype resulting from the degeneration or abnormal development of the adult compound eye structure. In candidate screening a selected set of mutation lines are used in a hypothesis-driven manner. (Marsh & Thompson 2006; Muqit & Feany 2002; Nichols 2006)

2.4 NEURONAL CEROID LIPOFUSCINOSES

Once I was like everybody else

Once I was just like them

Once I could do everything as the others and everything that I enjoyed

Once I could do all that

All that you can do when you can see

Once no longer exists

Once will never return

Once will never ever return

Once is no more

-Ida Bernhardsson (1979-2009)

In 1826, a Norwegian family of healthy parents had suffered a loss of their two eldest children from a disease manifesting with blindness, progressive mental deterioration, loss of speech and epilepsy. The remaining two children had a similar condition, which had started at the age of 6 years with deteriorating vision. The tragedy of this small town family was reported by Dr. Otto Christian Stengel, a physician at the Copper Mining Company of Røros ('Beretning om et maerkeligt Sygdomstilfaelde hos fire Sødskende i Naerheden af Røraas', Eyr et medicinsk Tidskrift, vol. 1, 1826, according to (Haltia 2006)).

In 1896, the American neurologist Bernard Sachs described a disease termed 'Familial Amaurotic Idiocy' with rapid progression of visual loss and mental retardation combined with accumulation of lipid material within swollen neurons. During the following decades further studies by Drs Batten, Vogt, Spielmeyer, Jansky, Bielschowsky, Haltia and Santavuori, among others, lead to the distinction of the neuronal ceroid lipofuscinosis (NCLs) from the disease now known as Tay-Sachs disease. Today, NCLs are defined as 'progressive degenerative diseases of the brain and, in most cases, the retina, in association with intracellular storage of material that is morphologically characterized as ceroid lipofuscin or similar'. Despite over 100 years of research and the vast accumulation of knowledge on genes, proteins and pathways, there is no treatment to cure children with NCL disease. (http://www.ucl.ac.uk/ncl/, Haltia 2006)

In the following sections, the NCL diseases are introduced focussing on the human disease symptoms and classification, together with the recent findings utilizing animal and cellular models. Two forms of NCLs and the corresponding proteins, CLN8 and CLN10/cathepsin

D are introduced more comprehensively (sections 2.4.4 and 2.4.5). The last section (2.4.8) focuses on phenomena that appear to be shared between different forms of NCL.

2.4.1 HUMAN NCL DISEASE

Collectively, the NCLs comprise the most common cause of progressive encephalopathies in children (Haltia 2006). Incidence is estimated to be 1:25 000-50 000 in the USA (according to The National Institute of Neurological Disorders and Stroke) and ranging between 1:25 000 and 1:200 000 in European countries (e.g. Norway, Germany and Italy; Augestad & Flanders 2006; Cardona & Rosati 1995; Claussen *et al.* 1992). The Finnish population is enriched with the infantile (CLN1), juvenile (CLN3), and late infantile (Finnish variant, CLN5) diseases and the progressive epilepsy with mental retardation (EPMR). Their respective incidences are 1:14 000, 1:19 000, 1:59 000 and 1:176 000 (Norio 2003a). Mutation carrier frequencies reach 1:60-1:70 in the whole population (CLN1, CLN3) but can be even higher than 1:50 in certain regions in Finland (CLN5, EPMR) (Kestila *et al.* 2010; Norio 2003a; Ranta *et al.* 1999; Savukoski *et al.* 1998).

Symptoms of NCL disease include epileptic seizures, ataxia, mental and motor regression, myoclonus and/or visual failure. NCL diagnosis is made based on genetic or enzymatic tests from a blood, skin biopsy or saliva sample from the patient. Prerequisite for NCL diagnosis is the existence of intracellular storage material (section 2.4.2.2), which can be studied using electron microscopy on skin or rectal biopsies, or in lymphocytes of a blood sample. Light microscopy may show the vacuolated lymphocytes typical for the juvenile onset CLN3 disease. Monitoring electroencephalogram (EEG), electroretinogram (ERG), measuring the visual and/or somatosensory evoked potentials (VEPs, SEPs) or performing neuroradiological analyses may assist the diagnosis of certain forms of NCL. (http://www.ucl.ac.uk/ncl/, Kousi *et al.* 2012)

Currently, while a treatment to slow down or reverse the symptoms of NCL remains unavailable, the therapies aim to improve patients' quality of life for as long as possible. Antiepileptic drugs are used to control the seizures. Palliative treatments include managing symptoms such as sleep disturbances, pain and feeding problems. According to the NCL subtype, symptom management may also target motor symptoms through antiparkinsonian drugs and/or physiotherapy and mental symptoms through combination therapy. (http://www.ucl.ac.uk/ncl/)

2.4.2 CLASSIFICATION OF THE NCL DISORDERS

The NCL diseases are classified based on molecular genetic findings, age of onset and the ultrastructural appearance of the storage material. Of the different NCL subtypes, causative

mutations have been reported in ten genes, *PPT1, TPP1, CLN3, DNAJC5, CLN5, CLN6, MFSD8, CLN8, CTSD, GRN* and *ATP13A2* (Table 2).

Table 2. The genetic basis of human NCL disorders.

NCL subtype	Defective gene /protein	Onset	Storage ultrastructure	Reference (genetic)
CLN1	*PPT1* /palmitoyl-protein thioesterase 1	Infancy (10-18 months)	GROD	Vesa *et al.* 1995
CLN2	*TPP1* / tripeptidyl-peptidase 1	Late infancy (2-4 years)	CL	Sleat *et al.* 1997
CLN3	*CLN3* /CLN3	Juvenile (5-10 years)	FP (CL, RL)	The Int. Batten Dis. Consortium 1995
CLN4	*DNAJC5* / DNAJ/HSP40 homolog, subfamily C, member 5	Adult	GROD	Noskova *et al.* 2011
CLN5	*CLN5* / CLN5	Late infancy (4-7 years)	RL, CL, FP	Savukoski *et al.* 1998
CLN6	*CLN6* / CLN6	Late infancy (3-8 years)	RL, CL, FP	Gao *et al.* 2002; Wheeler *et al.* 2002
		Adult	FP, granular	Arsov *et al.* 2011
CLN7	*MFSD8* / major facilitator superfamily domain-containing 8	Late infancy (2-7 years)	RL, FP	Siintola *et al.* 2007
CLN8	*CLN8* / CLN8	Late infancy (2-7 years)	RL, FP, CL	Ranta *et al.* 2004
		EPMR: juvenile (5-10 years)	CL-like, granular	Ranta *et al.* 1999
CLN10	*CTSD* / cathepsin D	At birth (or juvenile)	GROD	Siintola *et al.* 2006; Steinfeld *et al.* 2006
CLN11	*GRN* / granulin	Adult	FP[#]	Smith *et al.* 2012
CLN12	*ATP13A2* / ATPase type 13A2	Juvenile	lamellar[*]	Bras *et al.* 2012

Ultrastructural appearance of the storage material according to (Haltia 2006), except # according to Smith *et al.* 2012 and * according to (Tome *et al.* 1985). GROD, granular osmiophilic deposits; CL, curvilinear profiles; FP, fingerprint bodies; RL, rectilinear profiles.

2.4.2.1 Genetics

The NCLs are primarily classified based on genetic findings. Most NCL subtypes have a predominant clinical picture (depicted in Table 2), e.g. mutations in the *CLN3* gene predominately cause the juvenile onset disease. It is noteworthy, however, that most of the subtypes include variant phenotypes. Mutations in *CLN8* lead to two clearly different NCL diseases, late infantile and protracted forms (section 2.4.4). Apart from this phenotypic divergence, there is phenotypic convergence among the NCLs. The subtypes of late infantile onset NCLs show similar clinical findings but may be caused by mutations in a number of NCL genes. (Kousi *et al.* 2012)

2.4.2.2 Intracellular storage

The key finding in NCL neuropathology is the intracellular autofluorescent storage (Fig. 13). The disease was named after the accumulating material, lipofuscin and ceroid. Lipofuscin relates to normal aging, while ceroid accumulation is seen in pathological conditions including disease, cell stress and malnutrition (Seehafer & Pearce 2006). Lipofuscin and ceroid are fluorescent and positive for periodic acid-Schiff (PAS), Sudan black B and Luxol fast blue (LFB) stains. Storage material is largely composed of protein, which in most NCLs is the subunit c of mitochondrial F_1-F_0-ATP synthase. In certain subtypes, mainly in infantile and congenital disease, the main protein components of the storage material are sphingolipid activator proteins (saposins) A and D. The ultrastructural appearance of the storage material is still important in the NCL classification and diagnosis. Electron microscopic examination reveals storage patterns including curvilinear (late infantile), fingerprint (juvenile), rectilinear (late infantile variants) and granular (infantile) profiles (see Table 1). (Haltia 2003; Kousi *et al.* 2012)
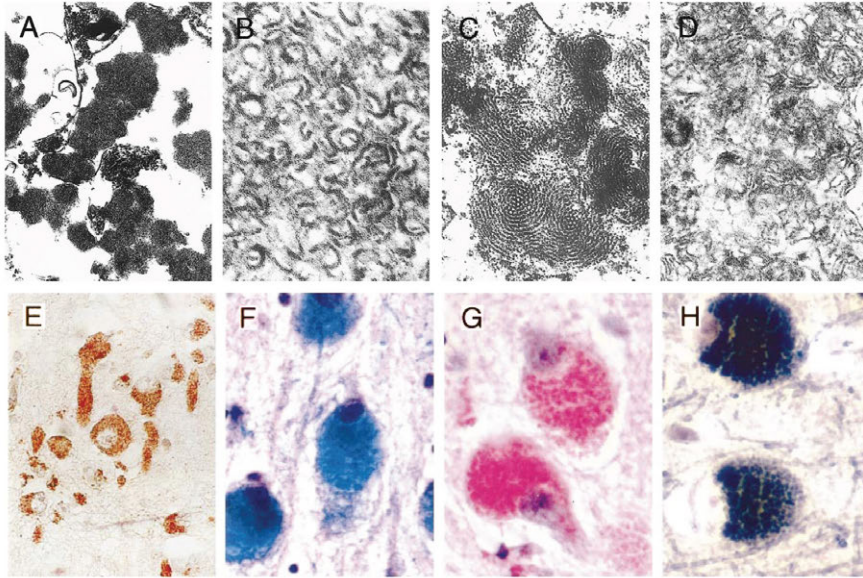
Figure 13. Storage material accumulation in NCL disease. The electron microscopic ultrastructural examination of the storage material shows A) granular osmiophilic deposits typical for CLN1 and CLN10, B) curvilinear profiles common in CLN2, C) fingerprint bodies of CLN3 and D) rectilinear profiles typical for most variant late infantile onset NCLs. In light microscopy, the accumulation of storage material can be visualized with E) immunostaining for subunit c of the mitochondrial ATP synthase (CLN5), F) Luxol fast blue, G) PAS and H) Sudan black B staining. Figures F-H are from CLN8 EPMR patient neurons. Magnifications A) x10000, B) x20000, C) x30000, D) x15000, E) x300, F-H) x1000. Adapted from Haltia 2003, reprinted with permission from Wolters Kluwer Health.

2.4.3 NCL DISEASE IN ANIMALS

NCL disease is not confined to humans but occurs widely in the animal kingdom. Disease has been described to affect various breeds of dogs, sheep and cattle but also affects domestic pig, goat, horse, cat and mouse. The naturally occurring models have been widely used in NCL research, especially prior to the development of techniques for the production of genetically modified mice. Two natural mouse models exist for the CLN8 and CLN6 disease (*Cln8mnd* and *Cln6nclf*, respectively) and both exhibit NCL pathology (Bronson *et al.* 1993; Bronson *et al.* 1998). The large animal models, especially the sheep model, have been widely studied (Cooper 2003).

In addition to the naturally occurring animal disease, various experimental animals have been generated to study NCL disease. The most used model system has been the mouse. The mouse models show a neurodegenerative phenotype with autofluorescent storage and, with few exceptions, ultrastructural appearance and protein components of the storage similar to the corresponding human disease. Loss of vision (see section 5.2.1.2 in Results),

thalamocortical pathology (sections 2.4.7.4, 5.2.1 and 5.2.2) and premature death are common hallmarks of murine NCL. (Jalanko & Braulke 2009)

Apart from mice, the NCL proteins CTSD, PPT1 and CLN3, which are well-conserved in evolution (Table 3), have been studied in *Drosophila*, *C. elegans* and unicellular yeasts *Saccharomyces cerevisiae* and *Schizosaccharomyces pombe*. *Drosophila* models that are deficient for *Ppt1*, *Cln3* and *cathepsin D* (*cathD*) (see sections 2.4.5.4 and 5.1.2.2) show modest neurodegenerative phenotypes and/or reduced lifespans (Hickey *et al.* 2006; Myllykangas *et al.* 2005; Tuxworth *et al.* 2011). The *Ppt1* and *cathD* deficient *Drosophila* also show storage material accumulation (Hickey *et al.* 2006; Myllykangas *et al.* 2005; Tuxworth *et al.* 2011). No obvious NCL phenotype has been detected in *C. elegans* models for CLN1 and CLN3 (de Voer *et al.* 2005; Porter *et al.* 2005). The *S. cerevisiae* and *S. pombe* models have been succesfully used to study the CLN3 homologue Battenin (Btn1p) (Rakheja *et al.* 2008).

2.4.4 CLN8

Two types of human NCL disease are caused by mutations in the *CLN8* gene. Late infantile onset CLN8 is clinically very similar to other late infantile variant NCLs while the progressive epilepsy with mental retardation (EPMR) exhibits a clinically atypical, protracted NCL subtype that so far has not been reported outside of Finland. Although these two diseases represent such different phenotypes, there appears to be no phenotype-genotype correlation in CLN8.

Apart from the naturally occurring *Cln8* mutant mouse, *Cln8^{mnd}*, an NCL phenotype due to a missense mutation in the canine *Cln8* gene has been reported in English Setter dogs (Katz *et al.* 2005). *CLN8* is only conserved in vertebrates although a distantly homologous gene exists in the *Drosophila* genome.

2.4.4.1 CLN8 disease, late infantile

The late infantile onset CLN8 disease begins at 2-7 years of age with seizures, developmental regression and/or motor impairment. Subsequently, myoclonus, cognitive decline, ataxia and impairment of vision and speech appear. Disease progression is rapid and loss of ambulation follows approximately 2 years after disease onset. Most patients with CLN8 late infantile disease have been alive at the time of reporting, with ages up to 18 years, while one patient had died at the age of 10 years (Vantaggiato *et al.* 2009). The disease was first described in a subset of Turkish NCL patients but currently, patients with various origins have been diagnosed with CLN8 disease (Allen *et al.* 2011; Cannelli *et al.* 2006; Kousi *et al.* 2009; Kousi *et al.* 2012; Ranta *et al.* 2004; Reinhardt *et al.* 2010; Vantaggiato *et al.* 2009; Zelnik *et al.* 2007).

Magnetic resonance imaging (MRI) has revealed cerebral and especially cerebellar atrophy, hyperintensity of deep white matter and the posterior limb of the internal capsule (Allen *et al.*

2011; Reinhardt *et al.* 2010; Striano *et al.* 2007; Topcu *et al.* 2004; Vantaggiato *et al.* 2009; Zelnik *et al.* 2007). In addition, hypointensity of the thalamus (Vantaggiato *et al.* 2009) as well as thinning of the corpus callosum (Striano *et al.* 2007) have been described. EEG of these patients is abnormal showing epileptiform activity. Visual impairment and blindness are accompanied by diminished/extinguished ERG and VEPs (Allen *et al.* 2011; Reinhardt *et al.* 2010; Striano *et al.* 2007; Topcu *et al.* 2004; Vantaggiato *et al.* 2009; Zelnik *et al.* 2007). In electron microscopy, the neuronal storage material mainly consists of rectilinear and fingerprint profiles but additional curvilinear profiles and osmiophilic inclusions have been observed (Allen *et al.* 2011; Cannelli *et al.* 2006; Reinhardt *et al.* 2010; Vantaggiato *et al.* 2009; Zelnik *et al.* 2007).

2.4.4.2 CLN8 disease, progressive epilepsy with mental retardation

The EPMR disease, also called as Northern Epilepsy is characterized by childhood-onset epilepsy followed by mental deterioration and was described in families in Kainuu, northeastern Finland (Hirvasniemi *et al.* 1994). Development of the affected children is normal until 5-10 years of age. The disease starts with seizures which are generalized tonic-clonic and, in some patients, complex partial seizures that first occur approximately once every 1-2 months. During puberty, seizure frequency increases to 1-2 seizures per week. Between 2-5 years after the onset of seizures, mental deterioration begins to manifest and progresses rapidly when seizures are most frequent. In adulthood, mental regression continues even when the seizures become more infrequent. Other symptoms include clumsiness in fine motor tasks and imbalance, dysphasic speech and behavioral problems. Visual acuity is decreased in approximately half of the patients but retinal degeneration has not been observed. All patients are moderate to profoundly retarded with IQs below 70 and need assistance in every day life in adulthood. Lifespan appears to be only slightly reduced, with death occurring after the fifth decade of life. (Hirvasniemi *et al.* 1994; Hirvasniemi *et al.* 1995; Ranta & Lehesjoki 2000)

Both magnetic resonance imaging (MRI) and computed tomography (CT) scans show progressive cerebellar and brain stem atrophy and, later in the disease, also cerebral atrophy (Hirvasniemi & Karumo 1994; Lauronen *et al.* 2001). EEG changes are mild until puberty, when slowing of the background activity, disappearance of the sleep patterns and scanty interictal epileptiform activity are obvious. VEPs were abnormal in some patients (Hirvasniemi *et al.* 1995). Neuropathological findings include the typical NCL storage material accumulation comprising of the mitochondrial ATP synthase subunit c and minor amounts of saposins A and D and amyloid β (Herva *et al.* 2000). Ultrastructurally, curvilinear profiles and granular appearance have been observed. However, the overall pathology is relatively mild compared to other NCLs and shows selective distribution. Especially the neocortical layer III

and V neurons and the hippocampal CA2 sector show extensive storage and pathological changes, while other regions remain only mildly affected (Herva *et al.* 2000).

2.4.4.3 CLN8 protein

The *CLN8* gene encodes a predicted 5-7 pass transmembrane protein that resides in the endoplasmic reticulum (ER) and partially in the ER-Golgi intermediate compartment (ERGIC). The protein has a C-terminal ER retention signal (lysine-lysine-arginine-proline, KKRP), the disruption of which causes the protein to be trapped in the Golgi apparatus (Lonka *et al.* 2000). None of the patient mutations studied so far disrupt the subcellular localization of CLN8 (Lonka *et al.* 2000; Vantaggiato *et al.* 2009). However, the pathological mouse mutation c.267–268insC (see section 2.4.4.4) was only found in the ER (Lonka *et al.* 2000). In transfected primary neurons the CLN8 protein is localized to ER, yet in mouse brain the protein fractionates differently from markers of ER and ERGIC (Lonka *et al.* 2004). While some NCL proteins show axonal and/or synaptic localization in neurons, this appears not to be the case for CLN8 (Lonka *et al.* 2004).

CLN8 is homologous to the yeast longevity assurance gene protein (Lag1p) and the translocating chain-associated membrane protein (TRAM) through the possession of a domain named TRAM-Lag1p-CLN8 or TLC (Winter & Ponting 2002). The human and mouse TLC domain family consists of six ceramide synthases (CerSs or longevity assurance, LASS proteins), three TRAMs, CLN8 and six other genes with unknown functions (Pewzner-Jung *et al.* 2006). These multipass transmembrane proteins reside in ER and are well-conserved in evolution (Levy & Futerman 2010). The ceramide synthase properties of TLC proteins were first discovered in yeast, where Lag1 and its paralogue Lac1 have been shown to be essential for the synthesis of very long fatty acid chain ceramides (Guillas *et al.* 2001). However, CLN8 is not likely to act as a ceramide synthase since the human CLN8 failed to rescue the yeast Lag1/Lac1 deficient phenotype, an opposite result to the human CerSs (Guillas *et al.* 2001; Guillas *et al.* 2003). Of the other TLC domain-containing proteins TRAM participates in the regulation of polypeptide translocation into the ER (Hegde *et al.* 1998; Voigt *et al.* 1996) and FAM57A (family with sequence similarity 57 member A) appears to be involved in amino acid transport (He *et al.* 2002).

2.4.4.4 *Motor neuron degeneration* mouse *Cln8^mnd*

The c.267–268insC mutation in the murine *Cln8* gene causes the NCL phenotype of the *Cln8^mnd* mouse (Fig. 14). This spontaneous mutation appeared in an inbred substrain of C57Bl/6, B6.KB2/Rn (Messer & Flaherty 1986). Initial descriptions considered the *motor neuron degeneration* mouse, *mnd,* as a model for amyotrophic lateral sclerosis (ALS). These mice were shown to develop hindlimb weakness and ataxia between 5-11 months of age, leading to severe spastic paralysis of all limbs and premature death (Messer & Flaherty 1986; Messer *et*

al. 1987). Yet the existence of autofluorescent storage inclusions consisting of mitochondrial ATP synthase subunit c with typical ultrastructural appearance indicated that these mice model the NCL disease (Bronson *et al.* 1993; Pardo *et al.* 1994). The mouse *Cln8^{mnd}* mutation was reported alongside the human EPMR mutation (Ranta *et al.* 1999).

Prior to the manifestation of motor deficits the *Cln8^{mnd}* mice show behavioural abnormalities such as increased aggression. Decreased habituation and altered fear-conditioning response indicated that *Cln8^{mnd}* mice display learning and memory related deficits (Bolivar *et al.* 2002). In addition, *Cln8^{mnd}* mice show spontaneous spiking activity in EEG and are susceptible to kainic acid induced seizures (Melo *et al.* 2010). However, retinal degeneration is the first pathological change described in *Cln8^{mnd}* mice. The thinning of retinal cell layers (Fig. 14D) and diminished ERG manifest already before one month of age. Retinal atrophy progresses to loss of the photoreceptor cell layer and degeneration of retinal ganglion cells by 3-4 months of age. ERG is extinguished by 6 months of age. (Chang *et al.* 1994; Guarneri *et al.* 2004; Messer *et al.* 1993).

Many studies have focussed on the pathology of the *Cln8^{mnd}* mouse spinal cord. Neuron loss concomitant with the onset of motor symptoms has been reported (Callahan *et al.* 1991; Gorio *et al.* 1999) while glial activation appears to precede these events (Mennini *et al.* 2004). In spinal cord, glutamate mediated excitotoxity has been proposed as a disease mechanism. The uptake of glutamate but not of GABA is decreased while the levels of ionotropic glutamate receptors are increased (Battaglioli *et al.* 1993; Mennini *et al.* 1998; Mennini *et al.* 2002). Treatments with glutamate receptor antagonists have shown mild beneficial effects on the motor symptom onset (Elger *et al.* 2006; Mennini *et al.* 1999).

Abnormalities in both excitatory and inhibitory neurotransmission have been proposed as disease mechanisms in the *Cln8^{mnd}* brain. Increased glutamatergic transmission has been observed in the hippocampus (Bigini *et al.* 2012), while the hippocampus and cerebral cortex show loss of inhibitory GABAergic interneurons (Cooper *et al.* 1999). Glial activation possibly precedes these changes, which were observed in 9 month old mice, since the hippocampus has been shown to contain activated glia at 5 months of age (Melo *et al.* 2010). Upregulation of TNFα, a microglial-secreted pro-inflammatory cytokine, and its receptors appears concomitantly or precedes the glial activation and may contribute to the neuroinflammation (Galizzi *et al.* 2011; Melo *et al.* 2010). In addition, TNFα has been shown to be upregulated in *Cln8^{mnd}* spinal cords (Ghezzi *et al.* 1998; Mennini *et al.* 2004). Oxidative stress and mitochondrial dysfunction have been suggested to contribute to the pathogenesis (Bertamini *et al.* 2002; Fujita *et al.* 1998; Kolikova *et al.* 2011) and recently, ER stress and unfolded protein response were shown to be activated in *Cln8^{mnd}* mice (Galizzi *et al.* 2011).
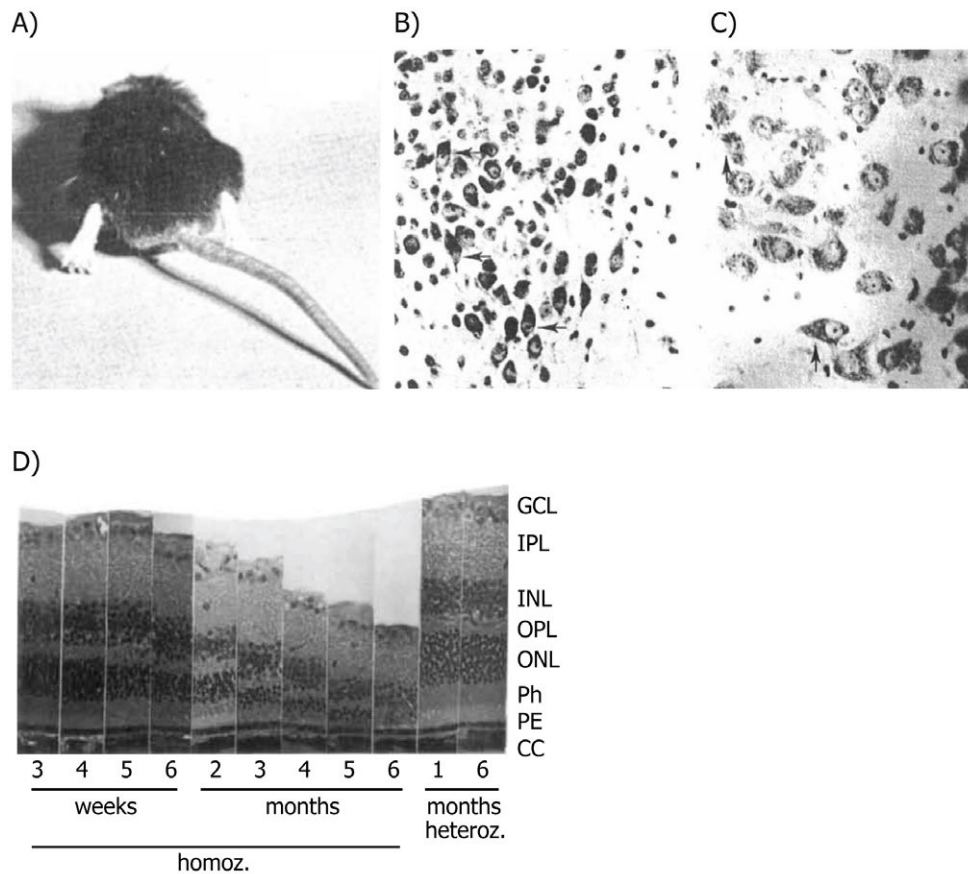
Figure 14. Symptoms of the *Cln8mnd* mouse include A) motor deficits (shown is an attempt to walk uphill) and motor neuron pathology in B) dorsal motor nucleus and C) hypoglossal nucleus of spinal cord. D) Retinal cell layer thinning is observed early. GCL = ganglion cell layer; IPL = inner plexiform layer; INL = inner nuclear layer; OPL = outer plexiform layer; ONL = outer nuclear layer; Ph = photoreceptors; RPE = retinal pigment epithelium; CC = choriocapillaris. Magnifications B and C) x250, D) x400. Adapted from Messer and Flaherty, 1986 (A, B, C) and Chang *et al.* 1994; reprinted with permissions from Informa Healthcare and the Association for Research in Vision and Ophthalmology, respectively.

2.4.5 CLN10/CTSD

The NCL causative mutations in the *CTSD* gene were originally found in sheep, and only recently in humans (Siintola *et al.* 2006; Tyynela *et al.* 2000). Apart from NCL, CTSD has also been connected to other human diseases such as Alzheimer's disease and cancer (Benes *et al.* 2008).

2.4.5.1 CLN10 disease

The earliest onset and most severe type of NCL disease is the congenital CLN10. Affected neonates die within hours to weeks after birth showing respiratory insufficiency and status epilepticus. Microcephaly, reduced brain size and the epileptic seizures have been suggested to start already during fetal development (Fritchie *et al.* 2009; Kousi *et al.* 2012; Sandbank 1968; Siintola *et al.* 2006). To date, only 10 cases of congenital NCL have been reported (Kousi *et al.* 2012). In two of the patients, mutations in *CTSD* have been described, and loss of CTSD protein in brain tissue has been confirmed in three additional patients (Siintola *et al.* 2006; Fritchie *et al.* 2009). Mutations in the *CTSD* gene have also been shown to cause juvenile onset NCL (Steinfeld *et al.* 2006). All *CTSD* mutations have been shown to result in abolished activity of CTSD enzyme (Fritchie *et al.* 2009; Kousi *et al.* 2012; Siintola *et al.* 2006; Steinfeld *et al.* 2006).

2.4.5.2 CTSD protein

The CTSD protein is a lysosomal aspartic protease. It mediates protein degradation, protease precursor activation and the processing of enzyme activators or inhibitors. CTSD has been suggested to process hormones, growth factors and antigens and to have a role in the regulation of apoptosis and plasma high density lipoprotein (HDL) cholesterol levels (reviewed in Benes *et al.* 2008).

CTSD is synthesized as an inactive prepro-enzyme, which is posttranslationally processed to the active form during transport from ER via trans-Golgi network and late endosomes to lysosomes. The mature CTSD has a pH optimum of 3-4 and prefers peptide bonds flanked by hydrophobic amino acid residues. *In vitro*, its enzymatic activity can be specifically inhibited by pepstatin A, and it has been suggested to be activated by ceramide and prosaposin, the precursor protein for saposins A, B, C and D (Heinrich *et al.* 1999; Heinrich *et al.* 2000). Interestingly, *in vitro* substrates of CTSD include the saposins A-D, of which A and D accumulate in the human and sheep CLN10 disease (Benes *et al.* 2008; Gopalakrishnan *et al.* 2004; Haidar *et al.* 2006). CTSD has been suggested to process amyloid precursor protein, apolipoprotein E (apoE) and tau, and thus be involved with Alzheimer's disease. Non-enzymatic functions have been suggested in cancer progression, since secreted pro-CTSD has mitogenic and growth factor-like properties on cancer cells (Benes *et al.* 2008; Liaudet-Coopman *et al.* 2006).

2.4.5.3 CLN10 disease in animals

Mutations in *CTSD* were first shown to cause a congenital NCL in the White Swedish Landrace sheep. The newborn lambs presented with weakness, tremor and death within a few days after birth. In autopsy, overt brain atrophy with abundant accumulation of neuronal

storage was detected. This disease was found to be due to a mutation in the *Ctsd* gene and an inactive CTSD enzyme. (Tyynela *et al.* 2000)

Ctsd deficient (*Ctsd*$^{-/-}$) mice were generated by disrupting the *Ctsd* open reading frame by the deletion of *Ctsd* exon 4 (Saftig *et al.* 1995). *Ctsd*$^{-/-}$ mice are apparently normal at birth but after two weeks severe neurodegenerative symptoms appear as epileptic seizures, tremor, muscle rigidity and blindness. In addition, the mice exhibit progressive pathology of the intestinal mucosa, loss of lymphoid cells of the spleen and thymus and death at the age of 25-27 days in a state of anorexia. CTSD enzymatic activity is abolished but increased levels and activity of lysosomal enzymes including cathepsin B (CTSB) and TPP1 have been described. Ultrastructurally, the *Ctsd*$^{-/-}$ intracellular storage resembles the human storage (granular osmiophilic deposits), but the main protein component is the mitochondrial ATP synthase subunit c instead of saposins A and D that accumulate in humans and sheep. Neuropathology is characterized by neuronal loss and glial activation in cerebral cortex and thalamus. (Jalanko & Braulke 2009; Koike *et al.* 2000; Koike *et al.* 2003; Partanen *et al.* 2008; Saftig *et al.* 1995)

In American bulldogs, a *CTSD* mutation and the consequently reduced enzymatic activity lead to young-adult onset NCL disease with ataxia, psychomotor retardation and premature death, but no loss of vision has been detected (Awano *et al.* 2006; Evans *et al.* 2005). Recently generated *ctsd* knockdown zebrafish shows disturbed eye and swim bladder development and reduced lifespan, but no lipofuscin storage was detected (Follo *et al.* 2011).

2.4.5.4 *Cathepsin D* deficient *Drosophila, cathD^1*

The *Drosophila cathepsin D* (*cathD; CG1548*) encodes for a protein which is 50% identical and 65% similar to the human CTSD. The *cathD* deficient *Drosophila* was generated through an imprecise excision of the transposable element EP2151 located 77bp upstream of the *cathD* open reading frame. In the resulting *cathD^1* mutant line more than 70% of the *cathD* coding sequence is lost and the mRNA expression of *cathD* is abolished. Development and lifespan are normal in *cathD^1* flies but they show modest late-onset neurodegeneration, observed through increased numbers of apoptotic nuclei in the 45-day-old *cathD^1* brain (Fig. 15). The typical NCL pathology was revealed by the progressive accumulation of autofluorescent and PAS/LFB positive storage material in neurons. Additionally, storage ultrastructure resembling the human infantile and human/ovine congenital NCL storage was observed. (Myllykangas *et al.* 2005)
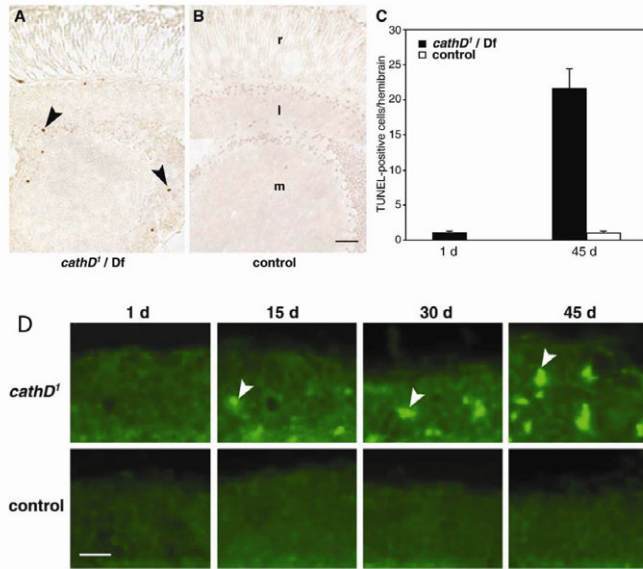
Fig. 15. *Cathepsin D* deficiency in *Drosophila*. A&B) The 45 day old *cathD* deficient *Drosophila* (A) show increased cell death as compared to the age-matched control fly (B), especially in the visual areas of the brain, where arrowheads point to individual TUNEL positive neurons (r, retina; l, lamina; m, medulla). C) Quantification of cells positive for TUNEL (terminal deoxynucleotidyl transferase dUTP nick end labeling) staining. D) Age-dependent accumulation of autofluorescent storage material in *cathD* deficient *Drosophila* in the cortex of medulla. Scale bars in A&B 15 μm, in D, 5 μm. Df, deficiency. Adapted from Myllykangas *et al.* 2005, reprinted with permission from Elsevier.

2.4.6 OTHER NCL DISEASES

2.4.6.1 Infantile onset NCL

The infantile onset CLN1 disease is caused by mutations in the palmitoyl-protein thioesterase 1 gene, *PPT1*. Disease symptoms usually begin with hyperexcitability, muscular hypotonia and psychomotor regression at 10-18 months of age, followed by seizures and ataxia. Loss of vision, speech and ambulation manifest by the age of 3 years and death occurs between 6-15 years of age (Santavuori *et al.* 2000). *PPT1* encodes a soluble hydrolase that removes thioester-linked fatty acid side chains from proteins. All of the reported *PPT1* mutations result in reduced PPT1 enzyme activity (Kousi *et al.* 2012).

2.4.6.2 Late infantile NCLs

CLN2 disease, classic late infantile, is caused by mutations in the tripeptidyl-peptidase 1, *TPP1*, gene. The disease starts with seizures between the age of 2-4 years and progresses rapidly with visual deterioration, cognitive and motor decline, myoclonus, ataxia and speech decline. Premature death occurs between 6-15 years of age. The majority of the identified *TPP1* mutations cause reduced activity of the lysosomal TPP1 enzyme, which cleaves

tripeptides from the N-terminus of small proteins. (Kousi *et al.* 2012; Santavuori *et al.* 2000; Sleat *et al.* 1997)

CLN5 disease represents one of the variant forms of late infantile disease onset. Previously named Finnish variant late infantile disease, it begins with motor clumsiness, concentration disturbances and learning difficulties at 4-7 years of age, followed by mental and motor decline, myoclonus, epilepsy, ataxia and visual failure. Disease leads to loss of ambulation by the age of 9-13 years and death between 14-36 years of age. The CLN5 protein function is unknown. (Kousi *et al.* 2012; Santavuori *et al.* 2000; Savukoski *et al.* 1998)

CLN6 disease, late infantile variant, is clinically highly similar to CLN2 late infantile disease, yet it shows a delayed onset and slower progression. Epileptic seizures and motor symptoms characterize the disease onset at 3-8 years of age. Mental decline, speech impairment, visual failure, myoclonus and ataxia follow. The disease leads to death in the third decade of life. To date, the function of CLN6 protein remains largely unknown. (Kousi *et al.* 2012; Mole *et al.* 2005)

CLN7 disease, variant late infantile, previously named as the Turkish variant late infantile disease, is caused by mutations in the major facilitator superfamily domain-containing 8*, MFSD8*, gene, encoding a lysosomal transporter (Siintola *et al.* 2007). To date, it has been described in patients of various origins with mostly family-specific mutations (Kousi *et al.* 2012). The disease is phenotypically indistinguishable from the CLN8 late infantile disease described in section 2.4.4.1.

2.4.6.3 Juvenile onset NCLs

The most common form of NCL is CLN3 disease, classic juvenile. In pathological examination vacuolated lymphocytes in the peripheral blood are a characteristic finding. Disease manifests between 5-10 years of age. The progressive visual loss is tin most cases the presenting symptom, followed by epileptic seizures. During the course of disease children show progressive motor disabilities, ataxia and motor decline, and towards the end-stage of the disease behavioral abnormalities including hallucinations develop. Patients die prematurely at an average age of 20-30 years. The most prevalent *CLN3* mutation is c.460-280_677+382del967, resulting in a 1.02 kb deletion in the *CLN3* mRNA. Function of CLN3 is still largely unknown (1995; Kousi *et al.* 2012; Mole *et al.* 2005; Santavuori *et al.* 2000)

A recent study described mutations in the *ATP13A2* gene in a Belgian family with juvenile onset NCL, CLN12 (Bras *et al.* 2012). Mutations in this gene encoding a predicted lysosomal P5-type ATPase have previously been shown to cause juvenile Parkinsonism with dementia, Kufor-Rakeb syndrome (Ramirez *et al.* 2006).

Another juvenile onset NCL disease, CLN9, was described as a separate subclass of NCLs after genetic and enzymatic exclusion of other NCLs and lysosomal storage disorders. To

date, the defective gene remains elusive. The four affected patients, with clinical phenotypes similar to the CLN3 classic juvenile disease, represent two families of Serbian and German origins. (Schulz *et al.* 2006)

2.4.6.4 Adult onset NCLs

Adult onset disease (ANCL) starts usually in the third decade of life and the patients die prematurely, approximately 12 years after disease onset. Visual loss is not typical but intracellular storage material accumulation is observed. The autosomal recessive and autosomal dominant adult onset NCLs present with very similar phenotypes (Haltia 2003). ANCL appears to be genetically very heterogenous. The original CLN number for ANCL, CLN4, has been designated to *DNAJC5* encoding a cysteine string protein were identified in heterozygous state in a subset of families affected with autosomal dominant disease (Benitez *et al.* 2011; Noskova *et al.* 2011; Velinov *et al.* 2012). A subset of patients with the autosomal recessive disease has CLN6 mutations (Arsov *et al.* 2011). Homozygous mutations in granulin (*GRN*) were recently described in two siblings with autosomal recessive adult onset NCL, designated as CLN11.

2.4.7 COMMON THEMES IN NCL PATHOGENESIS

Although genetically heterogeneous, NCLs show largely similar symptoms and storage material accumulation. Thus, the mechanisms leading to disease onset have been hypothesized to be similar. This section briefly introduces phenomena that appear to be shared between different NCL subtypes. The focus is on neuropathological findings and on alterations in lipid metabolism. First, current knowledge on the different NCL proteins is summarized (section 2.4.7.1 and Table 3).

2.4.7.1 Properties of NCL proteins

Most NCL proteins localize to lysosomes, whereas the CLN6 and CLN8 proteins are localized to ER (Table 3). Of soluble lysosomal proteins, PPT1, TPP1 and CTSD are enzymes while the function of CLN5 is unknown. The functions of membrane-bound NCL proteins CLN3, CLN6 and CLN8 remain largely unknown. MFSD8 and ATP13A2 have hypothetical transporter and ATPase functions, respectively, and DNAJC5 regulates the ATPase activity of 70 kDa heat shock proteins (HSP70). Certain NCL proteins have a differential localization in neuronal cells in comparison to non-neuronal cells. For example, PPT1 localizes to lysosomes in non-neuronal cells, but in neurons and in brain the protein is localized to axons and synaptic vesicles (Ahtiainen *et al.* 2003; Lehtovirta *et al.* 2001; Vesa *et al.* 1995)

Table 3. Functions and subcellular localization of NCL proteins.

Defective protein /NCL subtype	Function	Localization	Conservation
enzymes/soluble			
CTSD/CLN10	aspartic protease	lysosomal, secreted	Eukaryota
PPT1/CLN1	hydrolase, cleaves fatty acid side chains of proteins	lysosomal, lipid rafts, synaptic vesicles, axonal	Eukaryota
TPP1/CLN2	hydrolase, cleaves tripeptides from proteins	lysosomal	Vertebrata (+*Magnaporthe grisea*)
CLN5	unknown	lysosomal, axonal	Vertebrata
GRN/CLN11	cell growth regulation	secreted	Vertebrata
membrane proteins			
CLN3	unknown (cytoskeletal, transport, lysosomal acdification?)	lysosomal, endosomal, synaptosomal, lipid rafts	Eukaryota
CLN6	unknown (lysosomal acidification?)	ER	Vertebrata
MFSD8/CLN7	transporter	lysosomal, late endosomal	Vertebrata + Insecta
CLN8	unknown (lipid regulation?)	ER, ERGIC	Vertebrata
DNAJC5/CLN4	component of the synaptic chaperone	synaptic vesicles	Vertebrata + Insecta
ATP13A2/CLN12	P5-type ATPase	lysosomal	Vertebrata

Protein conservation based on HomoloGene, http://www.ncbi.nlm.nih.gov/homologene/, modified from Getty & Pearce 2011. *Magnaporthe grisea* = rice blast fungus.

The molecular pathways that are disrupted in NCL disease are mostly unknown. NCL proteins have been suggested to operate in a common pathway (Jalanko & Braulke 2009). Indeed, many of the NCL proteins interact or modulate each other (Lyly *et al.* 2008; Persaud-Sawin *et al.* 2007; Schulz *et al.* 2006; Vesa *et al.* 2002) and may have overlapping interactomes

(Lyly *et al.* 2008). While different NCL proteins may also affect distinct pathways, these pathways ultimately converge to result in lysosomal dysfunction and storage.

2.4.7.2 Abnormalities in the regulation of lipid metabolism

Before the storage material in NCLs was determined to be composed mainly of protein (Palmer *et al.* 1986; Palmer *et al.* 1989; Tyynela *et al.* 1993), many biochemical studies focussed on lipids. More recently, interest towards the involvement of lipid metabolism dysregulation in NCL pathogenesis has re-emerged mostly through the use of large-scale lipid and gene expression analyses in cellular and animal models. Alterations in all major lipid classes, sphingolipids, phospholipids and cholesterol, have been reported (Jalanko *et al.* 2006). In addition, through bioinformatics approaches amino acid sequence similarities have indicated putative roles for the CLN8 and CLN3 proteins in lipid metabolism regulation (Narayan *et al.* 2006; Winter & Ponting 2002).

CLN8

The TLC domain in the CNL8 sequence together with the subcellular localization of the protein indicate a role for CLN8 in lipid synthesis and/or transport of lipids between the ER and Golgi (Lonka *et al.* 2000; Winter & Ponting 2002). These hypotheses received further support through a large-scale lipid analysis of EPMR patient cerebral samples. The liquid chromatographic and mass spectrometric analyses revealed abnormal sphingo- and phospholipid levels depending on the disease stage (Hermansson *et al.* 2005). A patient with progressing disease showed reduced levels of ceramide, galactosyl- and lactosylceramide and sphingomyelin and the phospholipid plasmalogen. Accumulation of these lipids was observed in the advanced stage of the disease (Hermansson *et al.* 2005). CLN8 has been proposed to bind the sphingolipids GalC and ceramide in a lipid-protein binding assay performed in *Cln8mnd* mouse fibroblasts (Rusyn *et al.* 2008). In addition, mitochondria-associated ER-membranes extracted from *Cln8mnd* mouse liver were shown to have abnormal properties and defects in enzymes involved in phospholipid synthesis and trafficking (Vance *et al.* 1997).

CLN10/CTSD

CTSD has also been linked to metabolism since it is proposed to participate in the regulation of lipid trafficking and degradation. CTSD is proposed to control intracellular cholesterol levels by regulating apolipoprotein A-I (apoA-I) mediated lipid efflux. The inhibition of CTSD in human macrophages is associated with reduced expression and mislocalization of ATP-binding casette transporter A1 (ABCA1), which mediates cholesterol and phospholipid efflux to apolipoproteins apoA-I and apoE (Haidar *et al.* 2006). As a result, accumulation of free cholesterol was observed in late endosomes/lysosomes (Haidar *et al.* 2006). Parallel findings have been reported in the *Ctsd$^{-/-}$* mouse, with reduced ABCA1 protein levels and accumulation of cholesterol esters (Mutka *et al.* 2010).

CTSD is involved in the proteolytic maturation of prosaposin into active saposins A, B, C and D, which are required for sphingolipid degradation (Gopalakrishnan *et al.* 2004). In *Ctsd⁻/⁻* the amount of prosaposin is increased, suggesting reduced amounts of active saposins (Jabs *et al.* 2008) while the overexpression of CTSD leads to increased amounts of both prosaposin and processed saposins (Haidar *et al.* 2006). Thus, impaired lipid degradation may cause the observed accumulation of bis(monoacylglycero)phosphate (BMP) and gangliosides GM2 and GM3 in the symptomatic *Ctsd⁻/⁻* mouse brains (Jabs *et al.* 2008) and the accumulation of glycosphingolipids when CTSD is inhibited in human macrophages (Haidar *et al.* 2006).

Other NCLs

Apart from CTSD, at least PPT1 and CLN5 appear to be involved in the regulation of cholesterol metabolism. In primary neurons extracted from the *Ppt1ᐞᵉˣ⁴* mouse, altered expression of cholesterol biosynthesis related genes was accompanied with upregulated cholesterol biosynthesis (Ahtiainen *et al.* 2007). However, total cholesterol was unchanged in these neurons and in *Ppt1ᐞᵉˣ⁴* mouse brain (Ahtiainen *et al.* 2007). Increased neuronal apolipoprotein uptake suggested disturbed apolipoprotein metabolism (Lyly *et al.* 2008). Decreased amounts of large high density lipoprotein (HDL) particles and phospholipid transfer protein (PLTP) were observed in *Ppt1ᐞᵉˣ⁴* serum (Lyly *et al.* 2008). CLN5 deficiency appears to present with an opposite effect, since increased levels of serum cholesterol and PLTP were observed in *Cln5⁻/⁻* mice, together with increased apoA-I mediated cholesterol efflux from macrophages (Schmiedt *et al.* 2012). The CLN6 pathogenesis may also relate to cholesterol homeostasis since the CLN6 deficient fibroblasts show alterations in cholesterol precursor related genes and accumulate free cholesterol in lysosomes (Teixeira *et al.* 2006).

Many NCL proteins have been suggested to associate with lipid rafts, the sphingolipid and cholesterol rich plasma membrane microdomains proposed to be involved in membrane trafficking and signal transduction (Simons & Ikonen 1997). PPT1 (Goswami *et al.* 2005) and CLN3 (Hobert & Dawson 2007; Rakheja *et al.* 2004; Rusyn *et al.* 2008) have been proposed to regulate lipid raft properties such as glycosphingolipid content and transport. Glycosphingolipid transport defects were also observed in *Cln5⁻/⁻* mouse macrophages and fibroblasts (Schmiedt *et al.* 2012). Similarly with the *Ctsd⁻/⁻* mouse, accumulation of gangliosides has been observed in CLN6 patient fibroblasts and the mouse model (Jabs *et al.* 2008; Teixeira *et al.* 2006). CLN9, although the gene itself remains uncharacterized, has been suggested to act as a regulator of dihydroceramide synthase based on the properties of patient fibroblasts (Schulz *et al.* 2006).

The phospholipid species distribution has been shown to be altered in human CLN1 brain samples (Kakela *et al.* 2003) while only minor changes in phospholipid composition were observed in CLN2 patient fibroblasts (Granier *et al.* 2000) and in CLN3 patient brains (Kakela

et al. 2003). The levels of CLN3 and the phospolipid BMP appear to correlate, since BMP is reduced in patient fibroblasts and increased when CLN3 is overexpressed (Hobert & Dawson 2007). In addition, the yeast CLN3 homologue BTN1 has been shown to regulate phospholipid levels and their intracellular transport (Padilla-Lopez *et al.* 2012).

2.4.7.3 Selective neuropathological changes especially in thalamocortical pathways

NCL neuropathology is characterized by neuron loss that specifically affects distinct regions and neuron types of the brain. In general, neuron loss is preceded by gradual reactive changes in astrocytes and microglia. While most of these studies have been conducted using animal models, largely similar observations have been made in human post-mortem material. (Cooper *et al.* 2006; Cooper 2010)

Neuron types that appear selectively vulnerable in NCL pathology are inhibitory interneurons and thalamocortical relay neurons. The pathology of hippocampal and cortical GABAergic interneurons has been described in CLN1, CLN3, CLN5 and CLN8 mouse models and in CLN6 sheep (Bible *et al.* 2004; Cooper *et al.* 1999; Jalanko *et al.* 2005; Kopra *et al.* 2004; Oswald *et al.* 2001; Oswald *et al.* 2008; Pontikis *et al.* 2005). Particular effect of NCL disease is shown in the thalamocortical and corticothalamic pathways. Thalamic relay neurons appear to be lost prior to their projection sites in the animal models of most NCL subtypes (Kielar *et al.* 2007; Partanen *et al.* 2008; Pontikis *et al.* 2005; von Schantz *et al.* 2009; Weimer *et al.* 2006). This sequence is reversed in the *Cln5⁻/⁻* mouse (von Schantz *et al.* 2009). Especially the sensory thalamocortical pathways are affected early in disease progression (Bible *et al.* 2004; Kielar *et al.* 2007; Oswald *et al.* 2005; Partanen *et al.* 2008; von Schantz *et al.* 2009).

The activation of astrocytes and microglia is connected to NCL disease pathogenesis. Astrocytosis has been shown to precede neuron loss in the cerebral cortex, hippocampus, thalamus and cerebellum (Kielar *et al.* 2007; Macauley *et al.* 2009; Partanen *et al.* 2008; Pontikis *et al.* 2004; Pontikis *et al.* 2005; von Schantz *et al.* 2009). In many NCL subtypes, microglial activation follows astrocytosis but early microglial activation is observed in the CLN6 sheep (Kay *et al.* 2006; Oswald *et al.* 2005) and in *Cln5⁻/⁻* mouse (Schmiedt *et al.* 2012). It is not known whether glial response accelerates neurodegeneration or whether it has neuroprotective effects. A recent study in the CLN1 mouse model addressed this question: astrocyte activation was genetically attenuated (*Ppt1⁻/⁻*, *Gfap⁻/⁻*, Vimentin⁻/⁻), resulting in earlier appearing and more rapidly progressing pathology (Macauley *et al.* 2011). This indicates that the reactive astrocytes have at least partially beneficial effects in NCL brains.

3 AIMS OF THE STUDY

This study aimed to determine molecular events contributing to disease progression in the neuronal ceroid lipofuscinosis CLN8 and CLN10. Specific aims were

1) to investigate the genetic interactions and pathways of *cathepsin D* using the *cathepsin D* deficient *Drosophila* model for CLN10 disease, *cathD¹*

2) to characterize the neuropathology and spatio-temporal disease progression in the CLN8 disease model, *Cln8^mnd* mouse, by

2a) determining the sequence of pathological events in the *Cln8^mnd* mouse thalamocortical pathways,

2b) defining the role of white matter defects in the *Cln8^mnd* mouse, implicated by the galactolipid deficiency observed in a large-scale lipid analysis of *Cln8^mnd* brains.

4 MATERIALS AND METHODS

By three methods we may learn wisdom: First, by reflection, which is noblest; second, by imitation, which is easiest; and third by experience, which is the bitterest.

-Confucius

In this chapter, materials and methods utilized in Studies I, II and III are described. Roman numeral indicating the study in question is included in the title of each section.

4.1 MATERIALS

4.1.1 *DROSOPHILA* STRAINS, HUSBANDRY AND CROSSES (I)

The *Drosophila* strains used in this study were obtained from the Bloomington *Drosophila* Stock Center at Indiana University, The Exelixis Collection at the Harvard Medical School and individual research groups (for references, see Table 4). The overexpression lines for *cathepsin B (cathB)* and *cathD* were generated as described in I. The *cathD¹* genotype was verified with two polymerase chain reaction (PCR) setups, one with primers spanning the deletion (product size depends on the *cathD* genotype, see I) and one with primers within the deleted sequence of *cathD¹* (no product when *cathD¹* in homozygous state). Primers used for the latter PCR were F: AAC ATA GAA ATC AAA ATG CAG AAG G and R: GTT CTT GGT GTA GGT CTT CGA CTT (F and R for forward and reverse, respectively).

The stocks of the *Drosophila* strains were maintained at room temperature whereas crosses and aging of the flies were performed at 25°C. Flies were raised on standard media including agar, semolina, malt and yeast.

Table 4. *Drosophila* strains utilized in this study.

Gene name	Human homolog	Fly line	Genotype
cathD	cathepsin D (*CTSD*)	Myllykangas *et al.* 2005	$cathD^1/cathD^1$
		I	$elav\text{-}GAL4/+; cathD^1; UAS\text{-}cathD$
Ceramidase (CDase)	non-lysosomal ceramidase (*ASAH2*)	Acharya *et al.* 2003	$elav\text{-}GAL4/+; cathD^1; UAS\text{-}CDase/+$
CG10992 (cathB)	cathepsin B (*CTSB*)	Bourbon *et al.* 2002	$CG10992^{PG148}/+; cathD^1$
		I	$elav\text{-}GAL4/+; cathD^1; UAS\text{-}cathB/+$
CG17841	- (TLC protein domain containing)	Bourbon *et al.* 2002	$CG17841^{PL94}/+; cathD^1$
HMG Coenzyme A reductase *(Hmgcr)*	HMG-CoA reductase (*HMGCR*)	Tschape *et al.* 2002	$elav\text{-}GAL4/+; cathD^1; UAS\text{-}Clb/+$
Heat shock protein cognate 3 (Hsc70-3)	heat shock 70kDa protein 5 (*HSPA5*)	Bloomington #11815	$Hsc70\text{-}3^{G0102}/+; cathD^1$
Heat shock protein cognate 4 (Hsc70-4)	heat shock 70kDa protein 8 (*HSPA8*)	Bloomington #10286	$cathD^1; Hsc70\text{-}4^{L3929}/+$
Saposin-related (Sap-r)	prosaposin (*PSAP*)	Exelixis Collection	$cathD^1; Sap\text{-}r^{e01294}$
			$cathD^1; Sap\text{-}r^{e01294}/+$
schlank (lag1)	ceramide synthase 5 (*CERS5*)	Bloomington #11665	$lag1^{G0061}/+; cathD^1$
shibire (shi)	dynamin 1 (*DNM1*)	Bloomington #7068	$shi^1/+; cathD^1$
SNF4/AMP-activated protein kinase gamma subunit (loe)	protein kinase, AMP-activated, gamma 2 (*PRKAG2*)	Tschape *et al.* 2002	$cathD^1; SNF4^{loe}/+$
			$elav\text{-}GAL4/+; cathD^1; UAS\text{-}loeI/+$
Superoxide dismutase (Sod)	superoxide dismutase 1, soluble (*SOD1*)	Bloomington #4015	$cathD^1; Sod^{n1}/+$
swiss cheese (sws)	patatin-like phospholipase domain containing 7 (*PNPLA7*)	Exelixis Collection	$sws^{d07605}/+; cathD^1$
Target of rapamycin (Tor)	mechanistic target of rapamycin (*MTOR*)	Bloomington #7012	$elav\text{-}GAL4/+; cathD^1; UAS\text{-}Tor^{WT}/+$
		Bloomington #7013	$elav\text{-}GAL4/+; cathD^1; UAS\text{-}Tor^{TED}/+$
Thioredoxin reductase-1 (Trxr-1)	thioredoxin reductase 2 (*TXNRD2*)	Bloomington #10134	$Trxr\text{-}1^{481}/+; cathD^1$

Table 4 continued. *Drosophila* nomenclature used here is based on FlyBase (www.flybase.org). elav, embryonic lethal abnormal vision.

4.1.2 *Cln8^{mnd}* MOUSE (II, III)

Mouse strain B6.KB2-*Cln8^{mnd}*/MsrJ was obtained from the Jackson Laboratory, backcrossed to C57Bl/6JolaHsd and C57Bl/6JRccHsd and congenity verified as described in II and III. Homozygous *Cln8^{mnd}*/*Cln8^{mnd}* mice (*Cln8^{mnd}*) and their wild-type (wt) littermates were used. The experiments were performed in accordance with good practice of handling laboratory animals and using protocols approved by the ethical boards for animal experimentation of the National Public Health Institute and University of Helsinki, as well as State Provincial Offices of Finland (approval numbers ESLH-2008-00840/Ym-23, STH114A, ESLH-2008-10286/Ym-23, STH967A, ESAVI-2010-04382/Ym-23 and KEK09-061). Mice were housed at the Center for Laboratory Animals, University of Helsinki.

4.1.3 MOUSE PRIMARY CELL CULTURES (III)

Mouse primary neurons, astrocytes and oligodendrocytes were produced as described in III, modified from (Heinonen *et al.* 2000; Pedraza *et al.* 2008). Shortly, the hippocampal / cortical tissue was dissected from mouse embryos of the embryonic day (E) 15.5-17.5 and triturated to one-cell-stage using trypsin (Sigma). For neuron cultures, cells were plated in Neurobasal® Medium supplemented with 1x B-27, 1x GlutaMAX™-I, penicillin (50 U/ml) and streptomycin (50 µg/ml) (all from Gibco). Primary astrocytes were dissected similarly and cultured in DMEM (Dulbecco's Modified Eagle's Medium (DMEM) with 4.5 g/L Glucose, BioWhittaker®) with 10% fetal calf serum (FCS; Promo Cell®), 1x GlutaMAX™-I and antibiotics. Oligodendrocytes were differentiated in DMEM containing 1x B-27 and 3% FCS after the neural progenitor / oligodendrocyte progenitor cell expansion (according to Pedraza *et al.* 2008). Primary cells were differentiated for 7 days as described in III.

4.2 METHODS

Description of the key techniques utilized is presented in this section. Full list of methods is presented in Table 5.

Table 5. Methods used in this study.

Method	Used in
DNA extraction	I
Drosophila crosses	I
Molecular cloning	I
Polymerase chain reaction	I
Histologic processing	I, II, III
Light microscopy	I, II, III
(Immuno)histochemistry	I, II, III
Quantitative PCR	I, III
Reverse transcription	I, III
RNA extraction	I, III
Stereology	II, III
Statistical analysis	II, III
Cell culture	III
Cell proliferation assay	III
Enzyme activity measurement	III
Fractional anisotropy	III
Immunocytochemistry	III
Lipid mass spectrometry	III
Magnetic resonance imaging	III
Transmission electron microscopy	III
Myelin g ratio measurements	III
Western blotting	III
Nerve conduction velocity measurements	Unpublished

4.2.1 HISTOLOGICAL PROCESSING (I, II, III)

Adult *Drosophila* were fixed in 4% formalin at least overnight in +8°C at 1, 10, 20, 30 and 45 days of age. After fixation, flies were transferred to 70% ethanol and embedded in paraffin through a graded ethanol series (service provided by the Institute of Biomedicine/Anatomy,

University of Helsinki). Flies were decapitated and heads embedded in paraffin blocks. Coronal sections of 4 μm thickness were cut and transferred to SuperFrost Plus glass slides (Menzel-Gläser) and dried +37°C overnight.

The *Cln8^{mnd}* mice and their littermate controls were sacrificed at 1, 3, 5 and 8 months of age, when their brains were dissected and fixed in 4% paraformaldehyde in phosphate buffered saline (PBS). The cryoprotection and cryosectioning were performed as described in II. The mouse primary cell cultures were fixed for 15 min in 4% paraformaldehyde solution and stored in PBS +4°C until stained.

4.2.2 HISTOLOGY AND IMMUNOHISTOCHEMISTRY (I, II, III)

The staining methods utilized in this study are listed in Table 6. For *Drosophila* adult heads standard haematoxylin-eosin staining was used. Briefly, it consisted of paraffin elimination through a graded ethanol series, followed by standard haematoxylin-eosin staining and graded ethanol series to xylene. The phenotypic enhancements were estimated in these sections under the 40x objective. Compared to the *cathD^{1}* phenotype, enhancement was considered when more than 10 times vacuoles were present and weak enhancement, if more than 2 times but less than 10 times vacuoles were present.

Mouse brain sections for stereology were mounted onto gelatin-chrome alumin coated glass slides and air-dried. The slides were incubated for 30 minutes at 60°C in Nissl stain solution consisting of 0.05% Cresyl fast violet (VWR)/0.05% acetic acid, rinsed in distilled water, differentiated through a graded series of alcohols and xylene (VWR) and coverslipped with DPX (VWR). In addition, immunohistochemical stainings were performed to detect GFAP, CD68, NeuN, MBP and MOG (II, III). Mouse primary cells were stained as described in III. Details of the antibodies used are given in Table 6.

Table 6. Basis of the histological stains and antibodies used for immunohistology, immunocytochemistry and the immunostaining of protein blots. Antibody dilutions used in experiments are shown here; protocols in full are given in the original publications.

Staining	Basis	Used in
Histological stains		
Haematoxylin-Eosin	Hematoxylin is a basic dye staining nuclei and rough ER due to its affinity to nucleic acids; eosin is an acidic dye staining the cytoplasm.	I
Nissl (crecyl violet)	Stains cell nuclei and rough ER nucleic acids due to its affinity to nucleic acids.	II, III

Table 6 continued.

Staining	Basis	Used in
Immunohistochemistry		
GFAP	Glial fibrillary acidic protein, an astrocytic intermediate filament. Staining is regarded as highly specific for reactive astrocytes (Sofroniew & Vinters 2010). rabbit anti-GFAP, 1:4000, Z0334, DAKO	II
CD68	Cluster of differentiation 68 or macrosialin is a member of the lysosomal-associated membrane protein (LAMP) family expressed by macrophages (Sanchez-Guajardo *et al.* 2010). rat anti-CD68, 1:2000, MCA1957, AbD Serotec	II
NeuN	Neuronal Nuclei, recognizes the neuronal specific protein RBFOX3 (RNA binding protein, fox-1 homolog (C. elegans) 3) (Kim *et al.* 2009). mouse anti-NeuN, 1:1000, MAB377, Millipore	II
MBP	Myelin basic protein is a structural component of myelin and a marker for mature oligodendrocytes (Bradl & Lassmann 2010). rat anti-MBP, 1:500, MAB386, Millipore	III
MOG	Myelin and oligodendrocyte glycoprotein is a marker of differentiated oligodendrocytes (Bradl & Lassmann 2010). rat anti-MOG, 1:200, MAB2439, R&D Systems	III
Immunocytochemistry		
MBP	rat-anti-MBP 1:100, see above.	III
GalC	Galactoceramide is a myelin-enriched lipid and a marker for differentiating pre-oligodendrocyte and mature oligodendrocytes (Bradl & Lassmann 2010). anti-GalC 1:100, MAB142, Millipore	III
A2B5	Stains gangliosides and serves as a marker for oligodendrocyte progenitors and oligodendrocytes in their early-development (Baumann & Pham-Dinh 2001). anti-A2B5 1:200, MAB312, Millipore	III
Olig2	Transcription factor of the oligodendrocytic lineage, which is expressed throughout the oligodendrocyte development but higher in oligodendrocyte progenitors (Bradl & Lassmann 2010). anti-Olig2 1:500, AB9610, Millipore	III
Western blotting		
MBP	rat anti-MBP, 1:250, see above	III
PLP	Proteolipid-protein is a marker for differentiated oligodendrocytes (Bradl & Lassmann 2010). mouse anti-PLP, 1:1000, ab9311, Abcam	III
MOG	rabbit anti-MOG, 1:500, 12690-1-AP, ProteinTech Group	III
NG2	Chondroitin sulphate proteoglycan 4 is a marker for oligodendrocyte progenitors (Bradl & Lassmann 2010). rabbit anti-NG2, 1:500, AB5320, Millipore	III

4.2.3 LIGHT MICROSCOPY (I, II, III)

Immunostained mouse brain sections and adult *Drosophila* sections were observed and imaged using the using Zeiss Axioplan2 microscope, AxioCam HRc camera and AxioVision Release 4.6 software (Carl Zeiss). Images were processed (brightness/contrast, scaling) using the Adobe Photoshop CS4 software (Adobe Systems). Confocal microscope (LSM 510 Meta, Zeiss Inc.) was used for imaging the immunofluorescently stained oligodendrocytes as described in III.

4.2.4 STEREOLOGY (II, III)

A stereological optical dissector was used for the analysis of the neuron number and a Cavalieri estimator for the volumetric analyses. Analysis included 4-6 animals per genotype and age. From the one in six series of the Nissl-stained sections the appropriate anatomical region was defined using the Paxinos and Franklin mouse brain atlas (Paxinos & Franklin 2001) and performed using StereoInvestigator program (MBF Bioscience) as described in II and III. All analyses were performed with no prior knowledge of the genotype of the sample.

4.2.5 ELECTRON MICROSCOPY, G RATIO ANALYSIS (III)

For electron microscopy sample preparation, 1 and 4 month old mice were perfusion fixed with 4% PFA, the brains dissected and post-fixed in 6% glutaraldehyde solution overnight. Samples were cut to appropriate size (approximately 1mm^3) selecting the regions of brain stem and the frontal region of corpus callosum and transferred to phosphate buffer, pH 7.4. Sectioning and staining was provided as a service of the Institute of Biotechnology Electron Microscopy Unit, University of Helsinki. Under the electron microscope a set of representative pictures was taken choosing locations of bundles of myelinated axons. For g ratio analyses these pictures were analysed using the Fiji image analysis package by measuring the length of individual axon diameters versus corresponding fiber diameters as described in III.

4.2.6 MAGNETIC RESONANCE IMAGING, FRACTIONAL ANISOTROPY (III)

MRI was performed as described in detail in III resulting in data sets with and without diffusion weighting (diffusion tensor imaging, DTI). Volumetry for corpus callosum and internal capsule and the corpus callosum thickness were measured from the anatomical images without diffusion weighting. Diffusion tensor images were used from fractional anisotropy analyses. The region of interest (ROI) analysis for white matter structures is explained in III. In addition, a hypothesis free analysis method, track based spatial stastistics, TBSS (Smith *et al.* 2006; Smith *et al.* 2007), was applied to the DTI data set.

4.2.7 LIPID ANALYSES, ENZYME ACTIVITY MEASUREMENTS (III)

Mouse brain samples were homogenized with chloroform/methanol (9:1) and the lipids extracted as described in (Folch *et al.* 1957). Quantification of sphingolipids was performed using a liquid chromatography / mass spectrometry based analysis, as previously described for human EPMR samples (Hermansson *et al.* 2005). Free cholesterol was quantitated according to (Gamble *et al.* 1978).

For CGT enzyme activity measurements, mouse cerebral cortices were homogenized and protein concentrations determined to adjust them to 4 mg/ml (Zoller *et al.* 2005). Samples were incubated with the radioactive substrate, $[^{14}C]$-UDP-galactose (I). Radioactivity detection was performed as described in (Zoller *et al.* 2005).

4.2.8 WESTERN IMMUNOBLOTTING (III)

Mouse brain samples were lysed and prepared for polyacrylamide gel electrophoresis as described in III. Proteins were blotted and detected using immunostaining and either enhanced chemiluminiscence or infrared imaging based methods as described in III.

4.2.9 QUANTITATIVE PCR (I, III)

Total RNA was extracted from cells and tissues using the Qiagen RNeasy mini kit (Qiagen). Complementary DNA (cDNA) synthesis was performed using Moloney murine leukemia virus (MMLV) reverse transcriptase and random hexamers as primers (Promega) using a standard protocol (Joensuu *et al.* 2008). Real-time reverse transcriptase PCR was performed using commercial, mRNA specific primer/probe assays (III) or designed by the PrimerExpress software (Applied Biosystems). The *Drosophila* assays designed for *cathD*, *cathepsin B* (*cathB*) and *glyceraldehyde-3-phosphate dehydrogenase* (*Gapdh*) were as follows: *Gapdh* (F - AGC GCT GGT GCC GAA TAC, R - AGT GAG TGG ATG CCT TGT CGA T, probe - TGG AGT CCA CTG GCG TGT TCA CCA), *cathB* (F - TGC CGT GGA AGC CAT GT, R - CCG AAA AGT GGA AAT TCA CCT T, probe - CGA TCG CGT GTG CAT CCA TTC C), *cathD* (F - CAT CGG TGG TCA GTA TGT GGT T, R - CGC CCA GCA CAA ACT TGA TT, probe - CTT GCG ATC TCA TTC CCA AT TGC C). Probes contained 6-carboxyfluorescein (FAM) and tetramethylrhodamine (TAMRA) fluorophores at their 5' and 3' ends, respectively.

4.2.10 NERVE CONDUCTION MEASUREMENTS (UNPUBLISHED)

One and 4 month old mice (n=6 per genotype per age group) were analysed for peripheral nerve (sciatic) conduction velocity using a protocol modified from (Amadio *et al.* 2006; Haupt

& Stoffel 2004). The mice were anesthetized using 50 mg/kg sodium pentobarbital (Mebunat®, Orion) by intraperitoneal injection. During measurements, the mice were spontaneously breathing and their body temperature was maintained within the physiological range. To limit movement-related artefacts the hind limbs were fixed to a styrofoam base with thin needles.

For recordings of motor evoked potentials a concentric bipolar electrode (Rhodes NE-100) was inserted into the hind paw muscle. The signal was amplified and filtered using standard techniques. Stimulation electrodes (27G needles) were placed into 1) the lumbar spine, close to the emergence of the sciatic nerve roots, and 2) the metatarsal right below the calcaneum. The distance between these sites was measured with a calliper. The electrical stimuli were generated by a constant current stimulator (PSIU6 and Grass S88, Grass Instruments). For stimulation, 0.2 ms impulses with an intensity of 1.5x the motor threshold were used at a rate of 1 Hz.

At least 20 motor evoked potentials were acquired for each analysis. Data sampling was performed with a computer connected to a CED Micro 1401 interface and using Spike 2 software (Cambridge Electronic Design).

4.2.11 STATISTICAL ANALYSIS (II, III)

Results were statistically tested by Student's t-test, two-way analysis of variance (ANOVA) with Bonferroni post-hoc test, or Mann-Whitney U-test, when applicable, using Microsoft Excel and GraphPad Prism program (GraphPad Software Inc.). P values of <0.05 were considered significant.

5 RESULTS AND DISCUSSION

Who could have guessed that the lowly fruit fly might hold the key for decoding heredity? Or that the mouse might one day disclose astonishing evolutionary secrets?

-'Of Flies, Mice, and Men' by François Jacob, from the book description, Amazon.com

5.1 MODULATORS OF CLN10 NEUROPATHOLOGY IN *DROSOPHILA*

The *cathD¹ Drosophila* model for CLN10 disease is characterized by modest neurodegeneration and autofluorescent storage (Myllykangas *et al.* 2005). In this study, late-onset retinal degeneration was observed. In order to find modulators of the *cathD¹* phenotype and possible pathways relevant for CLN10 disease, the *cathD¹* retinal phenotype was utilized for hypothesis-based candidate modifier screening.

5.1.1 RETINAL PATHOLOGY OF *cathD¹ DROSOPHILA* (I)

The neuronal apoptosis in aged (45 days old) flies localizes especially to the brain areas receiving retinal input, the medulla and lamina (Myllykangas *et al.* 2005). Thus, the retinal pathology was further characterized in this study. The 45 days old *cathD¹* retina showed vacuolization (Fig. 2A in I), a finding indicative of cell death and typical for *Drosophila* models of neurodegenerative diseases (Kretzschmar 2009). Compared to many previously described neurodegenerative mutant *Drosophila*, the *cathD¹* retinal vacuolization was rather modest and late appearing. However, it was specific to the *cathD¹* mutation, since the phenotype was rescued by the expression of the *cathD* gene (Fig. 2B in I). This could be established through the use of the UAS-GAL4 system, where elav-GAL4 targeted the UAS-*cathD* expression to neurons and photoreceptor cells (Robinow & White 1988; Robinow & White 1991).

Pathological changes in the retina are consistent with the results from previously described CTSD deficiencies. The *Ctsd⁻/⁻* mouse shows prominent retinal atrophy and apoptotic photoreceptor cell death (Koike *et al.* 2000; Koike *et al.* 2003). In human disease both congenital and juvenile onset CLN10 is characterized by evident retinal atrophy (Brown *et al.* 1954; Steinfeld *et al.* 2006). A significant reduction in CTSD enzymatic activity may be required for the retinal pathology to develop since the CLN10 disease in American bulldogs

with residual CTSD activity does not present with visual impairment (Awano *et al.* 2006; Evans *et al.* 2005).

CTSD has been implicated as the major protease involved in photoreceptor turnover (Rakoczy *et al.* 1996; Regan *et al.* 1980). Retinal pigment epithelial cells are involved in the phagocytosis of photoreceptor debris by their microvilli that penetrate to photoreceptor cell layers (Strauss 2005). The presence of a mutated or inactive CTSD in retinal pigment epithelial cells correlates with the efficacy of photoreceptor clearance both *in vitro* and *in vivo* and affects the survival of these cells in aging mice (Rakoczy *et al.* 1996; Rakoczy *et al.* 1997; Rakoczy *et al.* 2002; Zhang *et al.* 2002; Zhang *et al.* 2005). Furthermore, the recently generated zebrafish model of CTSD deficiency was shown to lack the microvillar structures that are required for the phagocytosis (Follo *et al.* 2011). Since *Drosophila* and vertebrate retinal pigment cells share functional properties (Wang & Montell 2007), retinal degeneration observed in *cathD¹ Drosophila* could be caused by dysfunctional retinal pigment cells.

5.1.2 GENETIC MODIFIER STUDIES IN *cathD¹ DROSOPHILA* (I)

The retinal degenerative phenotype of *cathD¹* was utilized to screen for the effects of candidate modifiers, in order to to link *cathD* to genetic pathways relevant for NCL pathogenesis. Due to the relative mildness of *cathD¹* retinal pathology, only enhancement of the phenotype could be screened for. In addition, the requirement of histological analyses to observe modifications excluded the use of large-scale screening. However, 17 candidate mutant lines (Table 4) were studied representing biological processes previously described to be affected by CTSD deficiency and/or NCL disease (see Table 4 and Table 1 in I). An mRNA expression database FlyAtlas (www.flyatlas.org) was used to confirm the expression of these candidates in *Drosophila* eye. Based on the analysis of the *Drosophila* carrying *cathD¹* together with the candidate modifier mutation, 7 candidate mutants were shown to enhance the *cathD¹* retinal pathology. Here, the results of the screen are discussed focussing on *Drosophila* pathways of lipid metabolism regulation (section 5.1.2.1) and on the common themes found in the modifier screens in different *Drosophila* models for NCL disease (section 5.1.2.2).

5.1.2.1 Genes involved in lipid metabolism

The sphingolipid biosynthetic pathway is well-conserved and most genes in the pathway are shared between *Drosophila* and vertebrates (Acharya & Acharya 2005), Fig. 16. In this study, we focussed on the ceramide synthase *schlank*, a *Drosophila* homologue of the yeast longevity assurance gene, *lag1*. The homozygous lethal *lag1^G0061 Drosophila* line carries a P-element in the 5' coding sequence of the *lag1* gene. *lag1* was shown to act as a ceramide synthase that controls the balance between lipogenesis and lipolysis in *Drosophila* (Bauer *et al.* 2009).

lag1^G0061 enhanced the *cathD^1* degeneration, indicating that reduced ceramide synthesis has a detrimental effect on the *cathD* deficiency.
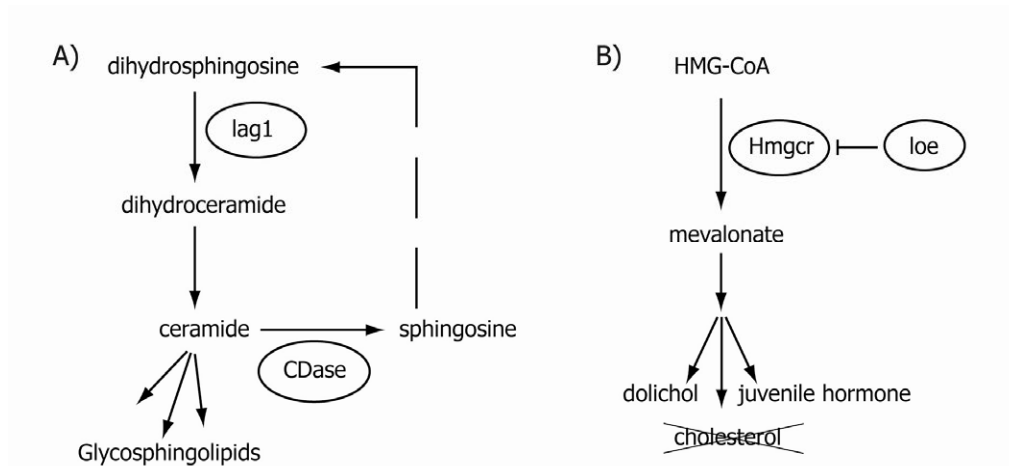

Figure 16. Sphingolipid and mevalonate pathways in *Drosophila*. Pathways are simplified to illustrate the selected candidate genes (circled) and their functions. The sterol branch of the mevalonate pathway is lost in insects. *lag1*, longevity assurance gene homologue; *CDase*, Ceramidase; HMG-CoA, 3-hydroxy-3-methyl-glutaryl coenzyme A; *Hmgcr*, HMG-CoA reductase; *loe*, AMP-activated protein kinase gamma subunit.

Overexpression of the *Drosophila* neutral ceramidase, *CDase*, which converts ceramide to sphingosine, did not have an effect on the retinal phenotype of *cathD^1*. Ceramide has been shown to bind and activate CTSD and affect its targeting, especially when excess ceramide is present (De Stefanis *et al.* 2002; Heinrich *et al.* 1999). However, since we did not test the effect of excess ceramide on the *cathD^1* pathology by overexpressing ceramide synthase *lag1* or deleting the *CDase* activity, this aspect requires further studies in *cathD^1 Drosophila*.

Saposins are involved in glycosphingolipid catabolism and have previously been reported to affect CTSD maturation and transport (Gopalakrishnan *et al.* 2004; Laurent-Matha *et al.* 2002; Zhu & Conner 1994). In addition, CTSD has a role in prosaposin maturation (Hiraiwa *et al.* 1997). Furthermore, saposins A and D are the major protein components of storage in human and ovine CLN10 disease (Siintola *et al.* 2006; Tyynelä *et al.* 2000). Mutated *Drosophila saposin-related*, a homologue of prosaposin, did not enhance retinal degeneration of *cathD^1* either in a heterozygous or homozygous state.

Overexpression of *Drosophila* HMG-CoA reductase homologue, *columbus* (*Hmgcr, clb*), enhanced the *cathD^1* phenotype in our study. The highly conserved HMGCR functions in the mevalonate pathway responsible for sterol and isoprenoid biosynthesis, and it is the primary target of therapies to regulate cholesterol levels (Burg & Espenshade 2011). Indeed, abnormal cholesterol levels and trafficking characterize CTSD deficiency both in mouse and in human macrophages (Haidar *et al.* 2006; Mutka *et al.* 2010). Furthermore, CTSD has been linked to

HMGCR by a study where atorvastatin, an HMGCR inhibitor, was shown to negatively regulate the level of CTSD expression in atherosclerotic plaques (Duran *et al.* 2007).

The *Drosophila* mevalonate pathway does not, however, participate in *de novo* cholesterol synthesis although many genes and regulatory mechanisms are conserved (Gertler *et al.* 1988, Fig. 16). The mevalonate pathway controls the biosynthesis of isoprenoids, which have been shown to act as chemoattractants in migrating germ cells in *Drosophila* (Santos & Lehmann 2004). Mevalonate is a precursor for the insect juvenile hormone, JH (Belles *et al.* 2005). While *cathD¹* does not appear to have a developmental phenotype, these pathways are not obvious mechanisms through which the *Hmgcr* would enhance the *cathD¹* adult-onset degenerative phenotype. It is of note that accumulation of isoprene compounds, dolichols, have been observed in many forms of NCLs (Rider *et al.* 1992). It is possible that the increased production of dolichols by *Hmgcr* overexpression contributes to the enhancement of retinal pathology in *cathD¹*.

The effect of AMP-activated protein kinase subunit γ homologue *löchrig* (*loe*) was selected as a candidate because of its inhibitory action towards *Hmgcr* (Tschape *et al.* 2002, Fig. 16). Since the *Hmgcr* pathway appears to affect the *cathD¹* induced degeneration, introducing extra copies of *loe* could be beneficial to the degeneration of *cathD¹* mutant. Unfortunately, due to not being able to observe suppressive effects to the *cathD¹* phenotype, we were unable to assess this in our study.

These results warrant further studies of the involvement of lipid metabolism regulation in CLN10. Specifically, ceramide synthesis and mevalonate pathway should be studied biochemically and in the *Ctsd⁻/⁻* mouse to clarify their role in CTSD functions and CLN10 disease. While the effects of genetic modifications are more laborious to study in the mouse, a treatment with HMGCR inhibiting statins could be an achievable assay to perform.

5.1.2.2 Common pathways with other NCL proteins?

Drosophila models have been generated for two other NCL diseases, CLN1 and CLN3 (Table 7). The *Drosophila Ppt1* and *Cln3* deficiencies present with NCL-like phenotypes (Hickey *et al.* 2006; Tuxworth *et al.* 2011). In addition, overexpression models have been generated which lead to rough eye phenotypes (Korey & MacDonald 2003; Tuxworth *et al.* 2009; Tuxworth *et al.* 2011). The CLN3 overexpression model also shows Notch-like wing, bristle and macrochaetae phenotype (Tuxworth *et al.* 2009). These models have been used for unbiased, large-scale genetic modifier screening (Table 7). While these screens have been performed in overexpression models, it is of note that our *cathD¹* screen utilized the loss-of-function model and may thus better indicate phenomena relevant for the CLN10 disease.

There are no individual modifier genes that would be shared between the three NCL proteins (Table 7). However, especially *cathD* and *Ppt1* may share genetic pathways of endocytosis/synaptic functions and lipid regulation (Buff *et al.* 2007). Both *Cln3* deficiency and overexpression appear sensitive to oxidative stress (Tuxworth *et al.* 2011) which may be the case for *cathD¹* as well. These pathways are discussed in more detail below.

The fact that *cathepsin B*, *CG10992,* was identified as a weak enhancer of *cathD¹* may indicate a role for cathepsin B in NCL pathogenesis. Interestingly, the Cathepsin B / Cathepsin L double knock-out mouse closely resembles the *Ctsd⁻/⁻* mouse and shows similar storage material accumulation (Koike *et al.* 2005).

Synaptic functions/endocytosis

CTSD is involved in the proteolysis of presynaptic α-synuclein, accumulation of which causes Parkinson's disease through a toxic effect (Cullen *et al.* 2009; Feany & Bender 2000). Aggregates of α-synuclein were found in human, mouse and sheep CLN10 tissue, indicating that α-synuclein toxicity might contribute to CLN10 disease (Cullen *et al.* 2009). These findings were confirmed *in Drosophila*, where enhanced retinal pathology was observed through the expression of human α-synuclein (the *Drosophila* genome itself lacks α-synuclein gene) in the *cathD¹* background (Cullen *et al.* 2009).

In our study mutated *Drosophila* dynamin, *shibire*, enhanced *cathD¹* degeneration. Dynamin/*shi* functions in endocytosis and synaptic vesicle recycling (Robinson 2007; Seto *et al.* 2002; van de Goor *et al.* 1995), yet the enhancement effect may be caused by the disturbed endocytic properties of *shi*. The temperature sensitive mutant *shi¹* used in this study was not activated, and no synaptic phenotype has been suggested for *shi¹* under permissive temperatures (Kawasaki *et al.* 2000; van de Goor *et al.* 1995). The mouse Dynamin 1 mutant also needs to be challenged for the synaptic phenotype, yet endocytic failure was observed without stimulation (Ferguson *et al.* 2007). In addition, *Drosophila shi¹* has been shown to modify the phenotype of *liquid facets*, a *Drosophila* epsin involved in clathrin dependent endocytosis even in permissive temperatures (Cadavid *et al.* 2000), suggesting that the *shi¹* allele may cause an effect combined with other mutations in the shared pathway. Further supporting the importance of endocytic defects in *cathD¹* pathology, *Target of rapamycin*, *Tor*, and *Hsc70-4* were identified as additional modifiers. A genetic interaction between *Tor*, *Hsc70-4* and *shi* has been described in substrate specific endocytic degradation (Hennig *et al.* 2006), a process to which *cathD* could logically connect.

The *Drosophila cathD¹* synaptic phenotype was examined in the 3rd instar larval neuromuscular junction, but the *cathD¹* mutation did not appear to have an obvious effect on the size and distribution of synaptic boutons (unpublished observations, M. Kuronen, R.I. Tuxworth, G. Tear). However, more comprehensive studies are required to determine the synaptic

properties in *cathD¹*, since presymptomatic accumulation of readily releasable synaptic vesicles and decreased frequency of miniature excitatory postsynaptic currents have been observed in *Ctsd⁻/⁻* mice (Koch *et al.* 2011; Partanen *et al.* 2008).

In the *Ppt1⁻/⁻* mouse model of CLN1 disease, abnormal synaptic properties have been observed in the cortical neuron cultures (Virmani *et al.* 2005). Synaptic changes have also been postulated to precede the pathology of these mice (Kielar *et al.* 2009; Kim *et al.* 2008). Indeed, a clear effect of the synaptic/endocytosis related genes to the *Drosophila Ppt1* overexpression phenotype has been observed (Buff *et al.* 2007, Table 7). Interestingly, *DNAJC5/CSPα*, a recent addition to the list of NCL causative genes, could be modelled with *Drosophila cysteine string protein* mutants that cause impaired presynaptic neurotransmission and neurodegeneration (Noskova *et al.* 2011; Umbach *et al.* 1994; Zinsmaier *et al.* 1994). Thus, synaptic pathology is one of the common themes not only between different NCL subtypes but also between different animal models of NCLs.

Oxidative stress

Another such theme may be the sensitivity to oxidative stress, which has been proposed as a mechanism of neurodegeneration in NCL pathogenesis (Wei *et al.* 2008). Antioxidant dietary supplementation has been of slight benefit in human CLN3 patients (Santavuori *et al.* 1989) and the antioxidant therapy with resveratrol has shown beneficial effects in the *Ppt1⁻/⁻* mouse (Wei *et al.* 2011) and in *Cln3* deficient mouse cells (Yoon *et al.* 2011). CTSD has also been linked to oxidative stress induced apoptosis (reviewed in Pivtoraiko *et al.* 2009). The *Drosophila cathD* may also participate to oxidative stress-related pathways, since we found that the mutated *thioredoxin-reductase*, *Trxr-1*, enhanced the *cathD¹* degenerative phenotype. *Trxr-1* and the *Superoxide dismutase (Sod)* / *catalase* constitute the most important defense systems against oxidative damage in *Drosophila* (Missirlis *et al.* 2001). Yet the *cathD¹* phenotype was unaffected by the *Sod* mutation, indicating that the *Trxr-1* pathway is of specific importance in *cathD¹* induced pathology. Oxidative stress related pathways appear also affected in the CLN3 *Drosophila* models. *Sod* and *catalase* overexpression rescued the eye phenotype of *Cln3* overexpressing *Drosophila* (Tuxworth *et al. 2011)*. The lifespan of *Cln3* deficient *Drosophila* was decreased under induced oxidative stress (Tuxworth *et al.* 2011), however, H_2O_2 induced oxidative stress showed no significant effect on the *cathD¹* lifespan (unpublished observations, M. Kuronen, M. Talvitie, L. Myllykangas).

Comparison between the different NCL *Drosophila* models is now possible. The modifier effects observed in one model could be tested in other models to achieve conclusions on the involvement of a genetic pathway for different *Drosophila* NCL genes. As such, assessment of highly conserved synaptic functions and oxidative stress pathways in *Drosophila* would benefit the field of NCLs by possibly generating novel, unbiased molecules for further studies.

Table 7. *Drosophila* models of NCL disease.

Model, phenotype	Modulators, pathways
cathD[1] Modest neurodegeneration, typical NCL storage material accumulation (1)	Endocytosis: *Shi* (I) Chaperone: *Hsc70-4* (I) Lipid metabolism-related: *lag1*, *Hmgcr* (I) Lysosomal: *CG10992 (Cathepsin B)* (I) Oxidative stress: *Trxr-1* (I) Synaptic: α-synuclein (2)
Ppt1 deficiency Modest reduction in lifespan, storage material accumulation (3), defective endocytic trafficking (4)	–
Ppt1 overexpression Rough eye (5)	Synaptic: *endophilin A, blue cheese, synaptotagmin, stoned A, IGF-II mRNA binding protein* (6, 4) Lipid metabolism: *phosphatidylserine decarboxylase, ATP-binding cassette homolog* (6) Chaperone: *Hsc70-3* (6) Zinc transport: *Fear of Intimacy* (4) Phosphorylation: *C-terminal Src kinase* (4) Sumoylation: *Smt3* (4) Bone morphogenetic protein signaling: *Twisted gastrulation* (4)
Cln3^{—1MB1} Modest reduction in lifespan, no storage, hypersensitivity to oxidative stress (7)	–
Cln3 overexpression Rough eye, Notch-like phenotype (7, 8)	JNK pathway: *basket, hemipterous, puckered* (8) Stress responses and apoptosis: *MAP kinase kinase kinase 1, thioredoxin peroxidase (JafRac2), Tollo, falafel, thread* (7) RNA processing and translation regulation: *boule, pumilio, alternative splicing factor (Rox8)* (7), *mago nashi, tsunagi* (8) Notch signaling: *Hairless, E(spl) region transcripts m5 and m7* (7) Neurodegenerative disease-associated genes: *Molybdenum cofactor biosynthesis protein 1* (7) Protein turnover and stability: *cullin-5, septin interacting protein 3, vihar* (7) Vesicle trafficking: *schizo, like-AP180, signal recognition particle 9kD* (7) Cytoskeletal regulation and small GTPase signaling: *tarsal-less, microtubule associated protein 205, Small Protein Effector of Cdc42, klarsicht* (7) Ras signaling: *MAP kinase phosphatase 3, daughter of sevenless, pointed* (7) Transcriptional regulation and chromatin remodeling: *without children, stonewall, jim, jing interacting gene regulatory 1, serendipity β, methyl-CpG-binding like, meiosis I arrest* (7)

Table 7 continued. Phenotypes for different models are summarized, together with the results from genetic modifier studies. References: I, Study I of this thesis, 1) Myllykangas *et al.* 2005, 2) Cullen *et al.* 2009, 3) Hickey *et al.* 2006, 4) Saja *et al.* 2010, 5) Korey & MacDonald, 2003, 6) Buff *et al.* 2007, 7) Tuxworth *et al.* 2011, 8) Tuxworth *et al.* 2009.

5.2 NEUROPATHOLOGY OF THE *Cln8^mnd* MOUSE

The *Cln8^mnd* mouse is characterized with retinal degeneration, behavioural abnormalities and motor deficits that lead to premature death (Bolivar *et al.* 2002; Chang *et al.* 1994; Messer & Flaherty 1986; Messer *et al.* 1987; Messer *et al.* 1993). In this part of the work, the brains of presymptomatic/early symptomatic (1-3 months of age), moderately symptomatic (5 months) and late symptomatic (8 months) *Cln8^mnd* mice were analysed. Observed neuron loss and glial activation is discussed in sections 5.2.1 and 5.2.2. A specific defect in galactolipid content and synthesis was accompanied by a myelination delay that preceded any observed pathological changes in the brains of the *Cln8^mnd* mouse (sections 5.2.3 and 5.2.4). Finally, the sequence of these changes and their possible significance for CLN8 disease are discussed in sections 5.2.5 and 5.2.6.

5.2.1 NEURON LOSS IN SENSORY AND MOTOR PATHWAYS (II, UNPUBL.)

We studied neuron loss in *Cln8^mnd* mouse brains by assessing stereological cell counting methods. Disease progression was analysed in sensory thalamocortical pathways, which have previously been shown to be affected in NCL disease (reviewed in Cooper 2010). Due to the motor neuron degeneration phenotype of the *Cln8^mnd* mouse (Messer *et al.* 1986; 1987) the pathology of the motor cortex was also investigated.

5.2.1.1 Somatosensory thalamocortical pathway is affected first in *Cln8^mnd*

Within the sensory pathways studied, neuron loss showed earliest onset in the *Cln8^mnd* somatosensory thalamocortical pathway (Fig 5 in II). The thalamic ventral posterior complex, VPM/VPL, had lost 20% of neurons at 5 months of age. Similar redution was seen in the somatosensory cortical layers IV and VI that receive thalamic inputs or project to the thalamus. The somatosensory pathway is also affected in other mouse models of NCLs (Kielar *et al.* 2007; Partanen *et al.* 2008; Pontikis *et al.* 2005; von Schantz *et al.* 2009). Abnormal somatosensory evoked potentials (SEPs) in NCL patients further underline the relevance of somatosensory defects in NCL disease (see section 5.2.6).

5.2.1.2 Visual thalamocortical pathway is affected late in comparison to the *Cln8^mnd* retinal pathology

Visual loss is a prominent symptom in most forms of human and animal NCL disease (Jalanko & Braulke 2009). Retinal degeneration, with varying onset and severity, is observed in most NCL mouse models. *Cln8^mnd* photoreceptor loss is evident from postnatal day (P) 15-21 (Messer *et al.* 1993; Seigel *et al.* 2005). ERG shows reduced photoreceptor responses from

2 months onward and becomes undetectable by 6 months (Chang *et al.* 1994). Thus, it is intriguing that in our thalamocortical analysis we found evidence of largely intact visual cortex and thalamus until the late symptomatic, 8 month old *Cln8^{mnd}* mouse (Fig. 9 in II), when 60% of the neurons in LGNd and 20% in visual cortex were lost. This suggests that the visual areas of the *Cln8^{mnd}* brain remain intact for a markedly long period of time after dimimished or lost input signal from the retina.

This sequence of events in the visual pathway distinguishes *Cln8^{mnd}* from previously characterized NCL mouse models (Fig. 17), although absolute comparisons cannot be made e.g. due to the effects of different strain backgrounds. A completely reversed sequence appears in *Cln3^{−/−}* mice where the retina remains functionally intact, as assessed by ERG at 12 months, and shows mild apoptosis only at 18 months (Seigel *et al.* 2002). The optic tract conduction velocity is reduced already at 6 months of age with a concomitant neuron loss in LGNd (Weimer *et al.* 2006). The visual cortex was not assessed in these mice, which carry an exon 1-6 deletion, yet in *Cln3^{−Δex7/8}*, with a deletion of *Cln3* exons 7 and 8, cortical thinning and neuron loss were observed at 12 months of age (Pontikis *et al.* 2005).

Yet another sequence is found in *Ppt1* and *Cln5* deficiency, where the retina and either one of the visual thalamocortical pathway components are affected concomitantly (Fig. 17). The *Ppt1^{−/−}* mice show reduced ERG response from 2 months onwards and significant loss of photoreceptors at 5 months (Griffey *et al.* 2005). Loss of LGNd neurons is evident from 3 months onwards, whereas cortical neuron loss begins at 5 months (Kielar *et al.* 2007). In *Cln5^{−/−}* mice visual cortical neurons are lost from 4 months onwards, but in thalamic LGNd neuron loss was observed only at 12 months (von Schantz *et al.* 2009). In these mice loss of vision occurs at 4-5 months of age, assessed by the forelimb extension test (Kopra *et al.* 2004).

Of other NCL mouse models, *Ctsd^{−/−}* shows retinal thinning at P12 and photoreceptors are nearly abolished by P25, while the mice die at P26±2 (Koike *et al.* 2003). Visual cortical thinning was observed at the end stage of the disease (Partanen *et al.* 2008), however, the visual pathway has not been systematically studied in these mice. The *Cln6^{nclf}* mouse is phenotypically very similar to *Cln8^{mnd}*, although demonstrating slightly delayed pathology (Bronson *et al.* 1998). Retinal cell loss is demonstrated by 4 months of age (Bronson *et al.* 1998), but to date thalamocortical pathology of *Cln6^{nclf}* has not been described.

Apart from the photoreceptor cell loss, which is observed early, the *Cln8^{mnd}* retinal ganglion cells appear to contain storage material as early as from P0 (Seigel *et al.* 2005; Chang *et al.* 1994) and may thus have compromised functions. It is not clear why the retina shows specific sensitivity in *Cln8^{mnd}* disease. *Cln8^{mnd}* retinal pathology has been linked to oxidative stress (Guarneri *et al.* 2004). CLN8 has been linked to many other mechanisms, which may have particular effect in the retina, such as mitochondrial dysfunction or calcium signalling (Bertamini *et al.* 2002; Kolikova *et al.* 2011; Pardo *et al.* 1994).
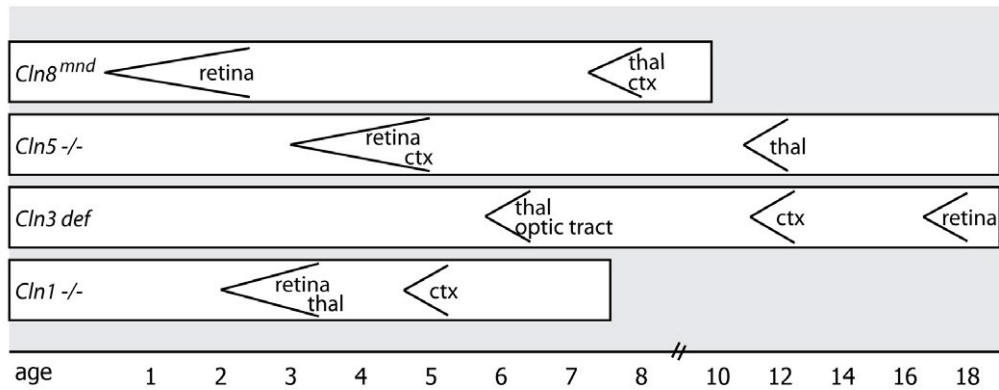
Figure 17. Comparison of the onset of retinal and visual thalamocortical pathology in the mouse models of NCL disease. The X axis represents mouse age in months and the reported lifespan of the models is indicated with boxes (*Cln3* and *Cln5* deficient mice survive beyond 18 months of age). *Ctsd*$^{-/-}$ and *Cln6*^{nclf} mice are not illustrated since the thalamocortical pathology is not well described. thal, thalamus (LGNd); ctx, cortex (V1).

5.2.1.3 Neuron loss progresses more rapidly in the *Cln8*^{mnd} thalamus

The sequence of thalamocortical pathology appears to vary within the NCL mouse models, which is also illustrated by Fig. 17. The thalamus appears to be the primary site of pathology in *Ppt1* and *Cln3* deficiencies, (Griffey *et al.* 2005; Kielar *et al.* 2007; Pontikis *et al.* 2005; Weimer *et al.* 2006) while cortical cell loss appeared first in the *Cln5*$^{-/-}$ mouse (von Schantz *et al.* 2009). In the *Cln8*^{mnd} mouse the thalamic and cortical areas were affected concomitantly, however, neuron loss was more pronounced and progressed more rapidly in the thalamic VPM/VPL and LGNd (Fig. 5 and 9 in II).

Thus it appears that thalamic neurons are more susceptible to NCL-related neuron loss than their cortical counterparts. This may arise from multiple causes. Thalamic neurons may be more sensitive to storage material accumulation, however, all NCL mouse models contain subcellular storage, yet the timing of thalamic pathology is different. The primary defect could be dysfunctional signalling from other regions of the CNS. This hypothesis would be favoured by a CLN3 study, where decreased optic nerve conductivity and LGNd pathology were concomitantly observed (Weimer *et al.* 2006). Since the thalamus is a major relay system in corticocortical pathways, thalamic neuron loss may arise from the dysfunction in cortical signalling. These aspects, such as determining the rate of storage material accumulation in different regions of the brain require further studies in all NCLs.

**5.2.1.4 Primary motor cortex shows late onset neuron loss in *Cln8^mnd*

Since *Cln8^mnd* mice present with the pathology of upper (motor cortical) and lower (spinal cord) motor neurons and progressive motor deficits, it was originally characterized as an ALS model (Messer and Flahety 1986; 1987), see Fig 14. Here, we studied the effect of the *Cln8^mnd* mutation in the primary motor cortex (M1). As with the visual cortex, *Cln8^mnd* motor cortex appears to retain its integrity until the end-stages of the disease, since neuron loss was observed only in 8 month old animals (Fig. 18; unpublished). At this age, approximately 20% of neurons in layers V and VI were lost. Layer V contains the large pyramidal neurons that send their axons to synapse with lower motor neurons in the spinal cord (Kandel *et al.* 2000). This neuron loss indicates diminished potential for motor commands from the cortex when motor symptoms are already evident.
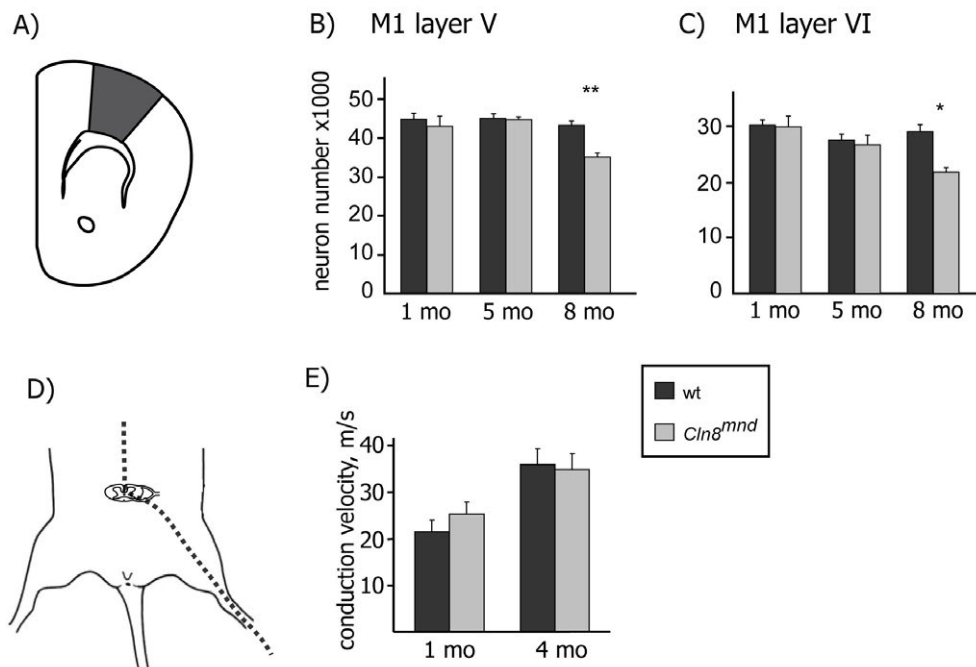
Figure 18. Late-onset neuron loss in the primary motor cortex (M1) of *Cln8^mnd* mouse and no presymptomatic abnormalities in the peripheral nerve conduction. A) Schematic representation of M1 in a bisected coronal section of a mouse brain. B, C) As quantified using the stereological optical fractionator, neuron numbers are reduced in layers V and VI by 20% in 8 month old *Cln8^mnd*. D) Schematic illustration of the mouse sciatic nerve. E) There was no reduction in *Cln8^mnd* nerve conduction velocity, measured from the motor evoked potentials of sciatic nerve in 1 and 4 month old mice. Data represented as mean + standard error (B,C) and standard deviation (E). mo, month(s) old.

The *Cln8^mnd* spinal cord pathology has been investigated in a number of studies, showing neurodegeneration, accumulation of storage material and glial activation (Callahan *et al.* 1991; Mennini *et al.* 2004; Messer *et al.* 1987; Messer & Plummer 1993). Unfortunately, no

systematically collected data exist on the quantity of neuron loss. Yet it appears to be quite mild (over 80% of neurons are spared at 7 months of age, Gorio *et al.* 1999) or not different from wildtype (a study in 8-9 month old *Cln8^{mnd}* mice by Zeman *et al.* 2004). Thus, it appears that the onset of motor symptoms is triggered by a dysfunction in upper and/or lower motor neurons rather than their overt loss. We preliminarily assessed this question by studying the *Cln8^{mnd}* mouse peripheral nerve function. We measured the motor evoked potentials prior to the onset of motor symptoms in 1 and 4 month old *Cln8^{mnd}* mouse sciatic nerve (Fig. 18; unpublished). The *Cln8^{mnd}* nerve conduction velocities were not different from wildtype, indicating that peripheral axonal conduction is not compromised in these early symptomatic mice. Unfortunately, our analysis did not include later stages of the disease or, despite repeated attempts, quantify the motor cortical potentials.

While our study does not form a complete picture of the motor pathway, we did comprehensively assess cortical integrity and peripheral nerve functionality. Our results combined with previous descriptions of the spinal cord pathology suggest that in the corticospinal motor pathway, the peripheral component degenerates concomitantly with the motor cortex and that these changes largely coincide with the observed motor symptom onset. The cerebellum, brain stem, thalamus and basal ganglia are also involved in motor functions and their regulation and furthermore, the motor systems receive feedback from the sensory pathways (Kandel *et al.* 2000). These aspects require further studies in the *Cln8^{mnd}* mouse.

5.2.2 GLIAL ACTIVATION (II, UNPUBL.)

Glial activation has been shown to precede neuron loss in previously analysed NCL models (Cooper 2010). Similarly, astrocytosis but especially microglial activation occurred early in the *Cln8^{mnd}* mouse. CD68 positive microglia with reactive appearing morphology were present at 3 months of age in *Cln8^{mnd}* somatosensory, visual and motor pathways. Microglial activation occurred well before neuron loss, especially in visual and motor pathways where neuron loss was observed only at 8 months (Fig. 19 and Figs 7, 8 in II). Similar findings have been reported in *Cln8^{mnd}* hippocampus and spinal cord where GFAP positive astrocytes and cluster of differentiation 11b (CD11b) positive microglia are present at 4-5 months of age (Mennini *et al.* 2004, Melo *et al.* 2010).

5.2.2.1 Role of glial activation in disease?

Dual roles for microglia have been proposed in neurodegenerative diseases such as Alzheimer's disease. Microglial activation appears to be neuroprotective through inducing amyloid β phagocytosis and proteolysis, while detrimental effects are mediated by the production of pro-inflammatory cytokines (Napoli & Neumann 2009). Microglia have been

suggested to phagocytose NCL storage material, implicated by the microglial localization of mitochodrial ATP synthase subunit c in *Ctsd*^{−/−} mouse brain. However, it appears that *Ctsd*^{−/−} microglia, not only neurons, accumulate storage material since *in vitro* microglia without neurons also contain subunit c (Nakanishi & Wu 2009). The presence of storage material might compromise normal functions and signalling of microglia and lead to neurotoxicity, for instance through nitric oxide overproduction which is observed in *Ctsd*^{−/−} mice (Nakanishi *et al.* 2001; Yamasaki *et al.* 2007).

In addition, there is evidence of increased pro-inflammatory signaling in the *Cln8^mnd* mouse. Levels of tumor necrosis factor alpha, TNFα, and its receptor have been shown to be elevated in *Cln8^mnd* mouse brain and spinal cord (Galizzi *et al.* 2011; Ghezzi *et al.* 1998; Melo *et al.* 2010; Mennini *et al.* 2004). Due to the pro-inflammatory nature of TNFα, its upregulation is likely to be detrimental to *Cln8^mnd* neurons.
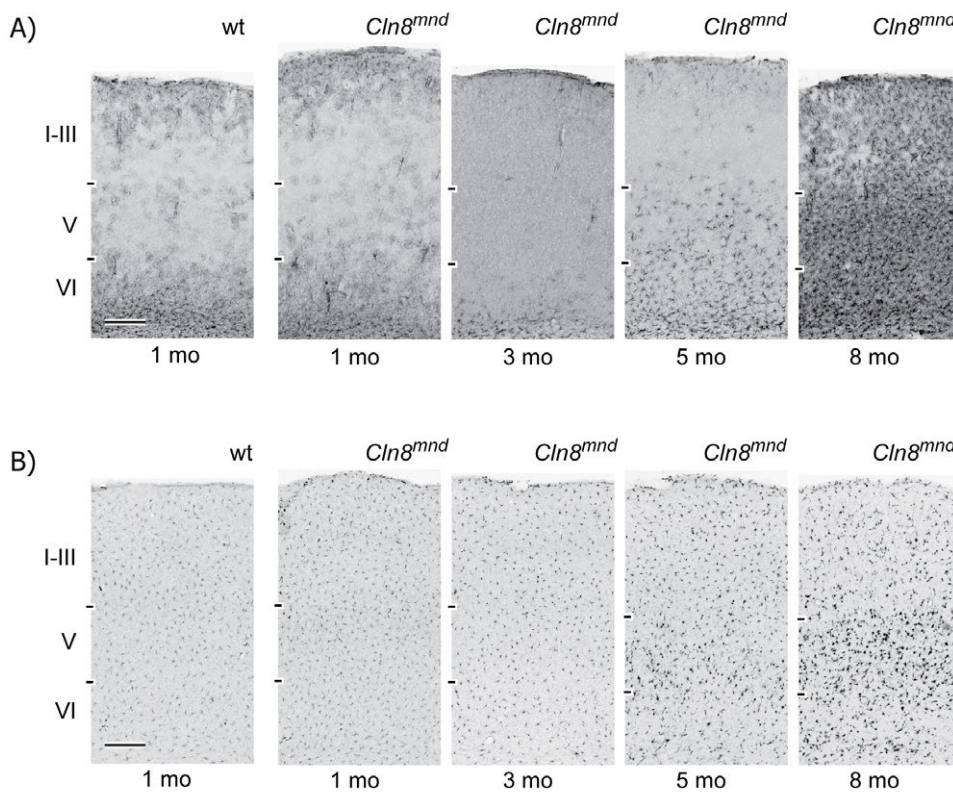
Figure 19. Glial activation precedes neuron loss also in the primary motor cortex of *Cln8^mnd* mice. A) GFAP staining shows activation of astrocytes, especially in layers V and VI, already at 5 months of age. B) Microglial activation is evident in CD68 staining especially in layer V. Scale bars 200 μm.

The major astrocytic glutamate transporter GLT-1 has been shown downregulated in *Cln8^mnd* spinal cord already at 3-4 months of age (Mennini *et al.* 1998). The concomitant increase in

GFAP expression indicates a specific reduction in the properties of glutamate recycling in *Cln8^{mnd}* reactive astrocytes (Mennini *et al.* 1998). Reduced expression of GLT-1 has been observed in various neurodegenerative diseases such as ALS and Alzheimer's disease (Maragakis & Rothstein 2006; Sofroniew & Vinters 2010). A defective glutamate cycle may cause excitotoxicity and contribute to the seizure phenotype of the *Cln8^{mnd}* mouse (Melo *et al.* 2010).

The function of reactive astrocytosis in NCL disease was recently investigated in a CLN1 mouse model without the ability to upregulate astrocytic intermediate filaments, a hallmark of reactive astrocytosis. The *Ppt1^{-/-}*, *Gfap^{-/-}*, Vimentin^{-/-} triple knockout mouse shows earlier disease onset and increased neurodegeneration, possibly due to increased neuroinflammation mediated by microglial activation, an overt increase in pro-inflammatory cytokines and immune cell infiltration to the CNS (Macauley *et al.* 2011). This implies that reactive astrocytes, by diminishing the inflammatory reaction in the brain, may have protective effects in NCLs.

5.2.2.2 Differential glial activation in *Cln8^{mnd}* thalamic pathways

While in the late stages of *Cln8^{mnd}* disease glial activation is widespread, it does not affect all areas of the brain identically (Table 8). Apart from primary sensory and motor thalamocortical pathways, the posterior thalamic nucleus – somatosensory cortex pathway showed obvious glial activation in *Cln8^{mnd}*. This pathway was not investigated for neuron loss in this study, and has not been analysed in other NCL models. Interestingly, in the mouse model of another neurodegenerative epilepsy syndrome, progressive myoclonus epilepsy EPM1, this pathway showed neuron loss and glial activation (Tegelberg *et al.* 2012).

The reticular thalamic nucleus, which performs the major inhibitory action in the rodent thalamus, showed activation of both microglia and astrocytes in *Cln8^{mnd}*. The *Ppt1^{-/-}* reticular nucleus is affected by neuron loss and glial activation (Kielar *et al.* 2007). Loss of the inhibitory influence of the reticular nucleus may contribute to the death of thalamic relay neurons or affect the seizure phenotype of *Cln8^{mnd}* mice (Melo *et al.* 2010).

The olfactory sensations from olfactory cortex (piriform cortex) are relayed by the thalamic medial dorsal nucleus, which appears affected in the *Cln8^{mnd}* mouse. Degenerative changes were observed in the olfactory pathway of the CLN2 mouse model, *Tpp1^{-/-}* (Sleat *et al.* 2004). The limbic system pathology may be significant in the *Cln8^{mnd}* mouse, since clear glial activation was observed in *Cln8^{mnd}* amygdala, cingulate cortex and hippocampus (data not shown).

Table 8. Microglial activation and astrocytosis in the 8 month old *Cln8mnd* mouse thalamocortical pathways.

THALAMIC NUCLEUS	MAJOR OUTPUTS	INFORMATION RELAYED
Specific relay nuclei		
Ventral posterior	Somatosensory cortex	Somatosensory
Lateral geniculate	Visual cortex	Visual
Medial geniculate	Auditory cortex	Auditory
Ventral anterior / ventral lateral	Motor cortex	Motor
Association nuclei		
Anterior group	Cingulate gyrus	Limbic
Medial dorsal	Prefrontal cortex	Limbic/olfactory
Lateral dorsal	Cingulate gyrus	Emotional expression
Posterior group	Somatosensory cortex	Integration of sensory information
Other		
Midline	Basal forebrain	Limbic
Intralaminar not different to wt	Basal ganglia and cortex	Attention/arousal
Reticular	Thalamic nuclei	Modulation of thalamic activity

Degree of glial activation was determined from GFAP and CD68 stained brain sections by observing the region full of intense staining (three symbols);less than half of the region stained (two symbols);or few scattered cells (one symbol) in *Cln8mnd* compared to wt). Yellow symbols represent microglial activation (CD68) and red astrocytosis (GFAP). n=6 per genotype and age.

5.2.3 MYELINATION (III, UNPUBL.)

Even prior to microglial activation, we observed a developmental delay in the myelination of *Cln8mnd* mouse brains. In addition, a specific function for CLN8 in myelin formation was indicated by the expression pattern of *Cln8*. In the developing brain the expression of *Cln8* mRNA was induced at the beginning of myelinogenesis and downregulated after 1 month of age (Fig 5A in III). Of the *in vitro* CNS cell types studied, *Cln8* was expressed most by the oligodendrocytes (Fig 5B in III). Similar results have been observed in previous studies, where the expression of *Cln8* was found to peak in early postnatal development (Lonka *et al.* 2005). *Cln8* mRNA has been found to be upregulated in *in vitro* oligodendrocytes and during

oligodendrocyte differentiation by comparative microarray analyses of different CNS cell types (Cahoy *et al.* 2008; Fulton *et al.* 2011). Of other NCL genes, expression of *Cln5* appears also to be induced during oligodendrocyte maturation (Cahoy *et al.* 2008; Fulton *et al.* 2011). and decreased myelination and oligodendrocyte maturation was shown to characterize the early disease of *Cln5*$^{-/-}$ mice (Schmiedt *et al.* 2012).

As a whole, myelination has not received detailed attention in NCL research, since it does not appear primarily affected in NCL disease. Myelination requires the repid and well-orchestrated synthesis and transport of the myelin membrane components (see section 2.1.3.1). Since the cellular transport pathways are probably affected in most NCLs, it is not surprising that there would be effects to the myelination process as well. In addition, myelinating cells could therefore be useful tools to study NCL-related trafficking defects.

5.2.3.1 Delayed myelin maturation in early *Cln8*^{mnd} disease

A moderate decrease in brain myelin was found to characterize especially the early symptomatic *Cln8*^{mnd} mice. The thinning of *Cln8*^{mnd} mouse white matter tracts, including the corpus callosum, anterior commissure and internal capsule, was evident in 1 and 3 month old mice (Fig. 3 in III). Likewise, reduced immunostaining of myelin markers MBP, PLP and MOG was observed in 1 month old *Cln8*^{mnd} brain samples (Fig. 2 and 5 in III). The mRNA expression of *Mbp* and *Mog* was also reduced (Fig. 5 in III). Ultrastructural analysis of myelin showed thinner myelin sheets in *Cln8*^{mnd} brains (Fig. 4 in III) suggesting that the myelination defect is due to the inability of *Cln8*^{mnd} to produce sufficient amounts of myelin membrane.

Indeed, *Cln8*^{mnd} oligodendrocytes showed reduced expression of mature, myelinating oligodendroglial markers *Mbp* and *Mog in vitro,* while the expression of early markers *Ng2* and *Olig2* were normal (Fig. 7 in III). Thus, we propose that the observed decrease in myelination is due to delayed oligodendrocyte maturation and myelin membrane production in the *Cln8*^{mnd} mouse. Functionally, the *Cln8*^{mnd} myelin itself appears normal, since we were unable to show dramatic disturbances in white matter integrity, as measured by diffusion tensor imaging in 4 month old *Cln8*^{mnd} mice. Nerve conduction velocity was also normal in *Cln8*^{mnd} peripheral nerves (Fig. 18), indicating preserved insulation capacity of *Cln8*^{mnd} myelin.

5.2.3.2 Increased myelination in late stages of the disease?

Reduction in myelin content was not observed later in disease and there was no evidence of late-onset demyelination in *Cln8*^{mnd} mouse. White matter tract volumes or the expression of myelin markers were not different from wildtype in *Cln8*^{mnd} mice of 4-5 months of age (Figs 2, 3 and 5 in III). At 8 months of age, the corpus callosum thickness of *Cln8*^{mnd} was similar to wildtype (Fig. 20 A).
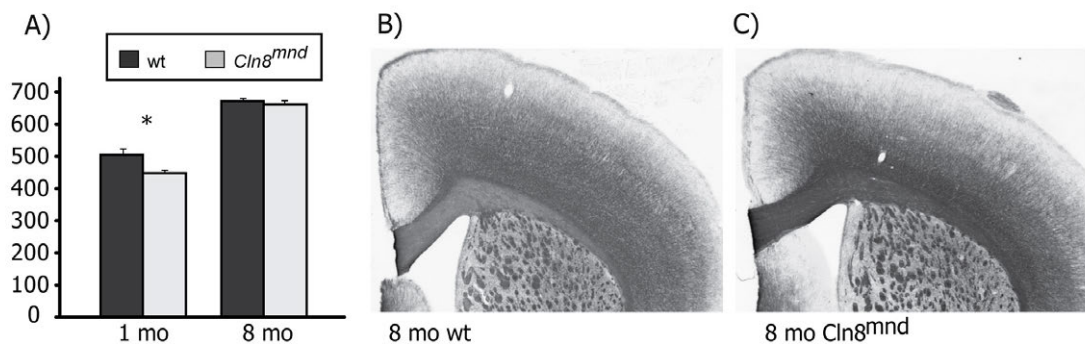
Figure 20. Increased MBP expression in the 8 month old *Cln8^mnd* mouse. A) Corpus callosum thickness did not differ from wildtype at 8 months of age B) Frontal brain section of an 8 month old wildtype mouse. C) Frontal brain section of an 8 month old *Cln8^mnd* mouse, showing increased MBP staining in corpus callosum, frontal cortex (motor and somatosensory areas) and in striatum.

Surprisingly, in the end stage of *Cln8^mnd* disease, we observed an increase in MBP staining in 8 month old *Cln8^mnd* mouse brains (Fig. 20 B, C). Since signals from reactive astrocytes promote myelination (Nash *et al.* 2011), increased MBP staining could reflect the presence of reactive glial cells in the *Cln8^mnd* brains at this stage.

5.2.4 ALTERATIONS IN LIPID METABOLISM (III, UNPUBL.)

A role for CLN8 in lipid metabolism regulation has been proposed through its TLC protein domain possession (Winter and Ponting, 2002) and through the observed abnormalities in brain lipid composition in EPMR patients (Hermansson *et al.* 2005). In addition, hints towards a lipid regulatory role for CLN8 have come from another lysosomal storage disease, as *CLN8* overexpression was recently shown to protect from severe phenotypes of Gaucher disease caused by glucocerebrosidase deficiency (Zhang *et al.* 2012).
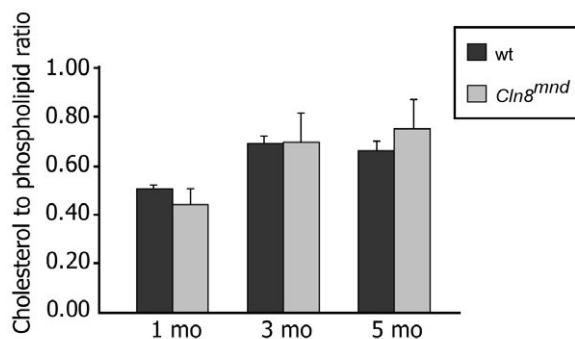

Fig 21. Free cholesterol content in the cerebral cortical tissue of mouse was similar to wildtype (wt). Ratio is given as cholesterol (nmol) to total phospholipids (nmol), error bars indicate standard deviation from mean.

A large-scale lipid profiling was performed to study the molecular events in the pathogenesis of *Cln8^{mnd}*. By liquid chromatography / mass spectrometry, a reduction in galactolipids GalC and sGalC was observed (Fig 1 in III). The reduction was significant only in the early period of the *Cln8^{mnd}* pathology (at one month of age). Later in disease, at 5 months, the level of sphingomyelin was slightly increased. The content of free cholesterol was normal (Fig 21). Since the galactolipids are myelin-specific, we analyzed the *Cln8^{mnd}* brains for their myelination status. These findings were discussed in the previous section 5.2.3.

In addition to the reduced galactolipid content, the key enzyme in galactolipid synthesis, CGT, showed moderately reduced activity in 1 and 5 month old *Cln8^{mnd}* mice (Fig 1 in III). This persistent decrease may link CLN8 to the CGT enzyme and galactolipid synthesis. Both CLN8 and CGT are expressed by oligodendrocytes and subcellularly reside in the endoplasmic reticulum (Lonka *et al.* 2000; Lonka *et al.* 2004; Neskovic *et al.* 1986; Nilsson & Warren 1994; Schulte & Stoffel 1993; van Meer 1998). CLN8 has also been suggested to bind GalC and ceramide (Rusyn *et al.* 2008). Taken together, CLN8 could act as a mediator of galactolipid synthesis, but further studies will be needed to pinpoint the exact mechanism.

Galactolipid synthesis deficient *Cgt^{-/-}* mice are viable but show tremor, hindlimb paralysis and death in the end of the myelination period (Bosio *et al.* 1996; Coetzee *et al.* 1996). Surprisingly, *Cgt^{-/-}* mutant mice display compacted myelin, yet the organization of myelin in the paranodal regions is abnormal, resulting in severe defects in myelin insulation properties (Bosio *et al.* 1996; Coetzee *et al.* 1996; Marcus & Popko 2002). Based on these findings galactolipids have been postulated to be essential for proper axon-glial interactions in the paranodes (Marcus & Popko 2002). The axon-oligodendrocyte signaling may also be disrupted *Cln8^{mnd}* mice, which show abnormal oligodendrocyte maturation and myelination defects.

5.2.5 SEQUENCE OF EVENTS

Taken together, we found notable effects of the *Cln8^{mnd}* mutation on the mouse phenotype. The temporal relationship of abnormal myelin maturation, reactive changes in microglia and astrocytes together with neuron loss in the *Cln8^{mnd}* mouse is presented in Fig. 22, which also summarises earlier knowledge on the *Cln8^{mnd}* mouse pathology.

Early studies on *Cln8^{mnd}* mice characterized the disease progression based on the motor symptoms, and considered mouse age points until 5-6 months to be asymptomatic (Callahan *et al.* 1991, Messer and Plummer, 1993, Plummer *et al.* 1995). It is clear, however, that disease progression in the *Cln8^{mnd}* mouse starts already earlier. This is evident especially in the *Cln8^{mnd}* retina but also indicated by the early changes in *Cln8^{mnd}* glial cells.

Indeed, while the precise timing of thalamocortical pathology varies in different pathways, glial and especially microglial activation appeared to predict later occurring neuron loss in all

pathways studied in *Cln8^mnd* mouse. Delayed myelination, which precedes these changes, was found in all *Cln8^mnd* white matter tracts studied and is not restricted to the thalamocortical pathways. Abnormal myelination may affect the stability of axonal integrity and the neural circuits they form (Barres 2008; Nave 2010) while galactolipid deficiency results in inproper axon-oligodendrocyte signalling (Marcus & Popko 2002). These effects may be pronounced on long axons that could contribute to the pathology of cortical pyramidal neurons and thalamic relay neurons in the *Cln8^mnd* mouse.
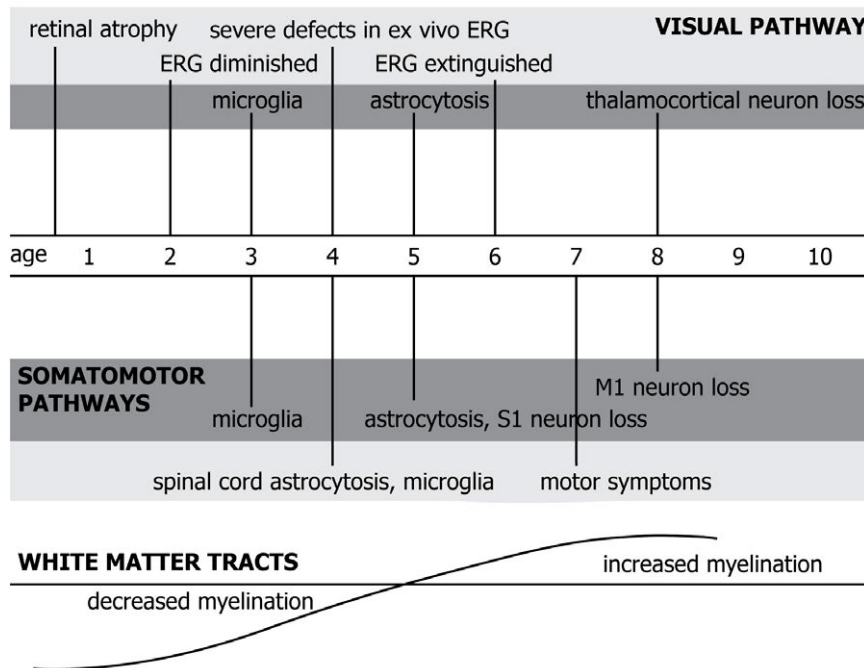

Figure 22. Neuropathology of the *Cln8^mnd* mouse. Mouse age is represented in months. Retinal/spinal cord pathology is represented by a light grey background and (thalamo)cortical changes by a dark grey background.

Microglia and astrocytes may respond to abnormalities in the signalling between neurons and glial cells, or to the accumulating neuronal storage material. Loss of inhibitory interneurons (Cooper *et al.* 1999) and defects in astrocytic glutamate recycling (Mennini 1998) may induce excitotoxicity in *Cln8^mnd* brain. This may be sensed by glial cells, which activate compensatory mechanisms such as microglia-mediated phagocytosis of excitatory synapses (Tambuyzer *et al.* 2009). However, the effects of glial activation may be detrimental in *Cln8^mnd* brain, as suggested by increased pro-inflammatory signaling (Galizzi *et al.* 2011, Ghezzi *et al.* 1998, Mennini *et al.* 2004, Melo *et al.* 2010).

While thalamocortical pathology is evident in *Cln8^mnd* brain, the origin of defects is not clear and may not be uniform across distinct pathways. The integrity of the somatosensory pathway is the first to be compromised in *Cln8^mnd* brain and appears to precede major

neurodegeneration in the spinal cord (Gorio *et al.* 1999; Zeman *et al.* 2004). Nevertheless, the pathology of sensory receptors connecting to spinal cord has not been studied. In the corticospinal motor pathway motor cortex and spinal cord show largely simultaneous pathology, although systematic analysis of these events is lacking and a thorough investigation of other regions involved in motor regulation would also be required. Finally, since these pathways are interconnected, the primary problems in the somatosensory pathway might be reflected as motor deficits in the *Cln8mnd* mouse.

The sequence appears clearer in the *Cln8mnd* mouse visual pathway, where an abnormal input from the retina is likely to induce the thalamocortical pathology. There is a considerable delay, however, that would make the *Cln8mnd* mouse an appealing model system for future therapies in trying to correct the NCL-related, retinal-onset visual loss. . One such approach could be a gene transfer based therapy with neurotrophic factors, supported by the beneficial effect of insulin-like growth factor 1 treatment to the *Cln8mnd* neuropathology (Cooper *et al.* 1999). However, in order to prevent cell loss in retina, it needs to be targeted very early.

5.2.6 SIGNIFICANCE TO HUMAN NCL DISEASE?

There are two distinct human NCL diseases caused by mutations in *CLN8*. Our findings indicate that the *Cln8mnd* mouse is a better model for the late infantile onset NCL than for the protracted EPMR disease. Patients with late infantile CLN8 disease show abnormal or extinguished ERG and diminished or loss of visual evoked potential (VEP) responses (Allen *et al.* 2011; Cannelli *et al.* 2006; Ranta *et al.* 2004; Reinhardt *et al.* 2010; Topcu *et al.* 2004; Vantaggiato *et al.* 2009). EPMR disease is not characterized with retinal degeneration and only a subset of patients has diminished visual acuity and abnormal VEPs (Hirvasniemi *et al.* 1995; Lang *et al.* 1997). Somatosensory pathology is indicated by the presence of myoclonus in late infantile CLN8 patients (Allen *et al.* 2011; Cannelli *et al.* 2006; Kousi *et al.* 2009; Kousi *et al.* 2012; Ranta *et al.* 2004; Reinhardt *et al.* 2010; Topcu *et al.* 2004; Vantaggiato *et al.* 2009; Zelnik *et al.* 2007). Myoclonus is not observed in EPMR and no alterations in somatosensory evoked magnetic fields were observed (Lauronen *et al.* 2001).

The *Cln8mnd* mouse mutation predicts a truncated CLN8 protein or degradation of the *Cln8* mRNA (Ranta *et al.* 1999). However, according to the current knowledge on genotype-phenotype correlations in CLN8 disease, the nature of the causative mutation does not explicitly underlie the differences between the two human CLN8 diseases. Most CLN8 disease mutations are missense mutations (Kousi *et al.* 2012). The EPMR mutation is a missense mutation outside of the TLC protein domain (Ranta *et al.* 1999). Mutations that are not within the TLC domain can also cause the more severe late infantile CLN8 disease, thus the more severe disease is not always caused by disruption of the TLC domain.

Studying the *Cln8mnd* mouse has provided information on disease progression in yet another NCL model. The recognition of early glial activation and the role for the thalamus in the NCL disease progression have evolved from studies in animal models (Cooper 2010). While human studies are limited to fairly low-resolution imaging methods and to the use of post mortem material, animal models are important in elucidating early events in NCL disease.

6 CONCLUSIONS

If you can look into the seeds of time,

And say which grain will grow and which will not,

Speak then to me.

-William Shakespeare

This thesis delineated cellular and molecular changes influencing the pathogenesis of neuronal ceroid lipofuscinosis (NCL) in two animal models, the *cathepsin D* deficient *Drosophila* model for CLN10 disease, *cathD¹*, and the *Cln8^{mnd}* mouse model for CLN8 disease. Since other NCL diseases have been previously modeled in mouse and *Drosophila*, we were able to compare our results to previous research. In addition, by utilizing these two systems, it was possible to compare the benefits and limitations of two different animal models.

In *Drosophila*, effects of second-site mutations on the *cathD¹* degenerative phenotype were tested *in vivo*, an approach that would have been limited to only a few candidates in mammalian model systems. While the *cathD¹ Drosophila* phenotype is recessive and relatively mild, a large-scale unbiased genetic modifier screen was infeasible, and thus the best potential of *Drosophila* modelling could not be exploited. However, by our hypothesis-based screen we were able to test different mechanisms that have been suggested relevant to CTSD induced neurodegeneration. Pathways related to endocytosis, oxidative stress and lipid regulation were proven applicable for future studies in *Drosophila*.

The most widely used model system for NCL disease is the mouse. With the comprehensive characterization of the *Cln8^{mnd}* mouse in this study, there is now a plethora of data from existing NCL mouse models. Some phenomena of NCL disease pathogenesis have specifically appeared through studying these mice, such as the relevance of neuron loss and glial activation in the thalamus. In human NCL patient brain imaging the thalamus shows pathological changes, which may prove to be important for the progression of the disease. Yet the cerebral cortical pathology is very pronounced in human NCLs while in mouse models such as *Cln8^{mnd}* the cortex is relatively spared. Differences in the regulation of thalamocortical pathways between mouse and human, such as the lack of local interneurons in the rodent thalamus, might explain some of these differences. However, thalamocortical pathways represent a well-characterized system where the NCL disease progression and interventions to it can be effectively monitored. Thus, our study has enabled the use of these pathways for the evaluation of treatment efficacy in the *Cln8^{mnd}* mouse. Of particular interest

might be the *Cln8^mnd* mouse visual system, where the relatively ample time frame between retinal and thalamocortical neuron loss could be utilized to target the NCL-related visual loss. However, therapies to prevent retinal cell loss need to be started very early.

It is probable, however, that markedly more information on the CLN8 protein will be needed before the development of such therapies become feasible. The function of the CLN8 protein was assessed in this study as well, and the link to galactolipid synthesis may open novel avenues for research. While this link indicates an oligodendrocyte-related function for CLN8, in other cell types CLN8 may execute other functions described in previous studies, such as regulation of calcium signaling and neurotransmitter balance. Indeed, robust involvement of glial cells in NCL pathogenesis suggests that the disease may involve abnormal function of both neurons and glial cells. These aspects are being dissected in other NCL models and in the future they should be tackled in CLN8 as well.

In this study, two NCL subtypes with defects in two very different proteins were investigated in two animal models. It was possible to pinpoint similarities, such as the vulnerability of retina and the involvement of lipid metabolism regulation, as common phenomena in the pathogenesis of these two NCL diseases. Yet when comparing the results to other NCL models it is not obvious that there would be a common cellular pathway disrupted in all NCLs. The thalamocortical pathology of the *Cln8^mnd* mouse differs from other NCL mouse models, and the *cathD* is linked to different genetic pathways in comparison to other NCL *Drosophila* models. In this regard, our study underlines the contradiction of NCLs: mechanisms leading to very similar diseases are similar and yet very different.

7 ACKNOWLEDGEMENTS

I wish to thank the appointed pre-examiners, **dos. Tapio Heino** and **Dr. Hannah Mitchison** for the thorough examination of my thesis during the summer holiday period... Your comments and considerations were extremely valuable.

I wish to express my deepest gratitude to my PhD supervisors, **dos. Outi Kopra and prof. Anna-Elina Lehesjoki. Anna-Elina** first hired me as a summer student 10 years ago, and the longest I've been away since that was for my Erasmus in Spain. I can still feel the enthusiasm for being accepted to work in your laboratory! During the years you have been an excellent example of a supervisor, taking care of collaborations, funding and developing the Folkhälsan Research Center facilities. My supervisor and lähiesimies **Outi** is thanked for nothing more but this project coming into an end and almost everything before that! You have been the absolute practical and mental driving force: I wouldn't have survived without your ideas, just-do-it attitude and constant encouragement and support. With your help I think I grew up quite a lot from that Harjoituskoululainen I was back in the days of UPJ…

I have been fortunate to have two more supervisors. I started my PhD studies in the *Drosophila* project, supervised by **dos. Liisa Myllykangas**. I am indebted to Liisa for introducing me to the grown-up scientific life and for letting me catch her never-ending passion for research. I wish to thank **prof. Jonathan D. Cooper**, who by no doubt is a key person in my PhD project. A warm welcome from Jon to his lab, not once, not twice but five times (!!) was invaluable in my CLN8 projects. I admire your wide knowledge on NCL disease but also your passion for keeping the patient-science interface so vivid.

I wish to thank my PhD follow-up group members, **prof. Anu Wartiovaara, dos. Tapio Heino** and **dos. Carina Holmberg-Still**, all of whom I admire a great deal!

My friends & fellows at Folkhälsan Institute of Genetics, past and present (as **Hanna** so adequately quoted, "you can check out any time of year / but you can't ever leave"): Because of you I came happily to work everyday! If it was for the morning coffee, sushi/Mountain lunch, wine tasting Fridays or Jalo's day, icecream at "luontokolmio"… There were other than food/drink-related activities as well: film shooting, Dragon racing, boxing, baseball tournaments and singing, not even mentioning the famous Folkhälsan garden parties / pikkujoulut / various karonkkas / cruises… It has been amazing to be part of the FIG crew! **Saara**, you've been there I suppose for all of the aforementioned, plus at least London, Washington DC and the Puschino trip (singing/whispering/giggling "Finlandia hymni" in the middle of Russian side Carelia in the non-sleepers cabin). Yay, good times! **Jaakko**, you're the best (and better) recycling buddy I've had at FH! And otherwise a Good Person and a vice-Google (KVJ). Special thanks for your patience and hands-on support with the image processing programs – for example in making the cover image! **Vilma**, there's so much craziness we still need to go through before the famous "liinavaatevarasto", and we will do it with style!(??!) I hate that we haven't really got beyond virsi numero 1 in our hymn singing efforts. **Anne**: My tutor! I owe you this Folkhälsan experience. Enjoy your beautiful children! **Ann-Liz**: for me you will always be the heart and soul of the whole lab. It's from you that I've received some perfectly-timed hugs of encouragement. Thank you. **Naula**: I've missed you at FH very very much! But it's been great to keep in touch with Härkälinna karonkkas! **Otto**: you don't actually know it ALL but you know a lot! Thanks for the lunch/coffee/beers/cigars company! **Tarja J**: my MSc thesis supervisor! Thanks for your continuous support and interest in my projects! **Hanna V**: Our Oscar-winning material! See you in sunny California! **Reetta V**: Our Forssa-born souls quickly bonded, wish you all the best with your wonderful trio! Other past PhD students and postdocs, **Kati, Liina, Jukka, Riikka, Kirsi, Juha I, Jodie, Tarja S.** and **Eija**, you are part of the Folkhälsan "furniture" and it's been great that you guys still are in the guest lists and show up (hope you show up in mine as well)! **Paula**: you are the true VIP in the lab! I admire your calm yet humoristic attitude to the everyday life in the lab. Plus it's been nice to share some mouse torturing guilt with you… **Mubashir**: We've had some interesting and touching talks! It's been great having you join the lab. **Maria S**: svenska kaffe never came to stay but your warm finlandsvensk attitude has been very comforting during all these years! **Anna V**.: great times in ASCB trip, various airports and snowstorms but we made it! Finally, **Anni, pH, Inken, Olesya, Marc, Katarin, Anna-Kaisa** - you've been the best company, keep the place in order and most of all, FUN! Last but not least, **Paula, Teija, Merja, Hanna H.** and **Marilotta**, you keep the chaotic researchers in order and I cannot thank you enough for that.

Tärkeääkin tärkeämmät ystävät: vaikka noiden kollegoidenkin kanssa on tullut hauskaa pidettyä niin te olette kuitenkin pitäneet tämän touhun tolkullisena!! **Forssatytöt** Minna, Janika, Junnu-Terhi, Peppi-Terhi ja TerhiS., olette ne vanhimmat (virkaiältään) ja nii-iin

tärkeät! **Turkurinki** eli Saara, Terhi, Antero, Reetta, Liisa, Lauri, Hanna-Leena, Manta, Tuula: biologian opinnoista tuntuu kyllä olevan ikuisuus mutta kiitos meidän ihanien pikkujoulujen, opiskeluaikojen ystävyys jatkuu! Ja sitten on se **Turkukaverit extended** eli Päivi, Iiris, Petra, Lyyli, Silja, Taina ja kumppanit, on ollut hienoa valloittaa Helsinkiä teidän kanssanne! Gracias mis **chicas** Minna, Isabel y Cornelia por amistad y nuestros viajes, durante 10 años ya! Kiitos **capoeiraystäville** Markus, Elli, Ressu, Ulla, Laurat ja muut: capoeira on avannut mun aivoihin, ruumiiseen ja sosiaaliseen elämään ihan uusia verkostoja ja se on upeaa!

Ja lopuksi kiitos äiti-Mirjalle ja isä-Erkille. Teidän geeneillä ja aikaansaamillanne ympäristövaikutuksilla olen tässä! Ja pikkuinen siskoni Marjo, olet hirvittävän tärkeä! Äiti olet aina mun äiti ja jaksat huolehtia siitä, olenko kunnossa ja turvassa reissuillani. Iskälle kiitokset erityisesti siitä, että olet elänyt mukana ja kannustanut, niin koulussa, musiikkikoulussa ja opinnoissa. Se on varmasti ollut edellytys sille, että olen sitkeästi jaksanut tehdä töitä hankalampinakin hetkinä. Kiitokset myös lähimmille sukulaisilleni, etenkin Riitalle ja mummulle kun olette olleet mukana koko elämän. Papan olisin kovasti halunnut pitää näkemässä väitöspäiväni ja kauas tästä eteenpäinkin.

Kiitollisena niin monesta ja niin monelle,

8 REFERENCES

Acharya U & Acharya JK. Enzymes of sphingolipid metabolism in *Drosophila melanogaster*. *Cell Mol Life Sci* 2005; 62: 128-42.

Acharya U, Patel S, Koundakjian E, Nagashima K, Han X, Acharya JK. Modulating sphingolipid biosynthetic pathway rescues photoreceptor degeneration. *Science* 2003; 299: 1740-3.

Aggarwal S, Yurlova L, Simons M. Central nervous system myelin: Structure, synthesis and assembly. *Trends Cell Biol* 2011; 21: 585-93.

Ahtiainen L, Kolikova J, Mutka AL, Luiro K, Gentile M, Ikonen E, Khiroug L, Jalanko A, Kopra O. Palmitoyl protein thioesterase 1 (Ppt1)-deficient mouse neurons show alterations in cholesterol metabolism and calcium homeostasis prior to synaptic dysfunction. *Neurobiol Dis* 2007; 28: 52-64.

Ahtiainen L, Van Diggelen OP, Jalanko A, Kopra O. Palmitoyl protein thioesterase 1 is targeted to the axons in neurons. *J Comp Neurol* 2003; 455: 368-77.

Allen NJ & Barres BA. Neuroscience: Glia - more than just brain glue. *Nature* 2009; 457: 675-7.

Allen NM, O'hici B, Anderson G, Nestor T, Ann Lynch S, King M. Variant late-infantile neuronal ceroid lipofuscinosis due to a novel heterozygous CLN8 mutation and de novo 8p23.3 deletion. *Clin Genet* 2011; 81: 602-4.

Amadio S, Pluchino S, Brini E, Morana P, Guerriero R, Boneschi FM, Comi G, Zaratin P, Muzio V, del Carro U. Motor evoked potentials in a mouse model of chronic multiple sclerosis. *Muscle Nerve* 2006; 33: 265-73.

Arcelli P, Frassoni C, Regondi MC, De Biasi S, Spreafico R. GABAergic neurons in mammalian thalamus: A marker of thalamic complexity? *Brain Res Bull* 1997; 42: 27-37.

Arsov T, Smith KR, Damiano J, Franceschetti S, Canafoglia L, Bromhead CJ, Andermann E, Vears DF, Cossette P, Rajagopalan S, McDougall A, Sofia V, Farrell M, Aguglia U, Zini A, Meletti S, Morbin M, Mullen S, Andermann F, Mole SE, Bahlo M, Berkovic SF. Kufs disease, the major adult form of neuronal ceroid lipofuscinosis, caused by mutations in CLN6. *Am J Hum Genet* 2011; 88: 566-73.

Augestad LB& Flanders WD. Occurrence of and mortality from childhood neuronal ceroid lipofuscinoses in norway. *J Child Neurol* 2006; 21: 917-22.

Austyn JM& Gordon S. F4/80, a monoclonal antibody directed specifically against the mouse macrophage. *Eur J Immunol* 1981; 11: 805-15.

Awano T, Katz ML, O'Brien DP, Taylor JF, Evans J, Khan S, Sohar I, Lobel P, Johnson GS. A mutation in the cathepsin D gene (CTSD) in american bulldogs with neuronal ceroid lipofuscinosis. *Mol Genet Metab* 2006; 87: 341-8.

Barres BA. The mystery and magic of glia: A perspective on their roles in health and disease. *Neuron* 2008; 60: 430-40.

Battaglioli G, Martin DL, Plummer J, Messer A. Synaptosomal glutamate uptake declines progressively in the spinal cord of a mutant mouse with motor neuron disease. *J Neurochem* 1993; 60: 1567-9.

Bauer R, Voelzmann A, Breiden B, Schepers U, Farwanah H, Hahn I, Eckardt F, Sandhoff K, Hoch M. Schlank, a member of the ceramide synthase family controls growth and body fat in *Drosophila*. *EMBO J* 2009; 28: 3706-16.

Baumann N & Pham-Dinh D. Biology of oligodendrocyte and myelin in the mammalian central nervous system. *Physiol Rev* 2001; 81: 871-927.

Belles X, Martin D, Piulachs MD. The mevalonate pathway and the synthesis of juvenile hormone in insects. *Annu Rev Entomol* 2005; 50: 181-99.

Benes P, Vetvicka V, Fusek M. Cathepsin D -many functions of one aspartic protease. *Crit Rev Oncol Hematol* 2008; 68: 12-28.

Benitez BA, Alvarado D, Cai Y, Mayo K, Chakraverty S, Norton J, Morris JC, Sands MS, Goate A, Cruchaga C. Exome-sequencing confirms DNAJC5 mutations as cause of adult neuronal ceroid-lipofuscinosis. *PLoS One* 2011; 6: e26741.

Bertamini M, Marzani B, Guarneri R, Guarneri P, Bigini P, Mennini T, Curti D. Mitochondrial oxidative metabolism in motor neuron degeneration (mnd) mouse central nervous system. *Eur J Neurosci* 2002; 16: 2291-6.

Bible E, Gupta P, Hofmann SL, Cooper JD. Regional and cellular neuropathology in the palmitoyl protein thioesterase-1 null mutant mouse model of infantile neuronal ceroid lipofuscinosis. *Neurobiol Dis* 2004; 16: 346-59.

Bier E. Drosophila, the golden bug, emerges as a tool for human genetics. *Nat Rev Genet.* 2005; 6: 9-23.

Bigini P, Milanese M, Gardoni F, Longhi A, Bonifacino T, Barbera S, Fumagalli E, Di Luca M, Mennini T, Bonanno G. Increased [(3) H]D-aspartate release and changes in glutamate receptor expression in the hippocampus of the mnd mouse. *J Neurosci Res* 2012; 90: 1148-58.

Bilen J & Bonini NM. *Drosophila* as a model for human neurodegenerative disease. *Annu Rev Genet* 2005; 39: 153-71.

Bolivar VJ, Scott Ganus J, Messer A. The development of behavioral abnormalities in the motor neuron degeneration (mnd) mouse. *Brain Res* 2002; 937: 74-82.

Bosio A, Binczek E, Stoffel W. Functional breakdown of the lipid bilayer of the myelin membrane in central and peripheral nervous system by disrupted galactocerebroside synthesis. *Proc Natl Acad Sci U S A* 1996; 93: 13280-5.

Bourbon HM, Gonzy-Treboul G, Peronnet F, Alin MF, Ardourel C, Benassayag C, Cribbs D, Deutsch J, Ferrer P, Haenlin M, Lepesant JA, Noselli S, Vincent A. A P-insertion screen identifying novel X-linked essential genes in *Drosophila. Mech Dev* 2002; 110: 71-83.

Bradl M& Lassmann H. Oligodendrocytes: Biology and pathology. *Acta Neuropathol* 2010; 119: 37-53.

Brand AH& Perrimon N. Targeted gene expression as a means of altering cell fates and generating dominant phenotypes. *Development* 1993; 118: 401-15.

Bras J, Verloes A, Schneider SA, Mole SE, Guerreiro RJ. Mutation of the Parkinsonism gene ATP13A2 causes neuronal ceroid-lipofuscinosis. *Hum Mol Genet* 2012; .

Bronson RT, Donahue LR, Johnson KR, Tanner A, Lane PW, Faust JR. Neuronal ceroid lipofuscinosis (nclf), a new disorder of the mouse linked to chromosome 9. *Am J Med Genet* 1998; 77: 289-97.

Bronson RT, Lake BD, Cook S, Taylor S, Davisson MT. Motor neuron degeneration of mice is a model of neuronal ceroid lipofuscinosis (Batten's disease). *Ann Neurol* 1993; 33: 381-5.

Brown NJ, Corner BD, Dodgson MC. A second case in the same family of congenital familial cerebral lipoidosis resembling amaurotic family idiocy. *Arch Dis Child* 1954; 29: 48-54.

Buff H, Smith AC, Korey CA. Genetic modifiers of *Drosophila* palmitoyl-protein thioesterase 1-induced degeneration. *Genetics* 2007; 176: 209-20.

Burg JS & Espenshade PJ. Regulation of HMG-CoA reductase in mammals and yeast. *Prog Lipid Res* 2011; 50: 403-10.

Cadavid AL, Ginzel A, Fischer JA. The function of the *Drosophila* fat facets deubiquitinating enzyme in limiting photoreceptor cell number is intimately associated with endocytosis. *Development* 2000; 127: 1727-36.

Cahoy JD, Emery B, Kaushal A, Foo LC, Zamanian JL, Christopherson KS, Xing Y, Lubischer JL, Krieg PA, Krupenko SA, Thompson WJ, Barres BA. A transcriptome database for astrocytes, neurons, and oligodendrocytes: A new resource for understanding brain development and function. *J Neurosci* 2008; 28: 264-78.

Callahan LM, Wylen EL, Messer A, Mazurkiewicz JE. Neurofilament distribution is altered in the mnd (motor neuron degeneration) mouse. *J Neuropathol Exp Neurol* 1991; 50: 491-504.

Campbell MJ& Morrison JH. Monoclonal antibody to neurofilament protein (SMI-32) labels a subpopulation of pyramidal neurons in the human and monkey neocortex. *J Comp Neurol* 1989; 282: 191-205.

Cannelli N, Cassandrini D, Bertini E, Striano P, Fusco L, Gaggero R, Specchio N, Biancheri R, Vigevano F, Bruno C, Simonati A, Zara F, Santorelli FM. Novel mutations in CLN8 in Italian variant late infantile neuronal ceroid lipofuscinosis: Another genetic hit in the mediterranean. *Neurogenetics* 2006; 7: 111-7.

Cardona F & Rosati E. Neuronal ceroid-lipofuscinoses in Italy: An epidemiological study. *Am J Med Genet* 1995; 57: 142-3.

Carson MJ, Bilousova TV, Puntambekar SS, Melchior B, Doose JM, Ethell IM. A rose by any other name? The potential consequences of microglial heterogeneity during CNS health and disease. *Neurotherapeutics* 2007; 4: 571-9.

Chang B, Bronson RT, Hawes NL, Roderick TH, Peng C, Hageman GS, Heckenlively JR. Retinal degeneration in motor neuron degeneration: A mouse model of ceroid lipofuscinosis. *Invest Ophthalmol Vis Sci* 1994; 35: 1071-6.

Chrast R, Saher G, Nave KA, Verheijen MH. Lipid metabolism in myelinating glial cells: Lessons from human inherited disorders and mouse models. *J Lipid Res* 2011; 52: 419-34.

Claussen M, Heim P, Knispel J, Goebel HH, Kohlschutter A. Incidence of neuronal ceroid-lipofuscinoses in west germany: Variation of a method for studying autosomal recessive disorders. *Am J Med Genet* 1992; 42: 536-8.

Coetzee T, Fujita N, Dupree J, Shi R, Blight A, Suzuki K, Suzuki K, Popko B. Myelination in the absence of galactocerebroside and sulfatide: Normal structure with abnormal function and regional instability. *Cell* 1996; 86: 209-19.

Cooper JD. The neuronal ceroid lipofuscinoses: The same, but different? *Biochem Soc Trans* 2010; 38: 1448-52.

Cooper JD, Russell C, Mitchison HM. Progress towards understanding disease mechanisms in small vertebrate models of neuronal ceroid lipofuscinosis. *Biochim Biophys Acta* 2006; 1762: 873-89.

Cooper JD. Progress towards understanding the neurobiology of Batten disease or neuronal ceroid lipofuscinosis. *Curr Opin Neurol* 2003; 16: 121-8.

Cooper JD, Messer A, Feng AK, Chua-Couzens J, Mobley WC. Apparent loss and hypertrophy of interneurons in a mouse model of neuronal ceroid lipofuscinosis: Evidence for partial response to insulin-like growth factor-1 treatment. *J Neurosci* 1999; 19: 2556-67.

Cullen V, Lindfors M, Ng J, Paetau A, Swinton E, Kolodziej P, Boston H, Saftig P, Woulfe J, Feany MB, Myllykangas L, Schlossmacher MG, Tyynela J. Cathepsin D expression level affects alpha-synuclein processing, aggregation, and toxicity in vivo. *Mol Brain* 2009; 2: 5.

De Stefanis D, Reffo P, Bonelli G, Baccino FM, Sala G, Ghidoni R, Codogno P, Isidoro C. Increase in ceramide level alters the lysosomal targeting of cathepsin D prior to onset of apoptosis in HT-29 colon cancer cells. *Biol Chem* 2002; 383: 989-99.

de Voer G, van der Bent P, Rodrigues AJ, van Ommen GJ, Peters DJ, Taschner PE. Deletion of the caenorhabditis elegans homologues of the CLN3 gene, involved in human juvenile neuronal ceroid lipofuscinosis, causes a mild progeric phenotype. *J Inherit Metab Dis* 2005; 28: 1065-80.

DeFelipe J. The evolution of the brain, the human nature of cortical circuits, and intellectual creativity. *Front Neuroanat* 2011; 5: 29.

Duran MC, Martin-Ventura JL, Mohammed S, Barderas MG, Blanco-Colio LM, Mas S, Moral V, Ortega L, Tunon J, Jensen ON, Vivanco F, Egido J. Atorvastatin modulates the profile of proteins released by human atherosclerotic plaques. *Eur J Pharmacol* 2007; 562: 119-29.

Elger B, Schneider M, Winter E, Carvelli L, Bonomi M, Fracasso C, Guiso G, Colovic M, Caccia S, Mennini T. Optimized synthesis of AMPA receptor antagonist ZK 187638 and neurobehavioral activity in a mouse model of neuronal ceroid lipofuscinosis. *ChemMedChem* 2006; 1: 1142-8.

Elston GN. Cortex, cognition and the cell: New insights into the pyramidal neuron and prefrontal function. *Cereb Cortex* 2003; 13: 1124-38.

Eroglu C & Barres BA. Regulation of synaptic connectivity by glia. *Nature* 2010; 468: 223-31.

Evans J, Katz ML, Levesque D, Shelton GD, de Lahunta A, O'Brien D. A variant form of neuronal ceroid lipofuscinosis in american bulldogs. *J Vet Intern Med* 2005; 19: 44-51.

Feany MB & Bender WW. A *Drosophila* model of Parkinson's disease. *Nature* 2000; 404: 394-8.

Ferguson SM, Brasnjo G, Hayashi M, Wolfel M, Collesi C, Giovedi S, Raimondi A, Gong LW, Ariel P, Paradise S, O'toole E, Flavell R, Cremona O, Miesenbock G, Ryan TA, De Camilli P. A selective activity-dependent requirement for dynamin 1 in synaptic vesicle endocytosis. *Science* 2007; 316: 570-4.

Folch J, Lees M, Sloane Stanley GH. A simple method for the isolation and purification of total lipides from animal tissues. *J Biol Chem* 1957; 226: 497-509.

Follo C, Ozzano M, Mugoni V, Castino R, Santoro M, Isidoro C. Knock-down of cathepsin D affects the retinal pigment epithelium, impairs swim-bladder ontogenesis and causes premature death in zebrafish. *PLoS One* 2011; 6: e21908.

Freeman MR & Doherty J. Glial cell biology in *Drosophila* and vertebrates. *Trends Neurosci* 2006; 29: 82-90.

Fritchie K, Siintola E, Armao D, Lehesjoki AE, Marino T, Powell C, Tennison M, Booker JM, Koch S, Partanen S, Suzuki K, Tyynela J, Thorne LB. Novel mutation and the first prenatal screening of cathepsin D deficiency (CLN10). *Acta Neuropathol* 2009; 117: 201-8.

Fujita K, Shibayama K, Yamauchi M, Kato T, Ando M, Takahashi H, Iritani K, Yoshimoto N, Nagata Y. Alteration of enzymatic activities implicating neuronal degeneration in the spinal cord of the motor neuron degeneration mouse during postnatal development. *Neurochem Res* 1998; 23: 557-62.

Fulton DL, Denarier E, Friedman HC, Wasserman WW, Peterson AC. Towards resolving the transcription factor network controlling myelin gene expression. *Nucleic Acids Res* 2011; 39: 7974-91.

Gagliardi C & Bunnell BA. Large animal models of neurological disorders for gene therapy. ILAR J. 2009; 50: 128-43.

Galizzi G, Russo D, Deidda I, Cascio C, Passantino R, Guarneri R, Bigini P, Mennini T, Drago G, Guarneri P. Different early ER-stress responses in the CLN8(mnd) mouse model of neuronal ceroid lipofuscinosis. *Neurosci Lett* 2011; 488: 258-62.

Gamble W, Vaughan M, Kruth HS, Avigan J. Procedure for determination of free and total cholesterol in micro- or nanogram amounts suitable for studies with cultured cells. *J Lipid Res* 1978; 19: 1068-70.

Gao H, Boustany RM, Espinola JA, Cotman SL, Srinidhi L, Antonellis KA, Gillis T, Qin X, Liu S, Donahue LR, Bronson RT, Faust JR, Stout D, Haines JL, Lerner TJ, MacDonald ME. Mutations in a novel CLN6-encoded transmembrane protein cause variant neuronal ceroid lipofuscinosis in man and mouse. *Am J Hum Genet* 2002; 70: 324-35.

Garcia-Marin V, Garcia-Lopez P, Freire M. Cajal's contributions to glia research. *Trends Neurosci* 2007; 30: 479-87.

Gertler FB, Chiu CY, Richter-Mann L, Chin DJ. Developmental and metabolic regulation of the *Drosophila melanogaster* 3-hydroxy-3-methylglutaryl coenzyme A reductase. *Mol Cell Biol* 1988; 8: 2713-21.

Getty AL & Pearce DA. Interactions of the proteins of neuronal ceroid lipofuscinosis: Clues to function. *Cell Mol Life Sci* 2011; 68: 453-74.

Ghezzi P, Bernardini R, Giuffrida R, Bellomo M, Manzoni C, Comoletti D, Di Santo E, Benigni F, Mennini T. Tumor necrosis factor is increased in the spinal cord of an animal model of motor neuron degeneration. *Eur Cytokine Netw* 1998; 9: 139-44.

Giaume C, Koulakoff A, Roux L, Holcman D, Rouach N. Astroglial networks: A step further in neuroglial and gliovascular interactions. *Nat Rev Neurosci* 2010; 11: 87-99.

Gopalakrishnan MM, Grosch HW, Locatelli-Hoops S, Werth N, Smolenova E, Nettersheim M, Sandhoff K, Hasilik A. Purified recombinant human prosaposin forms oligomers that bind procathepsin D and affect its autoactivation. *Biochem J* 2004; 383: 507-15.

Gorio A, Germani E, Lesma E, Rossoni G, Muller EE, Di Giulio AM. Long-term neuroprotective effects of glycosaminoglycans-IGF-I cotreatment in the motor neuron degeneration (mnd) mutant mouse. *Eur J Neurosci* 1999; 11: 3395-404.

Goswami R, Ahmed M, Kilkus J, Han T, Dawson SA, Dawson G. Differential regulation of ceramide in lipid-rich microdomains (rafts): Antagonistic role of palmitoyl:Protein thioesterase and neutral sphingomyelinase 2. *J Neurosci Res* 2005; 81: 208-17.

Granier LA, Langley K, Leray C, Sarlieve LL. Phospholipid composition in late infantile neuronal ceroid lipofuscinosis. *Eur J Clin Invest* 2000; 30: 1011-7.

Griffey M, Macauley SL, Ogilvie JM, Sands MS. AAV2-mediated ocular gene therapy for infantile neuronal ceroid lipofuscinosis. *Mol Ther* 2005; 12: 413-21.

Guarneri R, Russo D, Cascio C, D'Agostino S, Galizzi G, Bigini P, Mennini T, Guarneri P. Retinal oxidation, apoptosis and age- and sex-differences in the mnd mutant mouse, a model of neuronal ceroid lipofuscinosis. *Brain Res* 2004; 1014: 209-20.

Guillas I, Jiang JC, Vionnet C, Roubaty C, Uldry D, Chuard R, Wang J, Jazwinski SM, Conzelmann A. Human homologues of LAG1 reconstitute acyl-CoA-dependent ceramide synthesis in yeast. *J Biol Chem* 2003; 278: 37083-91.

Guillas I, Kirchman PA, Chuard R, Pfefferli M, Jiang JC, Jazwinski SM, Conzelmann A. C26-CoA-dependent ceramide synthesis of saccharomyces cerevisiae is operated by Lag1p and Lac1p. *EMBO J* 2001; 20: 2655-65.

Hafezparast M, Ahmad-Annuar A, Wood NW, Tabrizi SJ, Fisher EM. Mouse models for neurological disease. *Lancet Neurol* 2002; 1: 215-24.

Haidar B, Kiss RS, Sarov-Blat L, Brunet R, Harder C, McPherson R, Marcel YL. Cathepsin D, a lysosomal protease, regulates ABCA1-mediated lipid efflux. *J Biol Chem* 2006; 281: 39971-81.

Haltia M. The neuronal ceroid-lipofuscinoses: From past to present. *Biochim Biophys Acta* 2006; 1762: 850-6.

Haltia M. The neuronal ceroid-lipofuscinoses. *J Neuropathol Exp Neurol* 2003; 62: 1-13.

Hamilton NB & Attwell D. Do astrocytes really exocytose neurotransmitters? *Nat Rev Neurosci* 2010; 11: 227-38.

Hanisch UK & Kettenmann H. Microglia: Active sensor and versatile effector cells in the normal and pathologic brain. *Nat Neurosci* 2007; 10: 1387-94.

Harper A. Mouse models of neurological disorders--a comparison of heritable and acquired traits. *Biochim Biophys Acta* 2010; 1802: 785-95.

Haupt WF& Stoffel W. Nerve conduction velocity measurements reveal the functional deficit in ceramide galactosyl transferase-deficient (Cgt-/-) mice. *J Neurol Sci* 2004; 217: 83-8.

He X, Di Y, Li J, Xie Y, Tang Y, Zhang F, Wei L, Zhang Y, Qin W, Huo K, Li Y, Wan D, Gu J. Molecular cloning and characterization of CT120, a novel membrane-associated gene involved in amino acid transport and glutathione metabolism. *Biochem Biophys Res Commun* 2002; 297: 528-36.

Hegde RS, Voigt S, Rapoport TA, Lingappa VR. TRAM regulates the exposure of nascent secretory proteins to the cytosol during translocation into the endoplasmic reticulum. *Cell* 1998; 92: 621-31.

Heinonen O, Kyttala A, Lehmus E, Paunio T, Peltonen L, Jalanko A. Expression of palmitoyl protein thioesterase in neurons. *Mol Genet Metab* 2000; 69: 123-9.

Heinrich M, Wickel M, Winoto-Morbach S, Schneider-Brachert W, Weber T, Brunner J, Saftig P, Peters C, Kronke M, Schutze S. Ceramide as an activator lipid of cathepsin D. *Adv Exp Med Biol* 2000; 477: 305-15.

Heinrich M, Wickel M, Schneider-Brachert W, Sandberg C, Gahr J, Schwandner R, Weber T, Saftig P, Peters C, Brunner J, Kronke M, Schutze S. Cathepsin D targeted by acid sphingomyelinase-derived ceramide. *EMBO J* 1999; 18: 5252-63.

Hennig KM, Colombani J, Neufeld TP. TOR coordinates bulk and targeted endocytosis in the *Drosophila melanogaster* fat body to regulate cell growth. *J Cell Biol* 2006; 173: 963-74.

Hermansson M, Kakela R, Berghall M, Lehesjoki AE, Somerharju P, Lahtinen U. Mass spectrometric analysis reveals changes in phospholipid, neutral sphingolipid and sulfatide molecular species in progressive epilepsy with mental retardation, EPMR, brain: A case study. *J Neurochem* 2005; 95: 609-17.

Herva R, Tyynela J, Hirvasniemi A, Syrjakallio-Ylitalo M, Haltia M. Northern epilepsy: A novel form of neuronal ceroid-lipofuscinosis. *Brain Pathol* 2000; 10: 215-22.

Hickey AJ, Chotkowski HL, Singh N, Ault JG, Korey CA, MacDonald ME, Glaser RL. Palmitoyl-protein thioesterase 1 deficiency in *Drosophila melanogaster* causes accumulation of abnormal storage material and reduced life span. *Genetics* 2006; 172: 2379-90.

Hiraiwa M, Martin BM, Kishimoto Y, Conner GE, Tsuji S, O'Brien JS. Lysosomal proteolysis of prosaposin, the precursor of saposins (sphingolipid activator proteins): Its mechanism and inhibition by ganglioside. *Arch Biochem Biophys* 1997; 341: 17-24.

Hirvasniemi A, Herrala P, Leisti J. Northern epilepsy syndrome: Clinical course and the effect of medication on seizures. *Epilepsia* 1995; 36: 792-7.

Hirvasniemi A& Karumo J. Neuroradiological findings in the northern epilepsy syndrome. *Acta Neurol Scand* 1994; 90: 388-93.

Hirvasniemi A, Lang H, Lehesjoki AE, Leisti J. Northern epilepsy syndrome: An inherited childhood onset epilepsy with associated mental deterioration. *J Med Genet* 1994; 31: 177-82.

Hobert JA& Dawson G. A novel role of the Batten disease gene CLN3: Association with BMP synthesis. *Biochem Biophys Res Commun* 2007; 358: 111-6.

Iadecola C& Nedergaard M. Glial regulation of the cerebral microvasculature. *Nat Neurosci* 2007; 10: 1369-76.

The International Batten Disease Consortium. Isolation of a novel gene underlying Batten disease, CLN3. *Cell* 1995; 82: 949-57.

Jabs S, Quitsch A, Kakela R, Koch B, Tyynela J, Brade H, Glatzel M, Walkley S, Saftig P, Vanier MT, Braulke T. Accumulation of bis(monoacylglycero)phosphate and gangliosides in mouse models of neuronal ceroid lipofuscinosis. *J Neurochem* 2008; 106: 1415-25.

Jalanko A& Braulke T. Neuronal ceroid lipofuscinoses. *Biochim Biophys Acta* 2009; 1793: 697-709.

Jalanko A, Tyynela J, Peltonen L. From genes to systems: New global strategies for the characterization of NCL biology. *Biochim Biophys Acta* 2006; 1762: 934-44.

Jalanko A, Vesa J, Manninen T, von Schantz C, Minye H, Fabritius AL, Salonen T, Rapola J, Gentile M, Kopra O, Peltonen L. Mice with Ppt1Deltaex4 mutation replicate the INCL phenotype and show an inflammation-associated loss of interneurons. *Neurobiol Dis* 2005; 18: 226-41.

Joensuu T, Lehesjoki AE, Kopra O. Molecular background of EPM1-Unverricht-Lundborg disease. *Epilepsia* 2008; 49: 557-63.

Jones EG. Synchrony in the interconnected circuitry of the thalamus and cerebral cortex. *Ann N Y Acad Sci* 2009; 1157: 10-23.

Kakela R, Somerharju P, Tyynela J. Analysis of phospholipid molecular species in brains from patients with infantile and juvenile neuronal-ceroid lipofuscinosis using liquid chromatography-electrospray ionization mass spectrometry. *J Neurochem* 2003; 84: 1051-65.

Kandel E, Schwartz J, Jessell T (Editors). Principles of Neural Science. McGraw-Hill Medical, USA, 2000.

Katz ML, Khan S, Awano T, Shahid SA, Siakotos AN, Johnson GS. A mutation in the CLN8 gene in english setter dogs with neuronal ceroid-lipofuscinosis. *Biochem Biophys Res Commun* 2005; 327: 541-7.

Kawasaki F, Hazen M, Ordway RW. Fast synaptic fatigue in shibire mutants reveals a rapid requirement for dynamin in synaptic vesicle membrane trafficking. *Nat Neurosci* 2000; 3: 859-60.

Kay GW, Palmer DN, Rezaie P, Cooper JD. Activation of non-neuronal cells within the prenatal developing brain of sheep with neuronal ceroid lipofuscinosis. *Brain Pathol* 2006; 16: 110-6.

Kestila M, Ikonen E, Lehesjoki AE. Finnish disease heritage. *Duodecim* 2010; 126: 2311-20.

Kielar C, Wishart TM, Palmer A, Dihanich S, Wong AM, Macauley SL, Chan CH, Sands MS, Pearce DA, Cooper JD, Gillingwater TH. Molecular correlates of axonal and synaptic pathology in mouse models of Batten disease. *Hum Mol Genet* 2009; 18: 4066-80.

Kielar C, Maddox L, Bible E, Pontikis CC, Macauley SL, Griffey MA, Wong M, Sands MS, Cooper JD. Successive neuron loss in the thalamus and cortex in a mouse model of infantile neuronal ceroid lipofuscinosis. *Neurobiol Dis* 2007; 25: 150-62.

Kim KK, Adelstein RS, Kawamoto S. Identification of neuronal nuclei (NeuN) as fox-3, a new member of the fox-1 gene family of splicing factors. *J Biol Chem* 2009; 284: 31052-61.

Kim SJ, Zhang Z, Sarkar C, Tsai PC, Lee YC, Dye L, Mukherjee AB. Palmitoyl protein thioesterase-1 deficiency impairs synaptic vesicle recycling at nerve terminals, contributing to neuropathology in humans and mice. *J Clin Invest* 2008; 118: 3075-86.

Koch S, Molchanova SM, Wright AK, Edwards A, Cooper JD, Taira T, Gillingwater TH, Tyynela J. Morphologic and functional correlates of synaptic pathology in the cathepsin D knockout mouse model of congenital neuronal ceroid lipofuscinosis. *J Neuropathol Exp Neurol* 2011; 70: 1089-96.

Koike M, Shibata M, Waguri S, Yoshimura K, Tanida I, Kominami E, Gotow T, Peters C, von Figura K, Mizushima N, Saftig P, Uchiyama Y. Participation of autophagy in storage of lysosomes in neurons from mouse models of neuronal ceroid-lipofuscinoses (Batten disease). *Am J Pathol* 2005; 167: 1713-28.

Koike M, Shibata M, Ohsawa Y, Nakanishi H, Koga T, Kametaka S, Waguri S, Momoi T, Kominami E, Peters C, Figura K, Saftig P, Uchiyama Y. Involvement of two different cell death pathways in retinal atrophy of cathepsin D-deficient mice. *Mol Cell Neurosci* 2003; 22: 146-61.

Koike M, Nakanishi H, Saftig P, Ezaki J, Isahara K, Ohsawa Y, Schulz-Schaeffer W, Watanabe T, Waguri S, Kametaka S, Shibata M, Yamamoto K, Kominami E, Peters C, von Figura K, Uchiyama Y. Cathepsin D deficiency induces lysosomal storage with ceroid lipofuscin in mouse CNS neurons. *J Neurosci* 2000; 20: 6898-906.

Kolikova J, Afzalov R, Surin A, Lehesjoki AE, Khiroug L. Deficient mitochondrial ca(2+) buffering in the Cln8(mnd) mouse model of neuronal ceroid lipofuscinosis. *Cell Calcium* 2011; 50: 491-501.

Kopra O, Vesa J, von Schantz C, Manninen T, Minye H, Fabritius AL, Rapola J, van Diggelen OP, Saarela J, Jalanko A, Peltonen L. A mouse model for finnish variant late infantile neuronal ceroid lipofuscinosis, CLN5, reveals neuropathology associated with early aging. *Hum Mol Genet* 2004; 13: 2893-906.

Korey CA & MacDonald ME. An over-expression system for characterizing Ppt1 function in *Drosophila*. *BMC Neurosci* 2003; 4: 30.

Kousi M, Lehesjoki AE, Mole SE. Update of the mutation spectrum and clinical correlations of over 360 mutations in eight genes that underlie the neuronal ceroid lipofuscinoses. *Hum Mutat* 2012; 33: 42-63.

Kousi M, Siintola E, Dvorakova L, Vlaskova H, Turnbull J, Topcu M, Yuksel D, Gokben S, Minassian BA, Elleder M, Mole SE, Lehesjoki AE. Mutations in CLN7/MFSD8 are a common cause of variant late-infantile neuronal ceroid lipofuscinosis. *Brain* 2009; 132: 810-9.

Kretzschmar D. Swiss cheese et allii, some of the first neurodegenerative mutants isolated in *Drosophila*. *J Neurogenet* 2009; 1-8.

Lang AH, Hirvasniemi A, Siivola J. Neurophysiological findings in the northern epilepsy syndrome. *Acta Neurol Scand* 1997; 95: 1-8.

Laurent-Matha V, Lucas A, Huttler S, Sandhoff K, Garcia M, Rochefort H. Procathepsin D interacts with prosaposin in cancer cells but its internalization is not mediated by LDL receptor-related protein. *Exp Cell Res* 2002; 277: 210-9.

Lauronen L, Santavuori P, Hirvasniemi A, Kirveskari E, Huttunen J, Autti T. Northern epilepsy syndrome (NES, CLN8)--MRI and electrophysiological studies. *Eur J Paediatr Neurol* 2001; 5 Suppl A: 167-73.

Lehtovirta M, Kyttala A, Eskelinen EL, Hess M, Heinonen O, Jalanko A. Palmitoyl protein thioesterase (PPT) localizes into synaptosomes and synaptic vesicles in neurons: Implications for infantile neuronal ceroid lipofuscinosis (INCL). *Hum Mol Genet* 2001; 10: 69-75.

Lentz, T.L., Erulkar, S.D., Nervous system - evolution and development of the nervous system. Encyclopædia Britannica Online. 2012:.

Levy M & Futerman AH. Mammalian ceramide synthases. *IUBMB Life* 2010; 62: 347-56.

Liaudet-Coopman E, Beaujouin M, Derocq D, Garcia M, Glondu-Lassis M, Laurent-Matha V, Prebois C, Rochefort H, Vignon F. Cathepsin D: Newly discovered functions of a long-standing aspartic protease in cancer and apoptosis. *Cancer Lett* 2006; 237: 167-79.

Llinas RR. The contribution of Santiago Ramon y Cajal to functional neuroscience. *Nat Rev Neurosci* 2003; 4: 77-80.

Lonka L, Aalto A, Kopra O, Kuronen M, Kokaia Z, Saarma M, Lehesjoki AE. The neuronal ceroid lipofuscinosis Cln8 gene expression is developmentally regulated in mouse brain and up-regulated in the hippocampal kindling model of epilepsy. *BMC Neurosci* 2005; 6: 27.

Lonka L, Salonen T, Siintola E, Kopra O, Lehesjoki AE, Jalanko A. Localization of wild-type and mutant neuronal ceroid lipofuscinosis CLN8 proteins in non-neuronal and neuronal cells. *J Neurosci Res* 2004; 76: 862-71.

Lonka L, Kyttala A, Ranta S, Jalanko A, Lehesjoki AE. The neuronal ceroid lipofuscinosis CLN8 membrane protein is a resident of the endoplasmic reticulum. *Hum Mol Genet* 2000; 9: 1691-7.

Lyly A, Marjavaara SK, Kyttala A, Uusi-Rauva K, Luiro K, Kopra O, Martinez LO, Tanhuanpaa K, Kalkkinen N, Suomalainen A, Jauhiainen M, Jalanko A. Deficiency of the INCL protein Ppt1 results in changes in ectopic F1-ATP synthase and altered cholesterol metabolism. *Hum Mol Genet* 2008; 17: 1406-17.

Macauley SL, Pekny M, Sands MS. The role of attenuated astrocyte activation in infantile neuronal ceroid lipofuscinosis. *J Neurosci* 2011; 31: 15575-85.

Macauley SL, Wozniak DF, Kielar C, Tan Y, Cooper JD, Sands MS. Cerebellar pathology and motor deficits in the palmitoyl protein thioesterase 1-deficient mouse. *Exp Neurol* 2009; 217: 124-35.

Maragakis NJ & Rothstein JD. Mechanisms of disease: Astrocytes in neurodegenerative disease. *Nat Clin Pract Neurol* 2006; 2: 679-89.

Marcus J & Popko B. Galactolipids are molecular determinants of myelin development and axo-glial organization. *Biochim Biophys Acta* 2002; 1573: 406-13.

Markram H, Toledo-Rodriguez M, Wang Y, Gupta A, Silberberg G, Wu C. Interneurons of the neocortical inhibitory system. *Nat Rev Neurosci* 2004; 5: 793-807.

Marsh JL & Thompson LM. *Drosophila* in the study of neurodegenerative disease. *Neuron* 2006; 52: 169-78.

Melo T, Bigini P, Sonnewald U, Balosso S, Cagnotto A, Barbera S, Uboldi S, Vezzani A, Mennini T. Neuronal hyperexcitability and seizures are associated with changes in glial-neuronal interactions in the hippocampus of a mouse model of epilepsy with mental retardation. *J Neurochem* 2010; 115: 1445-54.

Mennini T, Bigini P, Cagnotto A, Carvelli L, Di Nunno P, Fumagalli E, Tortarolo M, Buurman WA, Ghezzi P, Bendotti C. Glial activation and TNFR-I upregulation precedes motor dysfunction in the spinal cord of mnd mice. *Cytokine* 2004; 25: 127-35.

Mennini T, Bigini P, Ravizza T, Vezzani A, Calvaresi N, Tortarolo M, Bendotti C. Expression of glutamate receptor subtypes in the spinal cord of control and mnd mice, a model of motor neuron disorder. *J Neurosci Res* 2002; 70: 553-60.

Mennini T, Cagnotto A, Carvelli L, Comoletti D, Manzoni C, Muzio V, Rizzi M, Vezzani A. Biochemical and pharmacological evidence of a functional role of AMPA receptors in motor neuron dysfunction in mnd mice. *Eur J Neurosci* 1999; 11: 1705-10.

Mennini T, Bastone A, Crespi D, Comoletti D, Manzoni C. Spinal cord GLT-1 glutamate transporter and blood glutamic acid alterations in motor neuron degeneration (mnd) mice. *J Neurol Sci* 1998; 157: 31-6.

Messer A & Plummer J. Accumulating autofluorescent material as a marker for early changes in the spinal cord of the mnd mouse. *Neuromuscul Disord* 1993; 3: 129-34.

Messer A, Plummer J, Wong V, Lavail MM. Retinal degeneration in motor neuron degeneration (mnd) mutant mice. *Exp Eye Res* 1993; 57: 637-41.

Messer A, Strominger NL, Mazurkiewicz JE. Histopathology of the late-onset motor neuron degeneration (mnd) mutant in the mouse. *J Neurogenet* 1987; 4: 201-13.

Messer A & Flaherty L. Autosomal dominance in a late-onset motor neuron disease in the mouse. *J Neurogenet* 1986; 3: 345-55.

Milligan ED & Watkins LR. Pathological and protective roles of glia in chronic pain. *Nat Rev Neurosci* 2009; 10: 23-36.

Missirlis F, Phillips JP, Jackle H. Cooperative action of antioxidant defense systems in *Drosophila. Curr Biol* 2001; 11: 1272-7.

Mole SE, Williams RE, Goebel HH. Correlations between genotype, ultrastructural morphology and clinical phenotype in the neuronal ceroid lipofuscinoses. *Neurogenetics* 2005; 6: 107-26.

Montell C. Visual transduction in *Drosophila. Annu Rev Cell Dev Biol* 1999; 15: 231-68.

Muqit MM& Feany MB. Modelling neurodegenerative diseases in *Drosophila*: A fruitful approach? *Nat Rev Neurosci* 2002; 3: 237-43.

Mutka AL, Haapanen A, Kakela R, Lindfors M, Wright AK, Inkinen T, Hermansson M, Rokka A, Corthals G, Jauhiainen M, Gillingwater TH, Ikonen E, Tyynela J. Murine cathepsin D deficiency is associated with dysmyelination/myelin disruption and accumulation of cholesteryl esters in the brain. *J Neurochem* 2010; 112: 193-203.

Myllykangas L, Tyynela J, Page-McCaw A, Rubin GM, Haltia MJ, Feany MB. Cathepsin D-deficient *Drosophila* recapitulate the key features of neuronal ceroid lipofuscinoses. *Neurobiol Dis* 2005; 19: 194-9.

Nakanishi H& Wu Z. Microglia-aging: Roles of microglial lysosome- and mitochondria-derived reactive oxygen species in brain aging. *Behav Brain Res* 2009; 201: 1-7.

Nakanishi H, Zhang J, Koike M, Nishioku T, Okamoto Y, Kominami E, von Figura K, Peters C, Yamamoto K, Saftig P, Uchiyama Y. Involvement of nitric oxide released from microglia-macrophages in pathological changes of cathepsin D-deficient mice. *J Neurosci* 2001; 21: 7526-33.

Napoli I& Neumann H. Microglial clearance function in health and disease. *Neuroscience* 2009; 158: 1030-8.

Narayan SB, Rakheja D, Tan L, Pastor JV, Bennett MJ. CLN3P, the Batten's disease protein, is a novel palmitoyl-protein delta-9 desaturase. *Ann Neurol* 2006; 60: 570-7.

Nash B, Thomson CE, Linington C, Arthur AT, McClure JD, McBride MW, Barnett SC. Functional duality of astrocytes in myelination. *J Neurosci* 2011; 31: 13028-38.

Nave KA. Myelination and support of axonal integrity by glia. *Nature* 2010; 468: 244-52.

Neskovic NM, Roussel G, Nussbaum JL. UDPgalactose:Ceramide galactosyltransferase of rat brain: A new method of purification and production of specific antibodies. *J Neurochem* 1986; 47: 1412-8.

Nichols CD. *Drosophila melanogaster* neurobiology, neuropharmacology, and how the fly can inform central nervous system drug discovery. *Pharmacol Ther* 2006; 112: 677-700.

Nilsson T & Warren G. Retention and retrieval in the endoplasmic reticulum and the golgi apparatus. *Curr Opin Cell Biol* 1994; 6: 517-21.

Norio R. The Finnish disease heritage III: The individual diseases. *Hum Genet* 2003a; 112: 470-526.

Norio R. Finnish disease heritage I: Characteristics, causes, background. *Hum Genet* 2003b; 112: 441-56.

Noskova L, Stranecky V, Hartmannova H, Pristoupilova A, Baresova V, Ivanek R, Hulkova H, Jahnova H, van der Zee J, Staropoli JF, Sims KB, Tyynela J, Van Broeckhoven C, Nijssen PC, Mole SE, Elleder M, Kmoch S. Mutations in DNAJC5, encoding cysteine-string protein alpha, cause autosomal-dominant adult-onset neuronal ceroid lipofuscinosis. *Am J Hum Genet* 2011; 89: 241-52.

Oswald MJ, Palmer DN, Kay GW, Barwell KJ, Cooper JD. Location and connectivity determine GABAergic interneuron survival in the brains of south hampshire sheep with CLN6 neuronal ceroid lipofuscinosis. *Neurobiol Dis* 2008; 32: 50-65.

Oswald MJ, Palmer DN, Kay GW, Shemilt SJ, Rezaie P, Cooper JD. Glial activation spreads from specific cerebral foci and precedes neurodegeneration in presymptomatic ovine neuronal ceroid lipofuscinosis (CLN6). *Neurobiol Dis* 2005; 20: 49-63.

Oswald MJ, Kay GW, Palmer DN. Changes in GABAergic neuron distribution in situ and in neuron cultures in ovine (OCL6) Batten disease. *Eur J Paediatr Neurol* 2001; 5 Suppl A: 135-42.

Padilla-Lopez S, Langager D, Chan CH, Pearce DA. BTN1, the saccharomyces cerevisiae homolog to the human Batten disease gene, is involved in phospholipid distribution. *Dis Model Mech* 2012; 5: 191-9.

Palmer DN, Martinus RD, Cooper SM, Midwinter GG, Reid JC, Jolly RD. Ovine ceroid lipofuscinosis. the major lipopigment protein and the lipid-binding subunit of mitochondrial ATP synthase have the same NH2-terminal sequence. *J Biol Chem* 1989; 264: 5736-40.

Palmer DN, Barns G, Husbands DR, Jolly RD. Ceroid lipofuscinosis in sheep. II. the major component of the lipopigment in liver, kidney, pancreas, and brain is low molecular weight protein. *J Biol Chem* 1986; 261: 1773-7.

Pardo CA, Rabin BA, Palmer DN, Price DL. Accumulation of the adenosine triphosphate synthase subunit C in the mnd mutant mouse. A model for neuronal ceroid lipofuscinosis. *Am J Pathol* 1994; 144: 829-35.

Partanen S, Haapanen A, Kielar C, Pontikis C, Alexander N, Inkinen T, Saftig P, Gillingwater TH, Cooper JD, Tyynela J. Synaptic changes in the thalamocortical system of cathepsin D-deficient mice: A model of human congenital neuronal ceroid-lipofuscinosis. *J Neuropathol Exp Neurol* 2008; 67: 16-29.

Paxinos G, Franklin KBJ. The Mouse Brain in Stereotaxic Coordinates. Academic Press, San Diego, CA, 2001

Pedraza CE, Monk R, Lei J, Hao Q, Macklin WB. Production, characterization, and efficient transfection of highly pure oligodendrocyte precursor cultures from mouse embryonic neural progenitors. *Glia* 2008; 56: 1339-52.

Pekny M & Nilsson M. Astrocyte activation and reactive gliosis. *Glia* 2005; 50: 427-34.

Pekny M & Pekna M. Astrocyte intermediate filaments in CNS pathologies and regeneration. *J Pathol* 2004; 204: 428-37.

Persaud-Sawin DA, Mousallem T, Wang C, Zucker A, Kominami E, Boustany RM. Neuronal ceroid lipofuscinosis: A common pathway? *Pediatr Res* 2007; 61: 146-52.

Pewzner-Jung Y, Ben-Dor S, Futerman AH. When do lasses (longevity assurance genes) become CerS (ceramide synthases)?: Insights into the regulation of ceramide synthesis. *J Biol Chem* 2006; 281: 25001-5.

Pivtoraiko VN, Stone SL, Roth KA, Shacka JJ. Oxidative stress and autophagy in the regulation of lysosome-dependent neuron death. *Antioxid Redox Signal* 2009; 11: 481-96.

Plummer J, Peterson A, Messer A. Accelerated and widespread neuronal loss occurs in motor neuron degeneration (mnd) mice expressing a neurofilament-disrupting transgene. *Mol Cell Neurosci* 1995; 6: 532-43.

Pontikis CC, Cotman SL, MacDonald ME, Cooper JD. Thalamocortical neuron loss and localized astrocytosis in the Cln3Deltaex7/8 knock-in mouse model of Batten disease. *Neurobiol Dis* 2005; 20: 823-36.

Pontikis CC, Cella CV, Parihar N, Lim MJ, Chakrabarti S, Mitchison HM, Mobley WC, Rezaie P, Pearce DA, Cooper JD. Late onset neurodegeneration in the Cln3-/- mouse model of juvenile neuronal ceroid lipofuscinosis is preceded by low level glial activation. *Brain Res* 2004; 1023: 231-42.

Porter MY, Turmaine M, Mole SE. Identification and characterization of caenorhabditis elegans palmitoyl protein thioesterase1. *J Neurosci Res* 2005; 79: 836-48.

Rakheja D, Narayan SB, Bennett MJ. The function of CLN3P, the Batten disease protein. *Mol Genet Metab* 2008; 93: 269-74.

Rakheja D, Narayan SB, Pastor JV, Bennett MJ. CLN3P, the Batten disease protein, localizes to membrane lipid rafts (detergent-resistant membranes). *Biochem Biophys Res Commun* 2004; 317: 988-91.

Rakoczy PE, Zhang D, Robertson T, Barnett NL, Papadimitriou J, Constable IJ, Lai CM. Progressive age-related changes similar to age-related macular degeneration in a transgenic mouse model. *Am J Pathol* 2002; 161: 1515-24.

Rakoczy PE, Lai CM, Baines M, Di Grandi S, Fitton JH, Constable IJ. Modulation of cathepsin D activity in retinal pigment epithelial cells. *Biochem J* 1997; 324 (Pt 3): 935-40.

Rakoczy PE, Baines M, Kennedy CJ, Constable IJ. Correlation between autofluorescent debris accumulation and the presence of partially processed forms of cathepsin D in cultured retinal pigment epithelial cells challenged with rod outer segments. *Exp Eye Res* 1996; 63: 159-67.

Ramirez A, Heimbach A, Grundemann J, Stiller B, Hampshire D, Cid LP, Goebel I, Mubaidin AF, Wriekat AL, Roeper J, Al-Din A, Hillmer AM, Karsak M, Liss B, Woods CG, Behrens MI, Kubisch C. Hereditary parkinsonism with dementia is caused by mutations in ATP13A2, encoding a lysosomal type 5 P-type ATPase. *Nat Genet* 2006; 38: 1184-91.

Ranta S, Topcu M, Tegelberg S, Tan H, Ustubutun A, Saatci I, Dufke A, Enders H, Pohl K, Alembik Y, Mitchell WA, Mole SE, Lehesjoki AE. Variant late infantile neuronal ceroid lipofuscinosis in a subset of Turkish patients is allelic to Northern Epilepsy. *Hum Mutat* 2004; 23: 300-5.

Ranta S & Lehesjoki AE. Northern epilepsy, a new member of the NCL family. *Neurol Sci* 2000; 21: S43-7.

Ranta S, Zhang Y, Ross B, Lonka L, Takkunen E, Messer A, Sharp J, Wheeler R, Kusumi K, Mole S, Liu W, Soares MB, Bonaldo MF, Hirvasniemi A, de la Chapelle A, Gilliam TC, Lehesjoki AE. The neuronal ceroid lipofuscinoses in human EPMR and mnd mutant mice are associated with mutations in CLN8. *Nat Genet* 1999; 23: 233-6.

Regan CM, de Grip WJ, Daemen FJ, Bonting SL. Degradation of rhodopsin by a lysosomal fraction of retinal pigment epithelium: Biochemical aspects of the visual process. XLI. *Exp Eye Res* 1980; 30: 183-91.

Rein K, Zockler M, Mader MT, Grubel C, Heisenberg M. The *Drosophila* standard brain. *Curr Biol* 2002; 12: 227-31.

Reinhardt K, Grapp M, Schlachter K, Bruck W, Gartner J, Steinfeld R. Novel CLN8 mutations confirm the clinical and ethnic diversity of late infantile neuronal ceroid lipofuscinosis. *Clin Genet* 2010; 77: 79-85.

Reiter LT, Potocki L, Chien S, Gribskov M, Bier E. A systematic analysis of human disease-associated gene sequences in *Drosophila melanogaster*. *Genome Res* 2001; 11: 1114-25.

Rider JA, Dawson G, Siakotos AN. Perspective of biochemical research in the neuronal ceroid-lipofuscinosis. *Am J Med Genet* 1992; 42: 519-24.

Robinow S& White K. Characterization and spatial distribution of the ELAV protein during *Drosophila melanogaster* development. *J Neurobiol* 1991; 22: 443-61.

Robinow S& White K. The locus elav of *Drosophila melanogaster* is expressed in neurons at all developmental stages. *Dev Biol* 1988; 126: 294-303.

Robinson PJ. Neuroscience. how to fill a synapse. *Science* 2007; 316: 551-3.

Rusyn E, Mousallem T, Persaud-Sawin DA, Miller S, Boustany RM. CLN3p impacts galactosylceramide transport, raft morphology, and lipid content. *Pediatr Res* 2008; 63: 625-31.

Ryder E & Russell S. Transposable elements as tools for genomics and genetics in *Drosophila*. *Brief Funct Genomic Proteomic* 2003; 2: 57-71.

Saftig P, Hetman M, Schmahl W, Weber K, Heine L, Mossmann H, Koster A, Hess B, Evers M, von Figura K. Mice deficient for the lysosomal proteinase cathepsin D exhibit progressive atrophy of the intestinal mucosa and profound destruction of lymphoid cells. *EMBO J* 1995; 14: 3599-608.

Saja S, Buff H, Smith AC, Williams TS, Korey CA. Identifying cellular pathways modulated by *Drosophila* palmitoyl-protein thioesterase 1 function. *Neurobiol Dis* 2010; 40: 135-45.

Sanchez-Guajardo V, Febbraro F, Kirik D, Romero-Ramos M. Microglia acquire distinct activation profiles depending on the degree of alpha-synuclein neuropathology in a rAAV based model of parkinson's disease. *PLoS One* 2010; 5: e8784.

Sanchez-Soriano N, Tear G, Whitington P, Prokop A. *Drosophila* as a genetic and cellular model for studies on axonal growth. *Neural Dev* 2007; 2: 9.

Sandbank U. Congenital amaurotic idiocy. *Pathol Eur* 1968; 3: 226-9.

Santavuori P, Lauronen L, Kirveskari E, Aberg L, Sainio K, Autti T. Neuronal ceroid lipofuscinoses in childhood. *Neurol Sci* 2000; 21: S35-41.

Santavuori P, Heiskala H, Autti T, Johansson E, Westermarck T. Comparison of the clinical courses in patients with juvenile neuronal ceroid lipofuscinosis receiving antioxidant treatment and those without antioxidant treatment. *Adv Exp Med Biol* 1989; 266: 273-82.

Santos AC & Lehmann R. Isoprenoids control germ cell migration downstream of HMGCoA reductase. *Dev Cell* 2004; 6: 283-93.

Savukoski M, Klockars T, Holmberg V, Santavuori P, Lander ES, Peltonen L. CLN5, a novel gene encoding a putative transmembrane protein mutated in finnish variant late infantile neuronal ceroid lipofuscinosis. *Nat Genet* 1998; 19: 286-8.

Schmiedt ML, Blom T, Blom T, Kopra O, Wong A, von Schantz-Fant C, Ikonen E, Kuronen M, Jauhiainen M, Cooper JD, Jalanko A. Cln5-deficiency in mice leads to microglial activation, defective myelination and changes in lipid metabolism. *Neurobiol Dis* 2012; *Neurobiol Dis.* 2012; 46: 19-29.

Schulte S& Stoffel W. Ceramide UDPgalactosyltransferase from myelinating rat brain: Purification, cloning, and expression. *Proc Natl Acad Sci U S A* 1993; 90: 10265-9.

Schulz A, Mousallem T, Venkataramani M, Persaud-Sawin DA, Zucker A, Luberto C, Bielawska A, Bielawski J, Holthuis JC, Jazwinski SM, Kozhaya L, Dbaibo GS, Boustany RM. The CLN9 protein, a regulator of dihydroceramide synthase. *J Biol Chem* 2006; 281: 2784-94.

Seehafer SS & Pearce DA. You say lipofuscin, we say ceroid: Defining autofluorescent storage material. *Neurobiol Aging* 2006; 27: 576-88.

Seigel GM, Wagner J, Wronska A, Campbell L, Ju W, Zhong N. Progression of early postnatal retinal pathology in a mouse model of neuronal ceroid lipofuscinosis. *Eye* 2005; 19: 1306-12.

Seigel GM, Lotery A, Kummer A, Bernard DJ, Greene ND, Turmaine M, Derksen T, Nussbaum RL, Davidson B, Wagner J, Mitchison HM. Retinal pathology and function in a Cln3 knockout mouse model of juvenile neuronal ceroid lipofuscinosis (Batten disease). *Mol Cell Neurosci* 2002; 19: 515-27.

Seto ES, Bellen HJ, Lloyd TE. When cell biology meets development: Endocytic regulation of signaling pathways. *Genes Dev* 2002; 16: 1314-36.

Sherman M & Guillery R. Exploring the Thalamus and its Role in Cortical Function. The MIT Press, Cambridge, MA, USA, 2006.

Siegel G, Agranoff B, Albers R, Fisher S, Uhler M (Editors). Basic Neurochemistry. Lippincott Williams & Wilkins, Philadelphia, PA, USA, 1999.

Siintola E, Topcu M, Aula N, Lohi H, Minassian BA, Paterson AD, Liu XQ, Wilson C, Lahtinen U, Anttonen AK, Lehesjoki AE. The novel neuronal ceroid lipofuscinosis gene MFSD8 encodes a putative lysosomal transporter. *Am J Hum Genet* 2007; 81: 136-46.

Siintola E, Partanen S, Stromme P, Haapanen A, Haltia M, Maehlen J, Lehesjoki AE, Tyynela J. Cathepsin D deficiency underlies congenital human neuronal ceroid-lipofuscinosis. *Brain* 2006; 129: 1438-45.

Simons K & Ikonen E. Functional rafts in cell membranes. *Nature* 1997; 387: 569-72.

Simons M & Trotter J. Wrapping it up: The cell biology of myelination. *Curr Opin Neurobiol* 2007; 17: 533-40.

Simons M & Trajkovic K. Neuron-glia communication in the control of oligodendrocyte function and myelin biogenesis. *J Cell Sci* 2006; 119: 4381-9.

Sleat DE, Wiseman JA, El-Banna M, Kim KH, Mao Q, Price S, Macauley SL, Sidman RL, Shen MM, Zhao Q, Passini MA, Davidson BL, Stewart GR, Lobel P. A mouse model of classical late-infantile neuronal ceroid lipofuscinosis based on targeted disruption of the CLN2 gene results in a loss of tripeptidyl-peptidase I activity and progressive neurodegeneration. *J Neurosci* 2004; 24: 9117-26.

Sleat DE, Donnelly RJ, Lackland H, Liu CG, Sohar I, Pullarkat RK, Lobel P. Association of mutations in a lysosomal protein with classical late-infantile neuronal ceroid lipofuscinosis. *Science* 1997; 277: 1802-5.

Smith KR, Damiano J, Franceschetti S, Carpenter S, Canafoglia L, Morbin M, Rossi G, Pareyson D, Mole SE, Staropoli JF, Sims KB, Lewis J, Lin WL, Dickson DW, Dahl HH, Bahlo M, Berkovic SF. Strikingly different clinicopathological phenotypes determined by progranulin-mutation dosage. *Am J Hum Genet.* 2012; 90 :1102-7.

Smith SM, Johansen-Berg H, Jenkinson M, Rueckert D, Nichols TE, Miller KL, Robson MD, Jones DK, Klein JC, Bartsch AJ, Behrens TE. Acquisition and voxelwise analysis of multi-subject diffusion data with tract-based spatial statistics. *Nat Protoc* 2007; 2: 499-503.

Smith SM, Jenkinson M, Johansen-Berg H, Rueckert D, Nichols TE, Mackay CE, Watkins KE, Ciccarelli O, Cader MZ, Matthews PM, Behrens TE. Tract-based spatial statistics: Voxelwise analysis of multi-subject diffusion data. *Neuroimage* 2006; 31: 1487-505.

Sofroniew MV& Vinters HV. Astrocytes: Biology and pathology. *Acta Neuropathol* 2010; 119: 7-35.

Sofroniew MV. Molecular dissection of reactive astrogliosis and glial scar formation. *Trends Neurosci* 2009; 32: 638-47.

Squire, L., Bloom, F., McConnell, S., Roberts, J., Spitzer, N., Zigmond, M., 2003, Fundamental Neuroscience. Academic Press, Orlando, FL, USA.

Steinfeld R, Reinhardt K, Schreiber K, Hillebrand M, Kraetzner R, Bruck W, Saftig P, Gartner J. Cathepsin D deficiency is associated with a human neurodegenerative disorder. *Am J Hum Genet* 2006; 78: 988-98.

Strauss O. The retinal pigment epithelium in visual function. *Physiol Rev* 2005; 85: 845-81.

Striano P, Specchio N, Biancheri R, Cannelli N, Simonati A, Cassandrini D, Rossi A, Bruno C, Fusco L, Gaggero R, Vigevano F, Bertini E, Zara F, Santorelli FM, Striano S. Clinical and electrophysiological features of epilepsy in Italian patients with CLN8 mutations. *Epilepsy Behav* 2007; 10: 187-91.

Tambuyzer BR, Ponsaerts P, Nouwen EJ. Microglia: Gatekeepers of central nervous system immunology. *J Leukoc Biol* 2009; 85: 352-70.

Tecott LH. The genes and brains of mice and men. *Am J Psychiatry* 2003; 160: 646-56.

Tegelberg S, Kopra O, Joensuu T, Cooper JD, Lehesjoki AE. Early microglial activation precedes neuronal loss in the brain of the Cstb-/- mouse model of progressive myoclonus epilepsy, EPM1. *J Neuropathol Exp Neurol* 2012; 71: 40-53.

Teixeira CA, Lin S, Mangas M, Quinta R, Bessa CJ, Ferreira C, Sa Miranda MC, Boustany RM, Ribeiro MG. Gene expression profiling in vLINCL CLN6-deficient fibroblasts: Insights into pathobiology. *Biochim Biophys Acta* 2006; 1762: 637-46.

Tome FM, Brunet P, Fardeau M, Hentati F, Reix J. Familial disorder of the central and peripheral nervous systems with particular cytoplasmic lamellated inclusions in peripheral nerves, muscle satellite cells, and blood capillaries. *Acta Neuropathol* 1985; 68: 209-17.

Topcu M, Tan H, Yalnizoglu D, Usubutun A, Saatci I, Aynaci M, Anlar B, Topaloglu H, Turanli G, Kose G, Aysun S. Evaluation of 36 patients from turkey with neuronal ceroid lipofuscinosis: Clinical, neurophysiological, neuroradiological and histopathologic studies. *Turk J Pediatr* 2004; 46: 1-10.

Tschape JA, Hammerschmied C, Muhlig-Versen M, Athenstaedt K, Daum G, Kretzschmar D. The neurodegeneration mutant lochrig interferes with cholesterol homeostasis and appl processing. *EMBO J* 2002; 21: 6367-76.

Tuxworth RI, Chen H, Vivancos V, Carvajal N, Huang X, Tear G. The Batten disease gene CLN3 is required for the response to oxidative stress. *Hum Mol Genet* 2011; 20: 2037-47.

Tuxworth RI, Vivancos V, O'Hare MB, Tear G. Interactions between the juvenile Batten disease gene, CLN3, and the notch and JNK signalling pathways. *Hum Mol Genet* 2009; 18: 667-78.

Tyynela J, Sohar I, Sleat DE, Gin RM, Donnelly RJ, Baumann M, Haltia M, Lobel P. A mutation in the ovine cathepsin D gene causes a congenital lysosomal storage disease with profound neurodegeneration. *EMBO J* 2000; 19: 2786-92.

Tyynela J, Palmer DN, Baumann M, Haltia M. Storage of saposins A and D in infantile neuronal ceroid-lipofuscinosis. *FEBS Lett* 1993; 330: 8-12.

Umbach JA, Zinsmaier KE, Eberle KK, Buchner E, Benzer S, Gundersen CB. Presynaptic dysfunction in *Drosophila* csp mutants. *Neuron* 1994; 13: 899-907.

van de Goor J, Ramaswami M, Kelly R. Redistribution of synaptic vesicles and their proteins in temperature-sensitive shibire(ts1) mutant *Drosophila. Proc Natl Acad Sci U S A* 1995; 92: 5739-43.

Van Horn SC, Erisir A, Sherman SM. Relative distribution of synapses in the A-laminae of the lateral geniculate nucleus of the cat. *J Comp Neurol* 2000; 416: 509-20.

van Meer G. Lipids of the Golgi membrane. *Trends Cell Biol* 1998; 8: 29-33.

Vance JE, Stone SJ, Faust JR. Abnormalities in mitochondria-associated membranes and phospholipid biosynthetic enzymes in the mnd/mnd mouse model of neuronal ceroid lipofuscinosis. *Biochim Biophys Acta* 1997; 1344: 286-99.

Wang T & Montell C. Phototransduction and retinal degeneration in *Drosophila. Pflugers Arch* 2007; 454: 821-47.

Vantaggiato C, Redaelli F, Falcone S, Perrotta C, Tonelli A, Bondioni S, Morbin M, Riva D, Saletti V, Bonaglia MC, Giorda R, Bresolin N, Clementi E, Bassi MT. A novel CLN8 mutation in late-infantile-onset neuronal ceroid lipofuscinosis (LINCL) reveals aspects of CLN8 neurobiological function. *Hum Mutat* 2009; 30: 1104-16.

Wawersik S & Maas RL. Vertebrate eye development as modeled in *Drosophila. Hum Mol Genet* 2000; 9: 917-25.

Wei H, Zhang Z, Saha A, Peng S, Chandra G, Quezado Z, Mukherjee AB. Disruption of adaptive energy metabolism and elevated ribosomal p-S6K1 levels contribute to INCL pathogenesis: Partial rescue by resveratrol. *Hum Mol Genet* 2011; 20: 1111-21.

Wei H, Kim SJ, Zhang Z, Tsai PC, Wisniewski KE, Mukherjee AB. ER and oxidative stresses are common mediators of apoptosis in both neurodegenerative and non-neurodegenerative lysosomal storage disorders and are alleviated by chemical chaperones. *Hum Mol Genet* 2008; 17: 469-77.

Weimer JM, Custer AW, Benedict JW, Alexander NA, Kingsley E, Federoff HJ, Cooper JD, Pearce DA. Visual deficits in a mouse model of Batten disease are the result of optic nerve degeneration and loss of dorsal lateral geniculate thalamic neurons. *Neurobiol Dis* 2006; 22: 284-93.

Velinov M, Dolzhanskaya N, Gonzalez M, Powell E, Konidari I, Hulme W, Staropoli JF, Xin W, Wen GY, Barone R, Coppel SH, Sims K, Brown WT, Zuchner S. Mutations in the gene DNAJC5 cause autosomal dominant kufs disease in a proportion of cases: Study of the parry family and 8 other families. *PLoS One* 2012; 7: e29729.

Vesa J, Chin MH, Oelgeschlager K, Isosomppi J, DellAngelica EC, Jalanko A, Peltonen L. Neuronal ceroid lipofuscinoses are connected at molecular level: Interaction of CLN5 protein with CLN2 and CLN3. *Mol Biol Cell* 2002; 13: 2410-20.

Vesa J, Hellsten E, Verkruyse LA, Camp LA, Rapola J, Santavuori P, Hofmann SL, Peltonen L. Mutations in the palmitoyl protein thioesterase gene causing infantile neuronal ceroid lipofuscinosis. *Nature* 1995; 376: 584-7.

Wheeler RB, Sharp JD, Schultz RA, Joslin JM, Williams RE, Mole SE. The gene mutated in variant late-infantile neuronal ceroid lipofuscinosis (CLN6) and in nclf mutant mice encodes a novel predicted transmembrane protein. *Am J Hum Genet* 2002; 70: 537-42.

Williams, R., 2000. Mapping genes that modulate mouse brain development: A quantitative genetic approach. In Mouse Brain Development. A. Goffinet , P. Rakic, eds. Springer Verlag, New York, NY, USA, pp. 21-22-49.

Winter E & Ponting CP. TRAM, LAG1 and CLN8: Members of a novel family of lipid-sensing domains? *Trends Biochem Sci* 2002; 27: 381-3.

Virmani T, Gupta P, Liu X, Kavalali ET, Hofmann SL. Progressively reduced synaptic vesicle pool size in cultured neurons derived from neuronal ceroid lipofuscinosis-1 knockout mice. *Neurobiol Dis.* 2005; 20: 314-23.

Voigt S, Jungnickel B, Hartmann E, Rapoport TA. Signal sequence-dependent function of the TRAM protein during early phases of protein transport across the endoplasmic reticulum membrane. *J Cell Biol* 1996; 134: 25-35.

von Schantz C, Kielar C, Hansen SN, Pontikis CC, Alexander NA, Kopra O, Jalanko A, Cooper JD. Progressive thalamocortical neuron loss in Cln5 deficient mice: Distinct effects in finnish variant late infantile NCL. *Neurobiol Dis* 2009; 34: 308-19.

Yamasaki R, Zhang J, Koshiishi I, Sastradipura Suniarti DF, Wu Z, Peters C, Schwake M, Uchiyama Y, Kira JI, Saftig P, Utsumi H, Nakanishi H. Involvement of lysosomal storage-induced p38 MAP kinase activation in the overproduction of nitric oxide by microglia in cathepsin D-deficient mice. *Mol Cell Neurosci* 2007; .

Yoon DH, Kwon OY, Mang JY, Jung MJ, Kim do Y, Park YK, Heo TH, Kim SJ. Protective potential of resveratrol against oxidative stress and apoptosis in Batten disease lymphoblast cells. *Biochem Biophys Res Commun* 2011; 414: 49-52.

Zelnik N, Mahajna M, Iancu TC, Sharony R, Zeigler M. A novel mutation of the CLN8 gene: Is there a mediterranean phenotype? *Pediatr Neurol* 2007; 36: 411-3.

Zeman RJ, Peng H, Etlinger JD. Clenbuterol retards loss of motor function in motor neuron degeneration mice. *Exp Neurol* 2004; 187: 460-7.

Zhang CK, Stein PB, Liu J, Wang Z, Yang R, Cho JH, Gregersen PK, Aerts JM, Zhao H, Pastores GM, Mistry PK. Genome-wide association study of N370S homozygous gaucher disease reveals the candidacy of CLN8 gene as a genetic modifier contributing to extreme phenotypic variation. *Am J Hematol* 2012; 87: 377-83.

Zhang D, Brankov M, Makhija MT, Robertson T, Helmerhorst E, Papadimitriou JM, Rakoczy PE. Correlation between inactive cathepsin D expression and retinal changes in mcd2/mcd2 transgenic mice. *Invest Ophthalmol Vis Sci* 2005; 46: 3031-8.

Zhang D, Lai MC, Constable IJ, Rakoczy PE. A model for a blinding eye disease of the aged. *Biogerontology* 2002; 3: 61-6.

Zhu Y& Conner GE. Intermolecular association of lysosomal protein precursors during biosynthesis. *J Biol Chem* 1994; 269: 3846-51.

Zinsmaier KE, Eberle KK, Buchner E, Walter N, Benzer S. Paralysis and early death in cysteine string protein mutants of *Drosophila. Science* 1994; 263: 977-80.

Zoller I, Bussow H, Gieselmann V, Eckhardt M. Oligodendrocyte-specific ceramide galactosyltransferase (CGT) expression phenotypically rescues CGT-deficient mice and demonstrates that CGT activity does not limit brain galactosylceramide level. *Glia* 2005; 52: 190-8.